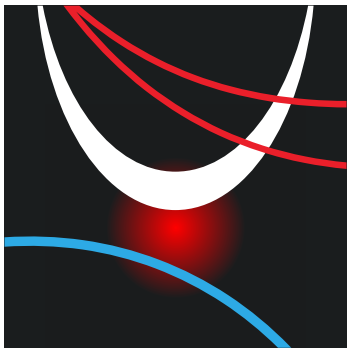
Advanced Properties And Processes In Optoelectronic Materials And Systems

20th APROPOS
BOOK OF ABSTRACTS

Vilnius
LITHUANIA

29 September –
2 October
2026



Advanced Properties And Processes In Optoelectronic Materials And Systems

20th APROPOS

BOOK OF ABSTRACTS

CENTER FOR PHYSICAL SCIENCES AND TECHNOLOGY

FTMC

Vilnius

2026

ORGANIZERS:

CENTER FOR PHYSICAL SCIENCES AND TECHNOLOGY

hermes PROJECT 25-29 — Funded by the European Union

ChipsC² LT

SUPPORTED BY:

attocube WITTENSTEIN group

EKSPLA

LIGHT CONVERSION

nanovita

TERAVIL

tespol engineering

BARNAS MASS SPECTROMETRY

Terahertz Technologies

MONO SPEKTRA

Embassy of Poland in Lithuania

ISBN 978-609-96355-1-4

CONTENTS

Committees	5
Introduction: A Word of Welcome	6
Programme	8
Tutorial Session: Frontier of Photonics & Semiconductor Technology	12
Section 1: Ultrafast Processes and THz Phenomena	17
Section 2: Novel Materials 1: Semiconductors	23
Section 3: Organics for Optoelectronics	30
Section 4: Special Session "Lublin Readings"	37
Section 5: Novel Materials 2: Metamaterials	41
Section 6: Quantum Materials and Technologies	47
Section 7: Novel Optoelectronic Systems	53
Section 8: Spectroscopy and Applications	59
Section 9: Wireless Communication Systems	65
Section 10: Integrated Photonics	71
Poster session	77
Best Student Awards	120
Author Index	122

COMMITTEES

CHAIR

Irmantas Kašalynas (Vilnius, Lithuania)

PROGRAMME COMMITTEE

Vidmantas Gulbinas (Vilnius, Lithuania)
Heinz-Wilhelm Hübers (Berlin, Germany)
Shang-Hua Yang (Hsinchu, Taiwan)
Saulius Juršėnas (Vilnius, Lithuania)
Wojciech Knap (Warsaw, Poland)
Polina Kuzhir (Joensuu, Finland)
Edmund H. Linfield (Leeds, U.K.)
Mažena Mackoit Sinkevičienė (Vilnius, Lithuania)
Linas Minkevičius (Vilnius, Lithuania)
Daniel Mittleman (Providence, RI, USA)
Chiko Otani (Sendai, Japan)
Hartmut G. Roskos (Frankfurt/M, Germany)
Agnieszka Siemion (Warsaw, Poland)
Gintautas Tamulaitis (Vilnius, Lithuania)
Gintaras Valušis (Vilnius, Lithuania)
Val Zwiller (Stockholm, Sweden)

LOCAL ORGANIZING COMMITTEE

Dovilė Čibiraitė–Lukenskienė (Director)
Rusnė Ivaškevičiūtė–Povilauskienė
Milda Tamošiūnaitė-Survilienė
Domas Jokubauskis
Ignas Grigelionis
Patricija Ivanauskaitė
Mindaugas Karaliūnas
Ramunė Kriaučionytė
Irma Luksienė
Ieva Bricienė
Laima Raginskaitė

A WORD OF WELCOME



Dear Colleagues, Dear Friends,

It is my honour and privilege to welcome you to the Sunrise Valley here in the lovely city of Vilnius for a historic milestone – the 20th APROPOS Conference.

We extend our deepest gratitude for your time, your brilliant insights, and your sincere efforts in contributing to this event. Your presence enables us to celebrate the beauty of physics, the elegance of optoelectronics, the charm of advanced nanostructures, and the fascinating phenomena that arise when optics meets electronics.

Since its inception in 1971 as a symposium on plasma and instabilities in semiconductors, this conference series has continually evolved. Over more than five decades, it has grown from "Ultrafast Phenomena in Semiconductors" into the modern APROPOS platform. Yet, throughout this journey, it has preserved its long-standing scientific traditions while pushing the boundaries of semiconductor research and industrial integration.

Nurturing the next generation remains a core pillar of our mission. Starting on September 29, the Tutorial Session, co-organized with the International Young Scientists' Symposium, offers students and young researchers an extraordinary masterclass – a tradition successfully launched back in 2022. With sessions exploring heterogeneous integration, terahertz electronics, photonic integrated circuits, and near-field optical microscopy, we are proud to foster Baltic and international scientific synergy.

This year, the conference is enriched by the traditional Lublin Readings session on Wednesday, September 30. We are privileged to host special guest Dr. Darius Staliūnas from the Lithuanian Institute of History, who will lecture on "Vilnius in the 19th Century: Memory Politics, Symbolic Geography, and Competitive Claims to the 19th-Century City". Following this deep dive into our regional identity, on Friday, October 2, we invite you to explore the city's multicultural heritage further with a tour of the Central Vilnius University Ensemble and the Old Town.

We gather today in a complex and challenging world. In 2026, the realities of geopolitical uncertainty and regional strain remind us that peace, security, and international collaboration cannot be taken for granted. In times of division, science must serve as a universal bridge. Bringing together minds from across Europe, the UK, Taiwan, Japan, the United States, and beyond reinforces the fact that democratic unity and shared knowledge are our greatest values. We are highly indebted to the Research Council of Lithuania, HERMES, and ChipsC^2 LT for making this event possible. Moreover, we extend our highest appreciation to our sponsors – attocube, EKSPLA, Light Conversion, TERAVIL, Terahertz Technologies, Barnas, and Monospektra – for sponsoring the tutorial session, the coffee breaks, and the establishment of the Researcher Awards.

I wish you a very productive week through illuminating conference tracks and enlightening debates as well as breakthrough ideas and encouraging discoveries that defy everyday routines. If APROPOS 2026 can spark a small step toward closer collaboration, we will be deeply fulfilled, knowing we have made a meaningful contribution to creating a more advanced, secure, and peaceful society.

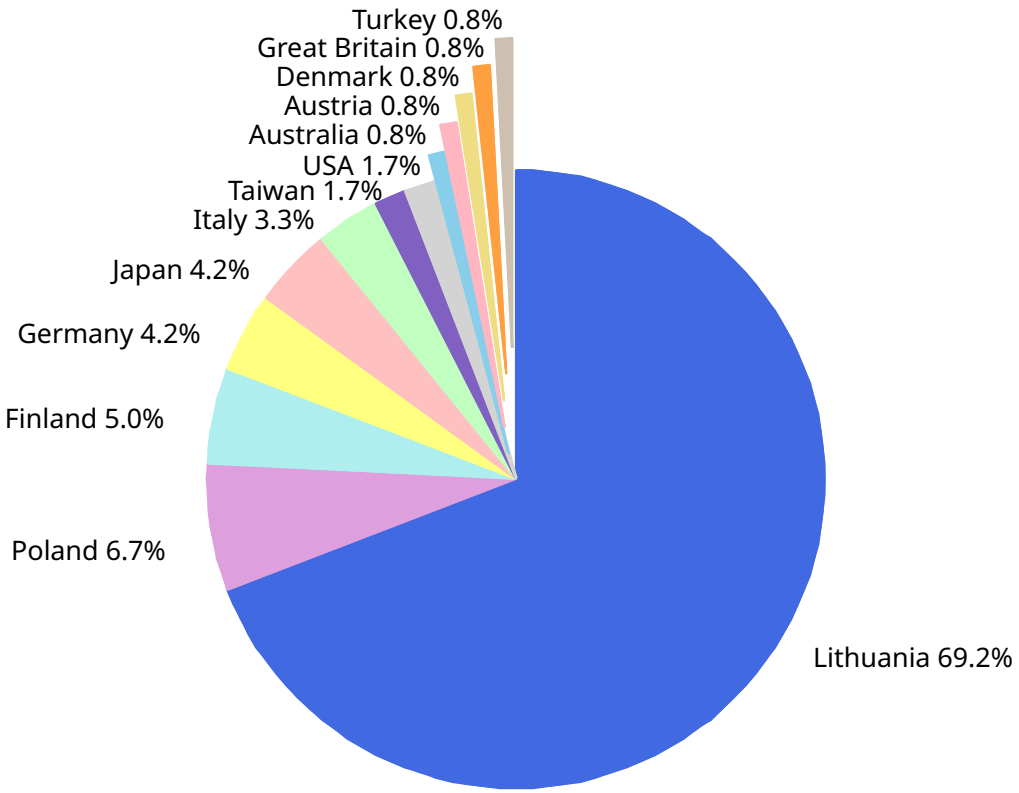
Prof. Dr. Irmantas Kašalynas

Chair of the 20^{th} APROPOS



Photo credit: Gabrielius Mackevičius, FTMC

Participants Statistics



Total number of participants: 120 from 3 continents

APROPOS 20

Advanced Properties And Processes In Optoelectronic Materials And Systems

PROGRAM

Tuesday (29th September)

TUTORIAL SESSION: *Vilnius University Life Sciences Centre, R402 (Saulėtekio ave. 7)*
Frontiers of Photonics & Semiconductor Technology

9:00 – 9:30 TUTORIAL WELCOME WORDS

9:30 – 11:00 **Viktor Krozer** | Ferdinand-Braun-Institut, Leibniz Institut für Höchstfrequenztechnik, Germany
Photonic-electronic heterogeneous integration technologies

11:00 – 11:15 Coffee break

11:15 – 12:45 **Alvydas Lisauskas** | Vilnius University & FTMC, Lithuania
Terahertz Generation and Detection in CMOS: State-of-the-Art, Physical Limits, and Emerging Applications

12:45 – 14:00 Lunch break

14:00 – 15:30 **Vladimir A. Zenin** | University of Southern Denmark, Denmark
Seeing light up close: Near-field Optical Microscopy

15:30 – 15:45 Coffee break

15:45 – 17:15 **Armandas Balčytis** | RMIT University & COMBS, Australia
Integrated Photonic Circuits: Enabling a New Era of Photonics

18:00 – 20:00 WELCOME RECEPTION *FTMC, Loby (Saulėtekio ave. 3)*

Wednesday (30th September)

FTMC, A101 (Saulėtekio ave. 3)

8:40 – 9:00 CONFERENCE OPENING CEREMONY

ULTRAFAST PROCESSES AND THz PHENOMENA (Chairperson Irmantas Kašalynas)

9:00 – 9:40 **Xi-Cheng Zhang** (Plenary) | University of Rochester, NY, U.S.A.
THz liquid photonics

9:40 – 10:05 **Gintaras Valušis** (Invited) | Vilnius University, Lithuania
Modern trends in compact terahertz systems and semiconductor chips

10:05 – 10:20 **Thomas B. Gill** | University of Leeds, U.K.
Chiral-Phonon Driven Ultrafast Spin Currents in a Non-Magnetic Ferroelectric

10:20 – 10:35 **Wataru Kimura** | The University of Tokyo, Japan
Three-dimensional analysis of femtosecond laser ablation in fused silica using dual-view interferometric imaging

10:35 – 10:50 **Simonas Driukas** | FTMC, Lithuania
Optical properties and time resolved THz spectroscopy of ion-implanted GeSn films

10:50 – 11:15 Coffee break

NOVEL MATERIALS 1: SEMICONDUCTORS (Chairperson Koichiro Tanaka)

11:15 – 11:40 **Taiichi Otsuji** (Invited) | ENSEMBLE3 Center of Excellence Ltd., Poland
Dirac plasmons in graphene/topological insulator heterostructures for THz lasers and amplifiers

11:40 – 12:05 **Wojciech Knap** (Invited) | Institute of High Pressure Physics & Warsaw University of Technology, Poland
Magnetoplasmonic Crystals

12:05 – 12:20 **Iryna B. Mikhailikova** | University of Cassino and Southern Lazio, Italy
Graphene-strip-loaded cylindrical Luneburg lens: effects of plasmon resonances on lens performance

12:20 – 12:35 **Evelina Dudutienė** | FTMC, Lithuania
Rapid thermal annealing of GaAsBi/(Al,Ga)As multiple-quantum-well structures

12:35 – 12:50 **Justinas Jorudas** | FTMC, Lithuania
Modification of β-Ga_2O_3 epilayer properties by direct laser micro-machining

12:50 – 14:00 Lunch break

ORGANICS FOR OPTOELECTRONICS (Chairperson Shang-Hua Yang)

14:00 – 14:25 **Polina Kuzhir** (Invited) | University of Eastern FInland, Finland
Multimodal Sensing with Single-Crystal Diamond Needles

14:25 – 14:50 **Karolis Kazlauskas** (Invited) | Vilnius University, Lithuania
Advanced strategies for efficient solid-state photon upconversion

14:50 – 15:05 **Titas Klepeckas** | FTMC, Lithuania
DIO-Induced Interface Intermixing Limits in Pseudo-Bilayer PM6:Y6 Organic Solar Cell Blends

15:05 – 15:20 **Faustino Wahaia** | Pontifical Catholic University of Chile, Chile
Analysis of Metal-Organic Framework Single Crystals for Possible THz Waves Emission and Sensing

15:20 – 15:35 **Shyantan Dasgupta** | FTMC, Lithuania
Bulk and interfacial ion dynamics in quasi-2D and 3D perovskite LEDs

15:35 – 16:00 Coffee break

SPECIAL SESSION: LUBLIN READINGS (Co-support by Embassy of Poland in Lithuania) (Chairperson Gintaras Valušis)

16:00 – 16:05 **Intro-word** | Polish Embassy

16:05 – 16:30 **Darius Staliūnas** | Vilnius University, Lithuania
Vilnius in 19th century: Memory Politics, Symbolic Geography, and Competitive Claims to the 19th-Century City

16:30 – 16:55 **Agnieszka Siemion** (Invited) | Warsaw University of Technology, Poland
Terahertz Beam Shaping with Diffractive Optics for medical applications with examination of scattering effects

16:55 – 17:20 **Rusnė Ivaškevičiūtė-Povilauskienė** (Invited) | FTMC, Lithuania
Digital Terahertz Holography Approach to Size-Dependent Scattering in Granular Materials

17:20 – 17:45 **Marcin Białek** (Invited) | Institute of High Pressure Physics, Poland
Deep Strong Light-Matter Coupling in Landau-Polaritons

17:45 – 20:00 POSTER SESSION

Thursday (1st October)

FTMC, A101 (Saulėtekio ave. 3)

NOVEL MATERIALS 2: METAMATERIALS (Chairperson Antonio Maffucci)

9:00 – 9:40 **Willie J. Padilla** (Plenary) | Duke University, NC, U.S.A.
Automated Deep Learning Inverse Design of Artificial Electromagnetic Materials

9:40 – 10:05 **Shang-Hua Yang** (Invited) | National Tsing Hua University, Taiwan
Terahertz Optical-Digital Neural Network Imaging

10:05 – 10:20 **Linas Minkevičius** (Invited) | FTMC, Lithuania
Recent Advances in Metasurface-based Optics for THz Imaging Systems

10:20 – 10:35 **Shotaro Kawano** | The University of Tokyo, Japan
Laser micromachining with a large-aperture metalens for a 1064-nm nanosecond laser

APROPOS 20

Advanced Properties And Processes In Optoelectronic Materials And Systems

10:35 – 10:50 **Aleksandr Saushin** | University of Eastern FInland, Finland
Control of polarization ellipticity of THz radiation with ultrathin metamaterial

10:50 – 11:15 Coffee break & **GROUP PHOTO**

QUANTUM MATERIALS AND TECHNOLOGIES (Chairperson Polina Kuzhir)

11:15 – 11:40 **Miriam Serena Vitiello** (Invited) | NEST, National Research Council CNR-NANO & Scuola Normale Superiore, Italy
Ultrafast, low-noise, THz graphene photodetectors and applications in quantum science

11:40 – 12:05 **Ronald Ulbricht** (Invited) | Max Planck Institute for Polymer Research, Germany
Characterizing the electronic structure of quantum defects in semiconductors using time-resolved spectroscopy

12:05 – 12:20 **Ifra Bibi** | FTMC, Lithuania
Laser-Induced Room-Temperature Single-Photon Emission from Defect Centers in Hexagonal Boron Nitride

12:20 – 12:35 **Paulius Rindzevičius** | FTMC, Lithuania
Temperature-dependent fluorescence of color centers in diamond structures

12:35 – 12:50 **Rokas Silkinis** | FTMC, Lithuania
Ab initio emission lineshape modeling of color centers in semiconductors

12:50 – 14:00 Lunch break

NOVEL OPTOELECTRONIC SYSTEMS (Chairperson Agnieszka Siemion)

14:00 – 14:25 **Erik Hagen Waller** (Invited) | Fraunhofer Institute for Industrial Mathematics ITWM, Germany
Terahertz systems and components in industry

14:25 – 14:50 **Kuniaki Konishi** (Invited) | The University of Tokyo, Japan
Fabrication of anti-reflective moth-eye structures using ultrashort-pulse laser processing and their application to radio astronomy observations

14:50 – 15:05 **Kazimieras Nomeika** | Light Conversion, Lithuania
Charge Carrier and Spin Diffusion in a Polycrystalline and Single Crystal Lead Halide Perovskite Semiconductor

15:05 – 15:20 **Regimantas Januškevičius** | Ekspla, Lithuania
Narrowband picosecond laser light sources for wide infrared spectral range based on nonlinear light conversion

15:20 – 15:35 **Adrian Cernescu** | Attocube Systems GmbH, Germany
Imaging and Spectroscopy at 10nm Spatial Resolution using s-SNOM

15:35 – 16:00 Coffee break

SPECTROSCOPY AND APPLICATIONS (Chairperson Georgy Fedorov)

16:00 – 16:25 **Heinz-Wilhelm Hübers** (Invited) | DLR Institute of Space Research & Humboldt University Berlin, Germany
High-resolution THz spectroscopy of the mesosphere and lower thermosphere of the Earth

16:25 – 16:50 **Koichiro Tanaka** (Invited) | RIKEN Centre for Advanced Photonics & Kyoto University, Japan
Saturation Spectroscopy of Rotational Transitions Toward the Molecular Clock Application

16:50 – 17:05 **Chia-Ming Mai** | National Tsing Hua University, Taiwan
Dual-mode Terahertz Time-Domain Spectroscopy for Versatile Characterization of Semiconductors

17:05 – 17:20 **Patricija Ivanauskaitė** | FTMC, Lithuania
Development of a portable optoelectronic system for terahertz gas spectroscopy
17:20 – 17:35 **Surya Revanth Ayyagari** | Vilnius University, Lithuania
Meta-Atom Photonic Sensor for THz Detection of Organic Molecules
18:30 – 21:00 CONFERENCE DINNER

Friday (2nd October)

FTMC, A101 (Saulėtekio ave. 3)

WIRELESS COMMUNICATION SYSTEMS (Co-organizer HERMES)
(Chairperson Heinz-Wilhelm Hübers)
9:00 – 9:40 **Tadao Nagatsuma** (Plenary) | The University of Tokyo, Japan
Terahertz Technologies for Wireless Communications: Achievements and Future Directions
9:40 – 10:05 **Antonio Maffucci** (Invited) | University of Cassino and Southern Lazio, Italy
Towards the integration of THz antennas in novel communication links: the Hermes project
10:05 – 10:20 **Paweł Komorowski** | Military University of Technology, Poland
High-speed terahertz communication in the W and J bands
10:20 – 10:35 **Justina Žemgulytė** | FTMC, Lithuania
Dielectric resonator array rectenna for radio frequency energy harvesting
10:35 – 10:50 **Gedminas Elertas** | Astrolight, Lithuania
Laser Communications in Action: Real-World Deployments from the Arctic to the Baltic Sea
10:50 – 11:15 Coffee break
INTEGRATED PHOTONICS (Co-organizers ChipsC2-LT & HERMES)
(Chairperson Willie J. Padilla)
11:15 – 11:40 **Timo Aalto** (Invited) | Silicon photonics, VTT, Finland
Photonic Integrated Circuits: from Pilot Line Access to Product
11:40 – 12:05 **Georgy Fedorov** (Invited) | University of Eastern FInland, Finland
Terahertz range electrodynamics and possible optoelectronic applications of carbon nanotube films
12:05 – 12:20 **Ubaid ur Rehman** | FTMC, Lithuania
Femtosecond Laser-Written Photonic Integrated Circuits for Quantum Applications
12:20 – 12:35 **Vytautas Janonis** | FTMC, Lithuania
Near-field investigation of GaN surface relief grating coupled plasmon phonon polaritons
12:35 – 12:50 **Armandas Balčytis** | RMIT University & COMBS, Australia
Engineering Thin-Film Lithium Niobate Cavities for On-Chip Frequency-Space Lattices
12:50 – 13:00 BEST STUDENT AWARDS & CONFERENCE CLOSING REMARKS
13:00 – 14:00 Lunch break
14:30 – 17:00 EXCURSION to old town and historical Astronomical Observatory of Vilnius University

TUTORIAL SESSION:

Frontier of Photonics & Semiconductor Technology

T1-L1

Photonic-electronic heterogeneous integration technologies

Viktor Krozer[1], Marko Rausch[1], Oleksandr Glubokov[1], Tanjil Shivan[1], Jonas Gläsel[2], Christoph Stölmacker[1], Adam Rämer[1,3], Christian Berger[1], Ralf Doerner[1], Maruf Hossain[1], Hady Yacoub[1], Patrick Runge[2], Wolfgang Heinrich[1], and Patrick Scheele[1]

[1] *Ferdinand-Braun-Institut, Leibniz Institut für Höchstfrequenztechnik Berlin, Germany.*
[2] *Heinrich Hertz Institut, Fraunhofer-Institut für Nachrichtentechnik Berlin, Germany*
[3]*now with Xavveo GmbH, Berlin, Germany*
Email: viktor.krozer@fbh-berlin.de.

Heterogeneous integration with large bandwidth approaching terahertz frequencies allow for higher speed and higher functional complexity in electronic circuits and enable heterogeneously integrated photonic electronic modules. Heterogeneous integration (HI) technology is an enabler for higher functional complexities and higher speeds, especially in More than Moore applications [1]. HI also allows for a reduction in size, weight, and power, enabling new capability and enhanced performance [2], [3]. In this presentation we discuss several technology approaches for semiconductor electronic and photonic integration. It is shown that bandwidth in excess of 300 GHz are attainable with interconnects placeable anywhere in a layout. A novel structure has be implemented for photonic electronic heterogeneous integration as depicted in Fig. 1. Here a photodiode in InP has been heterogeneously integrated with a transimpedance amplifier [4]. Bandwidth limitation will be discussed. It should be emphasized that for HI both components to be integrated have to be realized with a mirror layout. One advantage of the novel HI technology is the precise adjustment of the height between the two components.

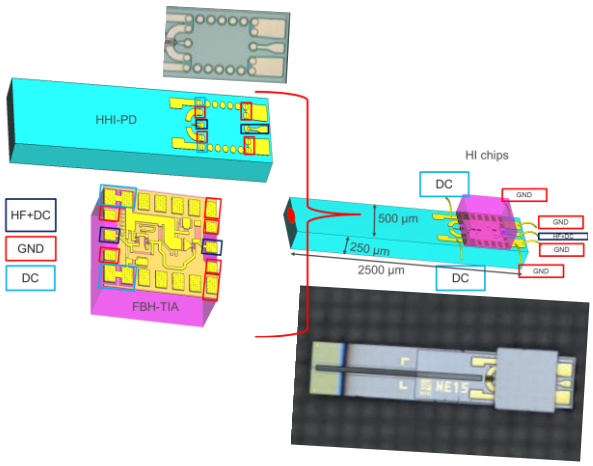


Fig. 1 Heterogeneous integration of photonic and electronic components into a compact module.

REFERENCES

[1] B. Bayraktaroglu, „Heterogeneous Integration Technology,“ AFRL-RY-WP-TR-2017-0168, 2017.
[2] N. Collaert, „Scaling up GaN- and InP-based technologies for 5G and 6G wireless communication“, Chip Scale Review, Vol. 28, 2024.
[3] H. Yacoub, C. Mangiavillano, M. Rausch, E. Dischke, W. Heinrich and P. Scheele, "InP-HBT MMIC for RF Applications: Technology Roadmap and Heterointegration," 2025 16th German Microwave Conference (GeMiC), Dresden, Germany, 2025, pp. 366-367.
[4] V. Krozer et al. „Towards Terahertz Bandwidth Heterogeneous Integration of Semiconductor Technologies“, CSW Conf. 2026, 2026.

T1-L2

Terahertz Generation and Detection in CMOS: State-of-the-Art, Physical Limits, and Emerging Applications

Alvydas Lisauskas[1,2]

[1]*Institute of Applied Electrodynamics and Telecommunications, Vilnius University, Saulėtekio av. 3, 10257 Vilnius, Lithuania .*
[2]*Optoelectronics Department, Center for Physical Sciences and Technology, Saulėtekio av. 3, 10257 Vilnius, Lithuania.*
Email: alvydas.lisauskas@ff.vu.lt

Abstract

Terahertz technologies are moving from laboratory-scale optical and cryogenic systems toward compact, room-temperature electronic platforms [1,2]. A key enabler of this transition is the use of complementary metal–oxide–semiconductor technology, which offers high-yield fabrication, reproducibility, low cost, and the possibility of large-scale integration with signal-processing circuitry [3,4]. This tutorial will review the state of the art in terahertz generation and detection using standard and advanced CMOS foundry processes, with emphasis on the physical mechanisms, circuit architectures, and system-level trade-offs relevant for frequencies from the sub-THz range toward 1 THz.

The generation part will cover CMOS oscillators, frequency multipliers, harmonic extraction, injection locking, phase locking, and power-combining concepts using on-chip and in-package antenna arrays. The detection part will focus on field-effect transistor detectors, Schottky diodes, antenna-coupling peculiarities, and integrated imaging arrays. Particular attention will be given to sensitivity, noise-equivalent power, bandwidth, output power, impedance matching, packaging, calibration, and comparison with III–V, photonic, and thermal THz technologies.

The tutorial is intended for PhD students and early-stage researchers who have a background in electromagnetics, semiconductor devices, or high-frequency electronics. By the end of the session, participants will understand why CMOS has become a serious platform for scalable THz systems, what its current limitations are, and how CMOS-based sources and detectors can be applied to spectroscopy, imaging, and sensing.

REFERENCES

[1] D. M. Mittleman, Optics Express, 26(8), 9417–9431, Apr. 2018.
[2] G. Valušis et al., Sensors, 21(12), 4092, Jan. 2021.
[3] E. Javadi et al., Sensors, 21(9), 2909, 2021.
[4] P. Hillger et al., IEEE Transactions on Terahertz Science and Technology, 9, 1–19, 2019.

T1-L3

Seeing light up close: Near-field Optical Microscopy

Vladimir A. Zenin

Center for Nano Optics, University of Southern Denmark, 5230 Odense, Denmark
Email: zenin@mci.sdu.dk

Near-field optical microscopy has transformed the way optical imaging is performed beyond the diffraction limit. This lecture will introduce the historical development of near-field optics, beginning with the early ideas of subwavelength optical probing and the emergence of scanning near-field optical microscopy (SNOM/NSOM) as a practical experimental technique. The discussion will then cover the main physical principles of SNOM, including evanescent fields, probe–sample interaction, aperture and apertureless configurations, and the role of scanning probe control in achieving nanoscale spatial resolution.

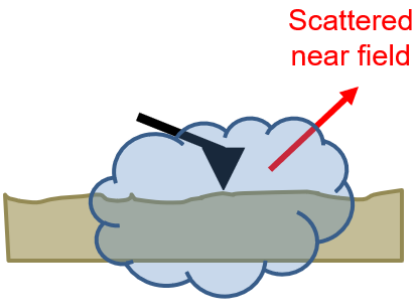


Fig. 1 Concept of near-field optical microscopy

Special attention will be given to how SNOM bridges optical spectroscopy and surface microscopy, enabling simultaneous access to structural, optical, and spectroscopic information at the nanoscale. The lecture will also review modern state-of-the-art approaches, including plasmonic and tip-enhanced techniques, near-field imaging of nanophotonic structures, two-dimensional materials, etc. By combining historical context, fundamental concepts, and recent advances, the lecture will provide a broad overview of near-field optical microscopy as a powerful tool for nanoscale optical characterization.

T1-L4

Integrated Photonic Circuits: Enabling a New Era of Photonics

Armandas Balčytis[1,2]

[1]*Integrated Photonics and Applications Centre, RMIT University, Melbourne, VIC 3000 Australia*
[2]*ARC Centre of Excellence in Optical Microcombs for Breakthrough Science (COMBS), Australia*
Email: armandas.balcytis@rmit.edu.au

Photonic integrated circuits (PICs) mark a pivotal stage in the evolution of optical wave routing, continuing the trend toward increased modal confinement seen in the transition from free-space benchtop setups to optical fiber circuits. Integration of multiple optical functions - such as waveguides, modulators, detectors, lasers, and nonlinear materials - on a single chip offer a path analogous to that of electronic integrated circuits, drastically reducing size, cost, and power consumption while improving reliability, robustness, and enabling new functionality.

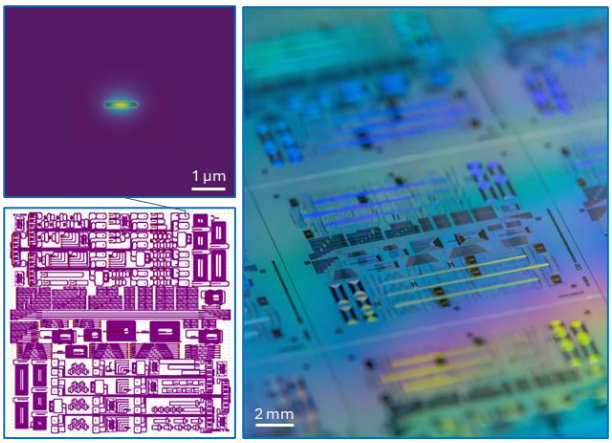


Fig. 1 SiN PIC workflow steps: mode simulation, circuit design, fabricated chip.

This tutorial introduces the principles, technologies, and applications of integrated photonics. Starting by laying out the case for PICs relative to alternative platforms, it will provide a concise summary of the platforms, including silicon [1], silicon nitride [2], III-V and piezoelectric material platforms [3], as well as emerging heterogeneous approaches. The tutorial will follow a representative photonic circuit path and introduce its key components – interfaces, couplers, modulators, and resonators, highlighting how well-defined primitives underlie the scalability of the PIC approach. It will also discuss the typical workflows for simulation, design, fabrication, and packaging of such devices.

A major focus will be on the role of integrated photonics in augmenting application areas, including communication systems, optical frequency metrology, and radio-over-fiber transmission. It will also survey emerging applications, such as integrated LiDAR for autonomous systems, biosensing platforms for healthcare diagnostics, frequency synthesis, and photonic processors for neuromorphic and quantum information processing.

Challenges such as optical losses, thermal effects, operation beyond the telecommunication wavelength region, packaging, and scalability will be discussed alongside recent advances in addressing these limitations. Finally, the tutorial will provide a forward-looking perspective on the emerging trends in integrated photonics, and how they are expected to shape the technological landscape across multiple domains.

REFERENCES

[1] Y. Yuan et al; *APL Photonics* **10** (2025) pp. 060901.
[2] K. A. Buzaverov et al; *Laser & Photonics Revie*ws **18** (2024) pp. 2400508.
[3] D. Zhu et al; *Advances in Optics and Photonics* **13** (2021) pp. 242-352.

SESSION 1:

Ultrafast Processes and THz Phenomena

S1-PL

THz liquid photonics

X.-C. Zhang
University of Rochester, Rochester, USA
Email: zhangxc@rochester.edu

I will present recent progress in THz liquid photonics—an extension of previous research on THz air photonics. Investigating THz generation from liquids may complete the final piece of the matter-phase puzzle in THz photonics.

2026 APROPOS

S1-I1

Modern trends in compact terahertz systems and semiconductor chips

Gintaras Valušis

Institute of Photonics and Nanotechnology, Department of Physics, Vilnius University Saulėtekio ave.3, LT-10254, Vilnius, Lithuania.
Email: gintaras.valusis@ff.vu.lt.

A particular interest in development of modern terahertz (THz) technology [1] is dedicated to the development of compact, solid-state-based room-temperature, high-power, stable and portable terahertz emitters and sensitive detectors as well as user-friendly THz imaging and spectroscopy systems containing flat optics components with minimized optical alignment [2].

In this presentation, modern trends in evolution of compact THz imaging and spectroscopic systems will be reviewed. Special attention will be given to innovations in THz semiconductor chips development as well as their hybrid integration schemes. Optical engineering will be also considered underlying an employment of THz structured light in imaging and 6G wireless communications systems. An exceptional view will be directed to a compact silicon diffractive optics and nonparaxial case in THz optics design aiming to find rational approaches for integration of optical components directly on the chip [3].

Contemporary scientific and technological challenges as well as extrapolations of possible further evolution in the field will be discussed.

REFERENCES

[1] A. Leitenstorfer et al, The 2023 terahertz science and technology roadmap, *Journal of Applied Physics D: Applied Physics,* 2023, Vol. **56**, 223001, 66 pages.

[2] G. Valušis et al, Roadmap of Terahertz Imaging 2021*, Sensors,* 2021, **21,** 4092, 51 page.

[3] S. Orlov et al, Light Engineering and Silicon Diffractive Optics Assisted Nonparaxial Terahertz Imaging, *Laser & Photonics Reviews*, 2024, **18,** 2301197, 27 pages.

S1-O1

Chiral-Phonon–Driven Ultrafast Spin Currents in a Non-Magnetic Ferroelectric

Thomas B. Gill[1], Ahmet Yagmur[2], Matthew Rogers[2], Nathan Fox[1], Ben Muggleton[1,3], Zabeada Aslam[4], Conor J. McCluskey[5], Phoenix Robinson[1,3], Bryan J. Hickey[2], Timothy Moorsom[2,3], J. Marty Gregg[5], Edmund H. Linfield[1], Sukhdeep Dhillon[6], Satoshi Sasaki[2], Joshua R. Freeman[1]

[1]*School of Electronic and Electrical Engineering, University of Leeds, Leeds, LS2 9JT, United Kingdom.*
[2]*School of Physics & Astronomy, University of Leeds, Leeds, LS2 9JT, United Kingdom.*
[3]*School of Chemical and Process Engineering, University of Leeds, Leeds, LS2 9JT, United Kingdom.*
[4]*LEMAS, Bragg Centre for Materials Research, University of Leeds, Leeds, LS2 9JT, United Kingdom.*
[5]*Centre for Quantum Materials and Technologies, School of Maths and Physics, Queen's University Belfast, Belfast, BT7 1NN, United Kingdom.*
[6]*Laboratoire de Physique de l'Ecole Normale Sup´erieur, ENS, Universit´e PSL, CNRS, Sorbonne Universit´e, Universit´e Paris Cit´e, Paris, 75005, France.*
Email: t.b.gill@leeds.ac.uk

Chiral phonons are a fundamental lattice vibration involving atoms moving in a circular motion, allowing the phonons to carry angular momentum [1]. This angular momentum allows for non-magnetic materials to exhibit properties previously only observable in magnetic materials. Here we present data showing that a non-magnetic ferroelectric material, In_2Se_3, can generate an ultrafast spin current through a chiral-phonon induced spin-Seebeck effect [2]. By adding a thin heavy metal layer, we utilise the inverse spin-Hall effect to convert the spin current in the In_2Se_3 layer into a transient charge current, which emits a pulse of terahertz radiation, similar to ferromagnetic terahertz spintronic emitters [3], but without the need for an external magnetic field. These emitted pulses were measured using polarisation resolved terahertz emission spectroscopy, revealing a strong elliptical polarisation, with the handedness being controlled by the polarisation of the optical pump beam. This indicates coherent transfer of phonon angular momentum on femtosecond timescales. This emission mechanism shows promise for developing circularly polarised terahertz emitters with controllable handedness, as well as a pathway for generating spin currents in non-magnetic materials.

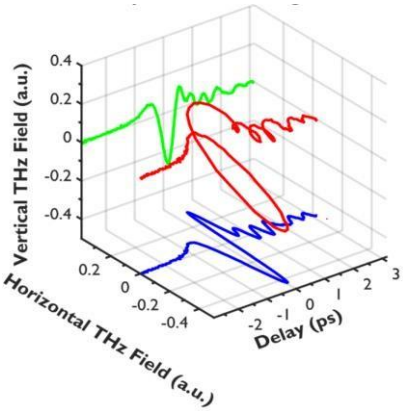


Fig. 1 Measured horizontal and vertical polarisation of a terahertz pulse emitted from In_2Se_3 with a layer of Pt.

REFERENCES

[1] D. M. Juraschek *et al.*; *Nature Physics* **21** (2025) pp. 1532–1540
[2] K. Kim *et al; Nature Materials* **22** (2023) pp. 322–328
[3] T. Seifert *et al.*; *Nature Photonics* **10** (2016) pp. 483–488

S1-O2

Three-dimensional analysis of femtosecond laser ablation in fused silica using dual-view interferometric imaging

Wataru Kimura[1], Shotaro Kawano[2], Haruyuki Sakurai[2], Kuniaki Konishi[1,2]

[1]*Department of Physics, Graduate School of Science, The University of Tokyo, Japan*
[2]*Institute for Photon Science and Technology, The University of Tokyo, Japan*
Email: kkonishi@ipst.s.u-tokyo.ac.jp

Femtosecond laser processing has been widely used for high-precision micromachining, yet its underlying physical mechanisms are often hard to track and control due to a myriad of coupled electronic, mechanical, and thermal processes that evolve in both space and time. To investigate these processes, interferometric pump-probe imaging [1,2] has proved to be a powerful technique due to its sensitivity to transient refractive-index changes induced by these processes. In our previous work, we had established a quantitative side-view Nomarski interferometer and demonstrated that electron density distributions in laser-induced air plasma were quantitatively reconstructed by using Abel inversion [3]. However, when this approach is applied to laser ablation, side-view imaging can lose information from the near-surface regions because of surface diffraction, although this depth can be comparable to the typical depth of the ablation crater.

In this study, we used a time-resolved dual-view interferometric imaging system to compare the experimentally observed top-view phase images with the top-view images numerically reconstructed from side-view images. Figure 1(a) and (b) respectively show the experimentally measured top-view and side-view phase images. The side-view phase image was analyzed using Abel inversion to reconstruct a cylindrical refractive-index-change distribution. Figure 1(c) shows the three-dimensional distribution reconstructed from the side-view image. The corresponding top-view image, shown in fig. 1(d), was then calculated by numerically propagating a probe wave through the reconstructed distribution using the angular spectrum method. By comparing this predicted image with the experimentally measured top-view image acquired simultaneously, we believe it is possible to evaluate whether the side-view reconstruction can explain the top-view observation and to examine near-surface contributions that may not be fully captured by the side-view analysis.

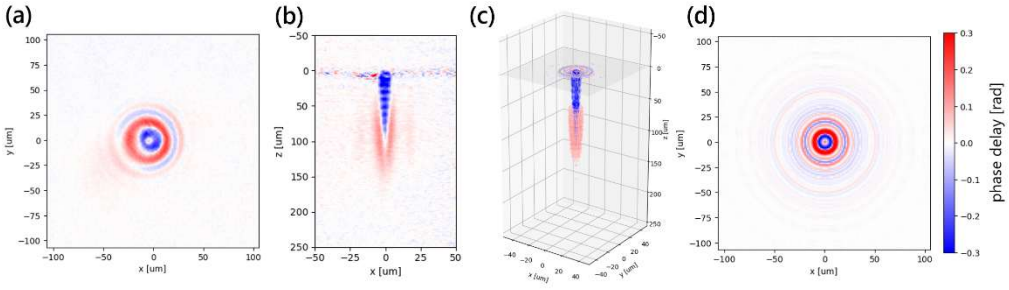


Fig. 1. (a)(b) Measured (a) top-view (b) side-view phase images. (c) 3D phase delay distribution reconstructed from (b) by Abel inversion. (d) A top-view image numerically reconstructed from side-view experimental image.

REFERENCES

[1] V. V. Temnov *et al.*, Appl. Phys. A Mater. Sci. Process. **78**, 483 (2004).
[2] B. Guo *et al.*, Int. J. Extrem. Manuf. **1**, 032004 (2019).
[3] W. Kimura *et al.*, Phys. Plasmas **32**, 062106 (2025).

S1-O3

Optical properties and time resolved THz spectroscopy of ion-implanted GeSn films

Simonas Driukas,[1] Chia-Ming Mai,[2] Ričardas Norkus,[1] Bronislavas Čehavičius,[1] Ignas Nevinskas,[1] Shang-Hua Yang,[2, 3, 4, 5] and Gintaras Valušis[6]

1)Department of Optoelectronics, Center for Physical Sciences and Technology, Saulėtekio Ave. 3, LT-10257, Vilnius, Lithuania

2)Institute of Electronic Engineering, National Tsing Hua University, Hsinchu City 300, Taiwan

3)Department of Electrical Engineering, National Tsing Hua University, Hsinchu City 300, Taiwan

4)Terahertz Optics and Photonics Center, National Tsing Hua University, Hsinchu City 300,Taiwan

5)College of Semiconductor Research, National Tsing Hua University, Hsinchu City 300, Taiwan

6)Institute of Photonics and Nanotechnology, Faculty of Physics, Vilnius University, Saulėtekio Ave. 3, LT-10257, Vilnius, Lithuania

Email: simonas.driukas@ftmc.lt

Among the emerging optoelectronic materials needed for the growing chip-integrated photonics industry, GeSn has attracted considerable attention due to its compatibility with existing CMOS fabrication processes and silicon-on-insulator technology, as well as its tunable bandgap enabling to reach 1.55 μm wavelength. While pure Ge is an indirect semiconductor, the incorporation of 7-9% Sn lowers the energy of the Γ conduction valley, leading to a direct bandgap GeSn material. [1] The alloy has already demonstrated strong potential for photodetectors, light-emitting diodes, and laser devices [2], however, its ultrafast performance at terahertz (THz) frequencies remains relatively unexplored. For THz applications and high frequency wireless data transfer, post-growth processing is required to reduce carrier lifetimes.

In this work, conventional structural characterization techniques and a range of THz spectroscopic methods are employed to investigate the structural, optical, and electrical properties of ion-implanted GeSn layers with varying implantation energies and ion doses. Structural characterization reveals a threshold beyond which implantation-induced damage becomes significant, while lower implantation parameters preserve the crystallinity of the material. Surface THz emission spectroscopy reveals THz emission at longer optical excitation wavelengths than those observed in the Ge substrate, indicating the Sn-induced bandgap reduction. Furthermore, optical-pump THz-probe spectroscopy unveils complex carrier dynamics governed by intervalley scattering and ion-induced defect states. A more than one order-of-magnitude reduction in carrier lifetime is achieved in ion-implanted samples, decreasing from 132 ps to 4.5 ps for an implantation dose of 5×10^{12} cm^{-2} and an implantation energy of 100 keV.

These results provide new insights into effects caused by ion implantation in GeSn alloys, enabling the identification of optimal implantation parameters for ultrafast optoelectronic applications.

REFERENCES

[1] Eales, T.D., Marko, I.P., Schulz, S. *et al.Sci Rep* **9**, 14077 (2019).
[2] A. Giunto and A. F. Morral, *Appl. Phys. Rev*. **11**, 041333 (2024).

ACKNOWLEDGMENT

This work is supported by the NSTC, Taiwan - grants "112-2221-E-007-089-MY3" and "113-2628-E-007-011-MY3".

SESSION 2:

Novel Materials 1: Semiconductors

S2-I1

Dirac plasmons in graphene/topological insulator heterostructures for THz lasers and amplifiers.

Taiichi Otsuji[1,2]

[1]*Photonic Elements Group, ENSEMBLE3 Ltd., Warszawa, Poland.*
[2]*Terahertz Laboratory, Institute of High Pressure Physics, PAN, Warszawa, Poland.*
Email: taiichi.otsuji@ensemble3.eu

Graphene is a two-dimensional (2D) Dirac semimetal with nontrivial topology. Its lattice chirality produces a Berry phase anomaly [1]. However, its weak spin-orbit coupling prevents it from being a topological insulator (TI). However, when graphene is in close proximity to a TI with strong spin-orbit coupling, such as Bi_2Te_3 or Bi_2Se_3, it can enter topological regimes [2, 3]. This paper proposes using a graphene-TI/semiconductor lamellar eutectic heterostructure as an electrostatically striped two-dimensional channel in Dirac plasmonic transistors. We will discuss the advantages of this heterostructure over simple graphene and/or TI 2D channels and address its potential for room-temperature, intense terahertz (THz) lasing and amplification.

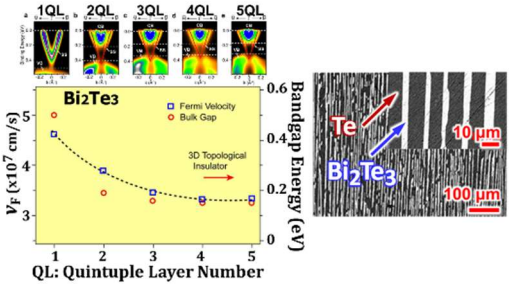


Fig. 1 QL-dependent band profile of Bi_2Te_3 (top) [4], Bi_2Te_3/Te eutectic lamellar heterostructure [5].

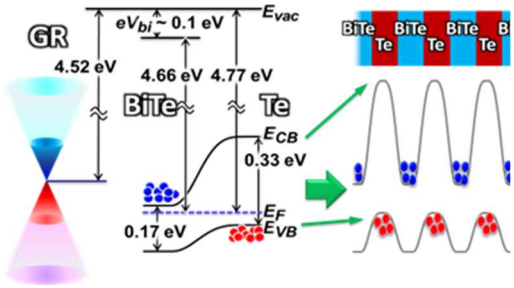


Fig. 2 Band diagrams of Bi_2Te_3/Te lamellar EuHetero [5].

First, we consider a lamellar eutectic heterostructure (EuHeter) consisting of Bi_2Te_3 TI and Te semiconductor grown via a self-organized directional solidification process (Fig. 1) [4, 5]. Each Bi_2Te_3 or Te lamellar layer has a thickness around 10 to 500 microns depending on the growth condition. Bi_2Te_3 is a topological insulator whose energy band dispersion varies depending on quintuple layer (QL) number, and $\geq$ 5 QLs of our case manifest the bulk semiconducting states rather than the surface topological states, saturating its bandgap energy around 0.17 eV [5]. The EuHetero growth process unintentionally n-type dopes the Bi2Te3 and p-type dopes the Te, resulting in repetitive p-n heterojunctions over the Bi2Te3/Te lamellar (Fig. 2) [5].

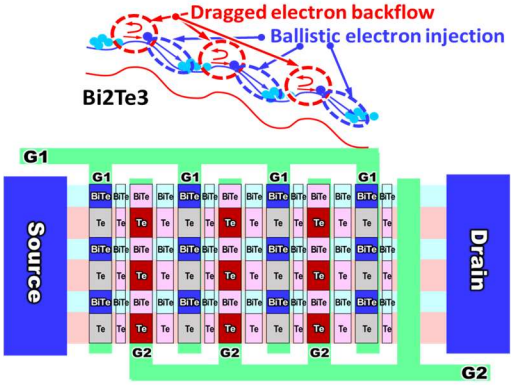


Fig. 3 Modulation-doped, striped channel formation in the graphene-Bi_2Te_3/Te EuHetero composite channel ADGG-FET [6].

Let us consider the Bi2Te3/Te lamellar Euhetero channel asymmetric dual-grating-gate (ADGG) transistor structure under a complementary ADGG (G1 and G2) biasing and a dc drain-source biasing. The n-doped Bi_2Te_3 and p-doped Te lamellar make the planar 2D

channel to be electrostatically “striped-out” channel (Fig. 3) [6], which can effectively suppress excitation of oblique plasmons, a killer of cavity modes of plasmon resonance [7]. One can form striped n- or p-type channels in the Bi2Te3 or Te layers with non-uniform potential slope with cliffs along the channel, leading to the promotion of Coulomb-drag plasmonic instability and resulting resonant self-oscillation in the THz range (Fig. 3) [8].

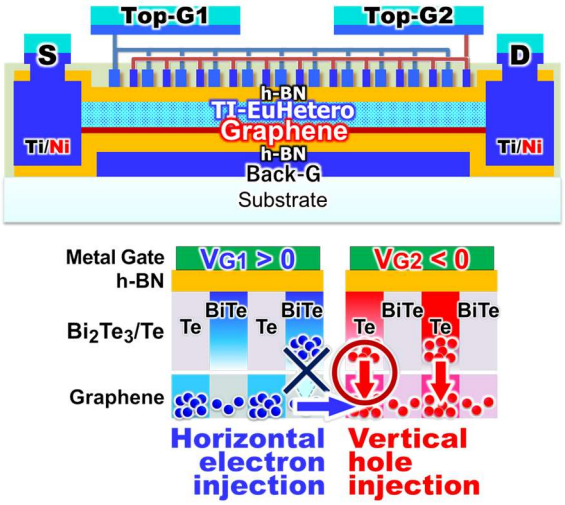


Fig. 4 Modulation-doped, striped channel formation in the graphene-Bi_2Te_3/Te EuHetero composite channel ADGG-FET [9]. Device cross sectional view (top) and diagonal doping from EuHetero to graphene (bottom) [9].

Next, we consider a composite channel where Bi_2Te_3/Te EuHetero is stacked on monolayer graphene. The energy band offsets between graphene and Bi_2Te_3/Te allow hole injection from the p-doped Te to graphene whereas it prohibits electron injection from the n-doped Bi_2Te_3 to graphene, enabling so called “diagonal” electron/hole injection to the graphene layer. This enormously prevent from heating the injected carriers, dramatically enhancing carrier population inversion and resulting THz gain (Fig. 4) [9, 10]. We further develop an asymmetric tri-grating-gate laser transistor structure using the graphene/EuHetero lamellar composite channel that can realize an integration of a population-inverted spontaneous THz emission regions and plasmon-instability-driven coherent THz amplification regions in a single monolithic die [11]. This will open a pathway towards room-temperature, intense THz lasing and coherent, giant amplification.

The author thanks K. Bandopadhyay, H.R. Darabian, K. Kouderis, A. Khamsavi, S. Mahdi, N. Khinevich, K. Markus, D.A. Pawlak, W. Knap, D. But, J. Kierdaszuk, J. Sitek, C. Kokacinski, M. Potemski, V. Ryzhii, S. Boubanga-Tombet, C. Tang, D. Yadav, A. Satou, K. Tamura, T. Suemitsu, H. Fukidome, M. Suemitsu, M. Ryzhii, K. Narahara, V. Mitin, and M. Shur for their contributions. He also acknowledges support by the “Centre of ExcelleNce for nanophotonicS, advancEd Materials and novel crystal growth-Based techno-LogiEs - ENSEMBLE3” project which is carried out within the 2.1 IRAP of the FNP co-financed by the EU under the European Funds for Smart Economy 2021-2027 (FENG.02.01-IP.05-0044/24), and the European Union Horizon 2020 research and innovation program Teaming for Excellence (GA. No. 857543). The publication was created as part of the project of the Minister of Science and Higher Education "Support for the activities of Centers of Excellence established in Poland under the Horizon 2020 program" (No. MEiN/2023/DIR/ 3797). He also acknowledges support by the Institute of High Pressure Physics of the Polish Academy of Sciences and the European Union through the ERC-ADVANCED grant TERAPLASM (No. 101053716).

REFERENCES

[1] M.I. Katsnelson, *Materials Today* **10** (2007) pp. 20-27.
[2] C. L. Kane et al., *Phys. Rev. Lett.*, **95**, (2005) p. 226801.
[3] I. Popov et al., *Phys. Rev. B* **90** (2014) p. 035418.
[4] Y. Li et al., *Adv. Mater.* **22**, (2010) p. 4002.
[5] K. Bandopadhyay et al., *Next Mater.* **5** (2024) p. 100252.
[6] T. Otsuji et al., Patent pending, P.452216 [WIPO ST 10/C PL452216], May 30, 2025.
[7] M. Dyakonov, *Semicond.* **42** (2008) pp. 984-988.
[8] V. Ryzhii et al., *V. Ryzhii et al., Phys. Rev. Appl.* **16** (2021) p. 014001.
[9] V. Ryzhii et al**.,** *Phys. Rev. B* **100** (2019) p. 115436.
[10] T. Otsuji et al., *Appl. Phys. Exp.* **19** (2026) p. 020103.
[11] T. Otsuji et al., to be presented at the 51st IRMMW-THz in Salt Lake City, UT, USA, Oct. 11-16, 2026.

S2-I2

Magnetoplasmonic Crystals

Pavlo Sai[1,2,3], Vadym Korotyeyev[1,4], Maksym Dub[1,3], Milan Orlita[5], Wojciech Knap[1,3]

[1]*CENTERA Labs Institute of High Pressure Physics PAS, Warsaw, Poland*

[2]*Department of Physics, University of Duisburg-Essen, Duisburg, Germany*

[3]*CENTERA, CEZAMAT, Warsaw University of Technology, Warsaw, Poland*

[4]*V. Ye. Lashkaryov Institute of Semiconductor Physics (ISP), NASU, Kyiv, Ukraine*

[5]*LNCMI, CNRS-UGA-UPS-INSA-EMFL, France*

*psai@unipress.waw.pl

Plasmonic crystals, consisting of periodic plasmonic cavities with subwavelength periodicity, enable engineering of plasmonic band structures and strong confinement of terahertz (THz) radiation. While electrical and structural tuning of plasmonic crystals has been extensively investigated [1,2], the impact of magnetic fields on their band structure remains largely unexplored. Here, we report studies on high magnetic field influence on plasmonic crystals formed by periodic arrangements of carrier cavities in grating-gate AlGaN/GaN with high-mobility two-dimensional electron gas (2DEG). We show strong modification of the crystal structures related to interaction of plasmonic collective excitation with harmonics of single particle cyclotron resonance (CR) electron excitations. The investigated structures were fabricated from AlGaN/GaN heterostructures grown on semi-insulating SiC substrates, with sub-micron grating gates patterned by electron-beam lithography. A schematic cross-section of the device is shown in Fig. 1(a). Magnetotransmission measurements were performed using Fourier-transform infrared spectroscopy in magnetic fields up to 16 T at 4.2 K.

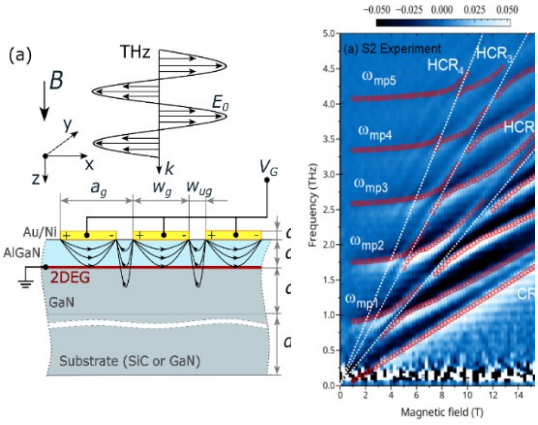


Fig.1. (a) Schematic view of AlGaN/GaN-based plasmonic crystal integrated with metal grating. (b) Magneto transmission of sample with 87% grating filling factor.

The key parameter that decides about the plasmonic crystal band structure is the filling factor (ratio of metalized and uncovered crystal surface). AlGaN/GaN grating-gate plasmonic crystals with different filling factors were investigated. We show that for plasmonic crystals with low grating filling factor, the fundamental plasmon mode exhibits anticrossing with higher harmonics of CR – HCR, leading to the formation of Bernstein modes and magnetic-field-induced band splitting. Increasing the grating filling factor results in excitation of multiple magnetoplasmon modes with energies up to 5 THz. As shown in Fig.1(b), these modes (ω_{mp}) strongly hybridize with HCR up to the fourth order modifying plasmonic crystal energy band structure by appearance of a complex spectrum of Bernstein modes.

The experimental observations are accurately reproduced by our electrodynamic model incorporating the magnetic-field-dependent conductivity tensor of the 2DEG without fitting parameters. The results demonstrate that plasmonic crystals provide a versatile platform for engineering tunable THz excitations in strong magnetic fields and open prospects for magnetoplasmonic THz devices.

1. P. Sai, et al., Phys. Rev. X 13, 041003 (2023).
2. P. Sai, et al., Advanced Optical Materials 13(21), 2500716 (2025).

S2-O1

Graphene-strip-loaded cylindrical Luneburg lens: effects of plasmon resonances on lens performance

Iryna O. Mikhailikova[1,2]

[1]*Department of Electrical and Information Engineering "Maurizio Scarano", University of Cassino and Southern Lazio, Cassino, 03043, Italy.*

[2]*EUt+ Institute of Nanomaterials and Nanotechnologies-EUTINN, European University of Technology, European Union.*

Email: iryna.mikhailikova@studentmail.unicas.it

The Luneburg lens (LL) focuses incident electromagnetic waves onto its surface through a radially graded permittivity profile that decreases from 2 at the center to 1 at the outer boundary [1]. Due to their quasi-optical properties, LL antennas are widely employed in radar, satellite communications, beamforming, and related electromagnetic systems. Since practical LLs are finite and discretized, they must be approximated by multiple concentric layers—typically about ten—to reproduce geometrical-optics performance. For electrically small lenses, the ideal focal point broadens into a finite focal region. Graphene strips placed within this region function as tunable plasmonic resonators that support quasi-surface-wave modes, leading to enhanced field localization through plasmon resonances and the electromagnetic-jet effect, similarly to the graphene-decorated dielectric rod studied in [2].

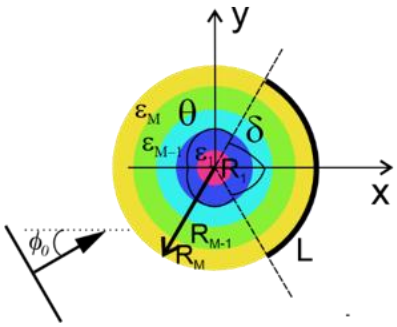


Fig. 1 Cross-section of an M-layer cylindrical Luneburg lens decorated with a conformal graphene strip of angular width 2δ. The black arrow shows the propagation direction of the incident plane wave, ϕ_0 is the incidence angle; R_p is the external radius and $\varepsilon_p = 2 - (p - 1/2)^2/M^2$ is the dielectric permittivity of the *p*-th layer, for $p = 1, \ldots, M$.

In this study, A hyper-singular integral equation (HSIE) formulation [3], discretized through a Nyström-type method [4], is considered to analyze a discretized Luneburg lens loaded with a conformal graphene strip. This approach ensures mathematically rigorous convergence while maintaining a relatively low discretization requirement, even for electrically large structures [5]. The graphene layer is represented as an infinitely thin conductive surface whose impedance is the reciprocal of the Kubo-based surface conductivity, determined by the frequency f, chemical potential μ_c, temperature T, and relaxation time τ [6].

REFERENCES

[1] R. K. Luneburg, *The Mathematical Theory of Optics*, Brown Univ. Press (1941).
[2] S. V. Dukhopelnykov et al., *J. Appl. Phys.* **126** (2019), no. 023104.
[3] D. Colton and R. Kress, *Integral Equation Methods in Scattering Theory*, Wiley (1983).
[4] J. L. Tsalamengas, *J. Comput. Phys.* **303** (2015), pp. 498–513.
[5] M. Lucido et al., *Phil. Trans. R. Soc. A* **383** (2025), no. 20240356.
[6] G. W. Hanson, *J. Appl. Phys.* **103** (2008), no. 064302.

S2-O2

Rapid thermal annealing of GaAsBi/(Al,Ga)As multiple-quantum-well structures

Evelina Dudutienė[1], Justas Žuvelis[1], Aivaras Špokas[1], Andrea Zelioli[1], Kipras Mažeika[2], Augustas Vaitkevičius[1,2], Sandra Stanionytė[3], Martynas Skapas[3], Piotr Wojnar[4] and Renata Butkutė[1]

[1]Department of Optoelectronics, State research institute Center for Physical Sciences and Technology, Saulėtekio av. 3 Vilnius, Lithuania.
[2]Institute of Photonics and Nanotechnology, Faculty of Physics, Vilnius University, Saulėtekio av. 3, Vilnius, Lithuania.
[3] Department of Characterisation of Materials Structure, State research institute Center for Physical Sciences and Technology, Saulėtekio av. 3 Vilnius, Lithuania
[4]Institute of Physics, Polish Academy of Sciences, Lotników av. 32/46, Warsaw, Poland.

Email: evelina.dudutiene@ftmc.lt.

Thermal annealing is widely used to tune the optical and structural properties of epitaxially grown III-V heterostructures. However, the response of GaAsBi multiple-quantum-well (MQW) systems to rapid thermal annealing (RTA) remains insufficiently understood, largely due to the complex interplay between Bi redistribution, interface intermixing, and defect evolution. In this work, we systematically investigate the effects of RTA in the 550 - 750 °C range on GaAsBi/GaAs and GaAsBi/AlGaAs MQWs with varying barrier thicknesses and compositions, enabling a direct comparison of design-dependent annealing behaviour.

Our results reveal that the impact of RTA is strongly governed by barrier design. GaAsBi MQWs structures incorporating narrow 7 nm GaAs barriers exhibit a degradation of room-temperature photoluminescence (PL) across all annealing temperatures. Although atomic force microscopy and X-ray diffraction measurements show preserved surface morphology and structural periodicity, the PL intensity decreases significantly, consistent with Bi redistribution that reduces the barrier thickness and weakens carrier confinement. In contrast, GaAsBi MQW with wider GaAs or AlGaAs barriers exhibit a qualitatively different response. For these structures, annealing up to 700 °C leads to a clear enhancement of room temperature PL intensity and reduced thermal quenching, attributed to a redistribution-driven reduction of alloy disorder and decreased density of point defects after RTA.

For all investigated structures, annealing at higher temperatures leads to the disappearance of the topmost QW and the formation of Bi quantum dots (QDs), as confirmed by transmission electron microscopy. Low-temperature cathodoluminescence measurements reveal sharp QD-like emission features; however, no corresponding PL signal is observed in the 4 - 300 K range, likely due to the low QD density or inefficient carrier capture into these states.

This work has received funding from the Research Council of Lithuania (LMTLT), agreement No. S-MIP-24-99.

S2-O3

Modification of β-Ga_2O_3 epilayer properties by direct laser micro-machining

Justinas Jorudas[1], Simonas Indrišiūnas[1], Maxim Moscotin[1], Giedrius Stalnionis[1], Ilja Ignatjev[1], Tomas Daugalas[1], Paulius Gečys[1], Ray-Hua Horng[2] and Irmantas Kašalynas[1]

[1]*Optoelectronics department, Center for Physical Sciences and Technology (FTMC), Lithuania.*
[2] *Institute of Electronics, National Yang Ming Chiao Tung University (NYCU), Taiwan.*
Email: justinas.jorudas@ftmc.lt

Direct laser micro-machining (DLM) is widely studied technique in material processing, due to its contactless nature, sub-micron precision, and high speed. In the case of compound semiconductors, DLM has been used for laser lift-off of the epitaxial layers [1], laser vertical interconnect accesses (VIAs) drilling [2], and laser dye dicing [3], [4]. However up to date – very little research has been reported on the usage of DLM for processing steps used in the semiconductor device formation such as mesa isolation formation or recessing for ohmic and Schottky contacts.

We investigated the structural and electrical properties of β-Ga_2O_3 epilayers modified via DLM with aim to realize the shallow recesses suitable for novel production of high-voltage semiconductor devices. Utilizing a 342 nm wavelength femtosecond laser and precisely controlling parameters of focused beam fluence and overlap, we developed the processes of forming the recesses on large semiconductor surface with the depth ranging from 200 nm down to 20 nm. The scanning electron microscopy, and Raman spectroscopy methods were also employed to reveal the morphology and perform structural analysis of the DLM-recessed areas and as-grown β-Ga_2O_3. By forming the DLM recesses shallower than 70 nm, we enable wide-range control of sheet resistance up to 100 MΩ/sq. while maintaining ohmic behavior. For depths exceeding 70 nm, recess resistance surpasses 10^{10} Ω, providing effective and maskless way for formation of intra-device isolation. Proof of principle DLM gate-recessed β-Ga_2O_3 MOSFET was fabricated also to prove versatility of DLM fabrication technique.

These findings highlight DLM as a viable, green and mask-less technique for high-precision mesa isolation and recess formation on the wide-bandgap semiconductor layers.

REFERENCES

[1] A. Tanaka et al., “Laser slice thinning of GaN-on-GaN high electron mobility transistors,” Sci. Rep., vol. 12, no. 1, p. 7363, May 2022, doi: 10.1038/s41598-022-10610-4.
[2] C. Sasaoka, Y. Ando, H. Takahashi, N. Ikarashi, and H. Amano, “Metal Stop Laser Drilling for Blind via Holes of GaN-on-GaN Devices,” Phys. status solidi, vol. 220, no. 16, Aug. 2023, doi: 10.1002/pssa.202200739.
[3] S. Indrišiūnas, E. Svirplys, J. Jorudas, and I. Kašalynas, “Laser Processing of Transparent Wafers with a AlGaN/GaN Heterostructures and High-Electron Mobility Devices on a Backside,” *Micromachines*, vol. 12, no. 4, p. 407, Apr. 2021, doi: 10.3390/mi12040407.
[4] Z. Sun *et al.*, “Laser stealth dicing of β-Ga2O3: Theoretical and experimental studies,” *J. Mater. Sci. Technol.*, vol. 238, pp. 303–312, Dec. 2025, doi: 10.1016/j.jmst.2025.03.044.

SESSION 3:

Organics for Optoelectronics

S3-I1

Multimodal Sensing with Single-Crystal Diamond Needles

Elena Filonenko[1], Yuliya Mindarava[2], Mateja Guimarães[2], Marlene Patraca Gonzalez[2], Sergei Malykhin[1], Dmitri Horoshko[2], Fedor Jelezko[2], and Polina Kuzhir[1]

[1] *Department of Physics and Mathematics, University of Eastern Finland, Joensuu, Finland*

[2] *Institute for Quantum Optics and Centre for Integrated Quantum Science and Technology (IQST), Ulm University, Ulm, Germany*

We report multimodal sensing based on single-crystal diamond needles as a platform for nanoscale metrology. Their high crystalline quality and well-defined geometry provide high sensitivity and stability for quantum and optothermal measurements.

The approach integrates complementary mechanisms, including nitrogen-vacancy (NV^-) center ODMR thermometry, silicon-vacancy (SiV^-) all-optical thermometry, and pH-sensitive photoluminescence for surface probing. Cross-validation between SiV^- and NV^- thermometry improves measurement reliability through independent sensing channels.

Surface-dependent photoluminescence variations further enable detection of local chemical environment changes, including pH, supporting multifunctional quantum sensing.

Overall, diamond needles offer a versatile platform for high-resolution, multi-parameter sensing with cross-validated accuracy across physical and chemical modalities.

S3-I2

Advanced strategies for efficient solid-state photon upconversion

Karolis Kazlauskas

[1]*Institute of Photonics and Nanotechnology, Faculty of Physics, Vilnius University, Saulėtekio av. 3, LT-10257 Vilnius, Lithuania*
Email: karolis.kazlauskas@ff.vu.lt.

Triplet–triplet annihilation upconversion (TTA-UC) provides a unique molecular route for converting low-energy, incoherent light into higher-energy emission, thereby enabling applications in solar energy harvesting, photocatalysis, bioimaging, optogenetics, and 3D printing [1]. However, translating high solution efficiencies into solid-state architectures, which are preferred for practical applications, requires a shift from empirical optimization to mechanism-guided materials design.

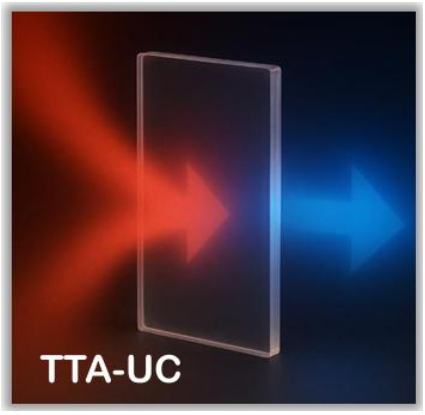


Fig. 1 Schematic illustration of TTA-UC process.

In this talk, we discuss how solid-state TTA-UC performance has advanced through the identification and control of coupled exciton-diffusion and loss processes. We first show that high annihilator loading, while needed for Dexter-type triplet hopping, can induce aggregation, emission quenching, and diffusion-assisted triplet loss at non-radiative sites [2]. We then describe strategies that turn these constraints into design rules: i) suppressing back-FRET from upconverted singlets with emissive singlet sinks [3]; ii) combining purification with melt-processing to obtain homogeneous, high-loading amorphous films with reduced singlet and triplet quenching [4]; and iii) using multi-resonant TADF emitters as advanced sink sites. Finally, we discuss recent routes to engineer the spin-statistical factor *f*, either by reducing losses to upper triplet states through annihilator design [5] or by exploiting aggregation-induced changes in the triplet manifold and spin–orbit coupling [6]. Together, these strategies define a route from managing exciton diffusion to actively engineering the fate of triplet-pair states in solid-state TTA-UC.

REFERENCES

[1] L. Zeng, L. Huang, J. Han, G. Han, *Acc. Chem. Res.* **55** (2022) 2604–2615.
[2] S. Raišys, K. Kazlauskas, S. Juršėnas, Y.C. Simon, *ACS Appl. Mater. Interfaces* **8** (2016) 15732–15740.
[3] S. Raišys, S. Juršėnas, Y.C. Simon, C. Weder, K. Kazlauskas, *Chem. Sci.* **9** (2018) 6796–6802.
[4] S. Raišys, S. Juršėnas, K. Kazlauskas, *Sol. RRL* **6** (2022) 2100873.
[5] L. Naimovičius, E. Radiunas, M. Dapkevičius, P. Bharmoria, K. Moth-Poulsen, K. Kazlauskas, *J. Mater. Chem. C* **11** (2023) 14826–14832.
[6] J. Lekavičius, E. Radiunas, G. Kreiza, A. Jozeliūnaitė, E. Orentas, K. Kazlauskas, *Chem. Sci.* **17** (2026) 6230–6237.

S3-O1

DIO-Induced Interface Intermixing Limits in Pseudo-Bilayer PM6:Y6 Organic Solar Cell Blends

Titas Klepeckas, Marius Franckevičius, Vidmantas Gulbinas

Center for Physical Sciences and Technology, Department of Molecular Compound Physics, Lithuania
Email: titas.klepeckas@ftmc.lt

Organic solar cells (OSCs) based on PM6:Y6 bulk heterojunction (BHJ) active layers have achieved power conversion efficiencies (PCEs) approaching 20%,[1] establishing them among the most promising non-fullerene acceptor systems. However, the inherent morphological disorder of single-step BHJ deposition introduces challenges in controlling donor–acceptor phase separation, promoting charge recombination and limiting long-term stability.[2] The two-step pseudo-bilayer heterojunction (PPHJ) architecture offers improved vertical phase separation control through sequential sublayer deposition,[3] yet PM6:Y6 PCEs typically plateau near 17%,[4] underscoring the need for a deeper understanding of interfacial intermixing and aggregation/phase separation dynamics.

In this work, we systematically investigate the role of the solvent additive 1,8-diiodooctane (DIO) on phase aggregation dynamics in PM6:Y6 PPHJ active layers cross four sublayer modification configurations: unmodified, acceptor-only, donor-only, and dual modification of both sublayers. Using UV-VIS absorption spectroscopy and time-resolved photoluminescence (TRPL), we track sublayer crystallinity, intermixing, and morphological evolution under thermal stress.

We demonstrate that unmodified PM6:Y6 PPHJ films are thermally unstable, exhibiting significant morphological evolution under thermal stress. Introducing DIO during deposition of a single sublayer partially mitigates this instability: the plasticising effect of DIO promotes sufficient initial intermixing, yielding a stable interface that is notably resistant to large-scale morphological disruption. However, this stabilising effect is highly sensitive to the modification strategy employed. Extending DIO treatment to both sublayers induces excessive phase separation, effectively collapsing the intermixed interface into a more discrete layer-by-layer morphology and disrupting the balance achieved through single-layer modification.

REFERENCES

[1] N. R. E. L. (NREL), Best research-cell efficiency chart, 2025. Accessed on 20th February 2025.
[2] S. Shoaee *et al.*, Adv. Mater., 36, 2302005, 2024.
[3] D. Luo *et al.*, Adv. Mater., 37, 2410880, 2025.
[4] X. Wang *et al.*, Adv. Funct. Mater., 31, 2102291, 2021.

S3-O2
Analysis of Metal-Organic Framework Single Crystals for Possible THz Waves Emission and Sensing

Faustino Wahaia[1,2], Irmantas Kašalynas[3], Daniil Pashnev[3], Gintaras Valušis[3], Andrzej Urbanowicz3, Mindaugas Karaliunas[3], Dinesh Pratap Singh[2,4], Francisco Hernán Capdeville Lienqueo[1,2], Birger Seifert[1,2]

[1]*Facultad de Física, Pontificia Universidad Católica de Chile, Chile*
[2]*ANID – Millennium Science Initiative Program – Millennium Institute for Research in Optics, Chile*
[3]*FTMC - Terahertz Photonics Laboratory, Optoelectronics Department, Center for Physical Sciences and Technology, Vilnius, Lithuania*
[4]*Department of Physics, Universidad de Santiago de Chile, Santiago*

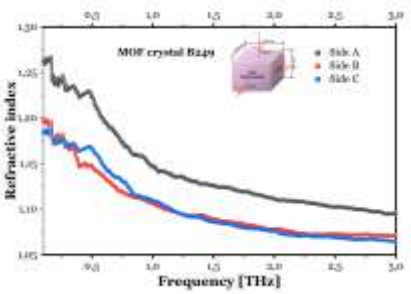
Correspondence author: Faustino Wahaia, Email: faustino.wahaia@uc.cl

Abstract

The use of metal-organic frameworks (MOFs) for terahertz (THz) emission and sensing is still at its early development stage. Our motivation for a deep study on the present non-centrosymmetric MOF crystal, [Zn(3-ptz)2]n, produced using a novel solvothermal technique created by a Startup**,** "**MAQI**" from the University of Santiago de Chile is to widening the list of these hybrid materials capable to generate and detect THz waves. To follow through THz time-domain spectroscopy (TTDS), to obtain the optical constants parameters and dielectric properties, such as refractive index $n_{MOF(THz)}(\omega)$, absorption coefficient $\alpha_{MOF(THz)}(\omega)$, and conductivity (σ), from this MOF single crystals. The TTDS measurements were carried out inner the frequency range of 0.1 to 3 THz. The results support the research outputs published in our earlier work, shown its promising position as a material for THz waves transceiver and applications in optoelectronics, photonics, and materials science.

Introduction

Over the past few years, THz technologies working in the spectral range 0.1 - 10 THz, 3 mm to 30 μm in wavelength [1], located between FIR and $\mu - waves$ band of the electromagnetic spectrum, have made giant strides since the development of materials and methods for the emission and detection THz radiation. It has generated a field for highly encouraging in basic sciences, including biomedical, materials characterization, wireless communications, homeland security and myriad others. The motivation driving this work was integrate the studied of [Zn(3-ptz)2]n MOF crystals into nowadays gingerly increasing list of THz photonic new materials [2].



Obtained through $\boldsymbol{n_{MOF}(\omega) = 1 + \frac{c}{\omega_{THz} d} arg[H(\omega)]}$ RI for the MOF crystals B249, according to THz wave propagation direction through

Conclusions

In summary, the two, B248 and B249, millimeter-sized crystals derived from the same batch, Zn(3-ptz)2 MOF crystals, studied in this work, showed promising potentialities as THz transceiver material. Further confirmation through extensive and exhaustive experimental work is needed to establish it as a reliable material for this purpose, including its potential use in novel photonic and optoelectronic devices.

REFERENCES

[1]. X. C. Zhang, *Introduction to THz wave photonics*. 2010. doi: 10.1007/978-1-4419-0978-7.
[2]. P. D. Cunningham *et al*, "Optical properties of DAST in the THz range," *Opt. Express*, vol. 18, no. 23, p. 23620, 2010, doi: 10.1364/oe.18.023620.

S3-O3

Bulk and interfacial ion dynamics in quasi-2D and 3D perovskite LEDs

Shyantan Dasgupta[1], Liutauras Vaiciulis[1], Lukasz Gelczuk[2], Edoardo Mosconi[3], Muyi Zhang[4], Feng Gao[4] and Vidmantas Gulbinas[1]

[1]Center for Physical Sciences and Technology (FTMC), Saulėtekio al. 3, LT-10257 Vilnius,

[2]Department of Experimental Physics, Faculty of Fundamental Problems of Technology, Wroclaw University of Science and Technology, 50-370 Wroclaw, Poland

[3]Computational Laboratory for Hybrid and Organic Photovoltaics - Istituto CNR di Scienze e Tecnologie Chimiche (SCITEC-CNR) c/o Department of Chemistry, Biology and Biotechnologies, University of Perugia Via Elce di Sotto 8, 06123 Perugia, Italy

[4]Department of Physics Chemistry and Biology (IFM) Linköping University, Linköping 58183, Sweden

Email:Shyantan.dasgupta@ftmc.lt.

The optimal performance of both photovoltaic and electroluminescent devices necessitates minimal nonradiative recombination losses. In perovskites, such losses are significantly influenced by carrier traps associated with mobile ions and vacancies, resulting in I–V hysteresis in solar cells and affecting the performance of perovskite-based optoelectronic devices, including photodetectors and LEDs.[1][2] Ideally in a perovskite LED (PeLED) operation, there are cations at the hole injection layer (HIL)/perovskite interface and anions at the electron injection layer (EIL)/perovskite interface, and upon the application of a forward bias, there is a redistribution of the ions at opposite interfaces under sufficient time scales. This consequently alters the energy landscape in a manner that promotes increased radiative recombination in the bulk.[3] In this work, we study ion dynamics at both the HIL and EIL interfaces along with the bulk of quasi-2D and 3D PeLEDs with time-resolved electroluminescence (TrEL) measurements, where we observed that with shorter pulse periods and longer pulse durations, the electroluminescence of quasi-2D PeLEDs underwent significant degradation compared to their 3D counterpart, which showed an opposite trend under similar conditions. We attribute this to the screening of the field at the HIL and EIL interfaces in the quasi-2D PeLEDs due to the presence of bulky spacer cations of the 2D perovskite lattice, which hamper the ionic redistribution at interfaces [4], thus mitigating the radiative recombination in the bulk. The presence of a large number of grain boundaries in quasi-2D PeLEDs is another factor contributing to strong ionic migration pathways under pulsed operations in their bulk. [5] In this work we corroborate the TrEL results with cross-section Kelvin probe force microscopy (KPFM) analysis and conductive atomic force microscopy (cAFM) studies performed under similar pulsed operations to study the ionic dynamics at the interface and the bulk. We also plan to investigate qualitatively the ionic species, mainly uncoordinated lead (Pb_i) and lead vacancies (V_{Pb}) formed under such pulsed operations through Deep Level Transient Spectroscopy (DLTS) under similar pulsed conditions implemented in TrEL measurements. Finally, to mitigate these field-induced traps, targeted bulk and interface passivation strategies will be deployed, incorporating novel charged dopants to passivate ionic species, suppress non-radiative recombination centers, and stabilize the quasi-2D PeLED lattice.

REFERENCES

[1] [1] R. Gegevičius, M. Franckevičius, J. Chmeliov, W. Tress, V. Gulbinas, “Electroluminescence Dynamics in Perovskite Solar Cells Reveals Giant Overshoot Effect” J. Phys. Chem. Lett. 2019, 10, 1779–1783.

[2] [1] S. Dasgupta, W. Żuraw, T. Ahmad, L. A. Castriotta, E. Radicchi, W. Mróz, M. Ścigaj, Ł. Pawlaczyk, M. Tamulewicz-Szwajkowska, M. Trzciński, J. Serafińczuk, E. Mosconi, A. Di Carlo, F. De Angelis, A. Dudkowiak, K. Wojciechowski, “Modification of a Buried Interface with Bulky Organic Cations for Highly Stable Flexible Perovskite Solar Cells” ACS Appl. Energy Mater. 2022, 5, 15114–15124.

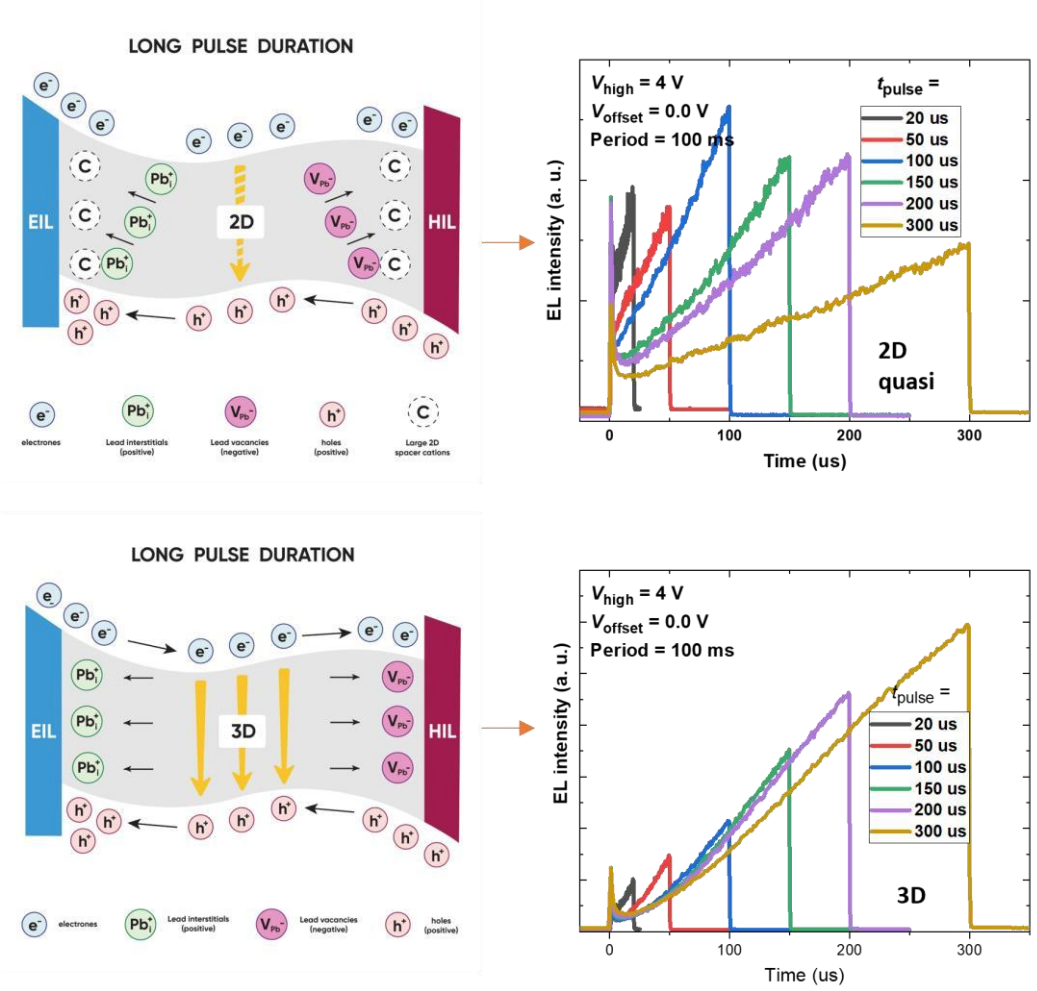
[3] [1] M. A. Torre Cachafeiro, N. K. Kumawat, F. Gao, W. Tress, “Pulsed operation of perovskite LEDs: a study on the role of mobile ions” Natl. Sci. Rev. 2025, 12, DOI 10.1093/nsr/nwae128.

[4] [1] M. Pegu, S. Kazim, T. Bu, D. M. Bassani, S. Ahmad, “Deciphering the Orientation of the Aromatic Spacer Cation in Bilayer Perovskite Solar Cells through Spectroscopic Techniques” 2021,

[5] [1] W. Bai, T. Xuan, H. Zhao, H. Dong, X. Cheng, L. Wang, R. J. Xie, “Perovskite Light-Emitting Diodes with an External Quantum Efficiency Exceeding 30%” Adv. Mater. 2023, 35, 1–8.

Acknowledgments:
The presenting author acknowledges funding from the Research Council of Lithuania LMT project (2400- PL 789).

TOC:



SPECIAL SESSION:

Lublin Readings

S4-I1

Terahertz Beam Shaping with Diffractive Optics for medical applications with examination of scattering effects

Adrianna Nieradka[1], Rusnė Ivaškevičiūtė-Povilauskienė[2], Lukas Stacevičius[2], Mateusz Kaluza[1], Ignas Grigelionis[1], Gintaras Valušis[3], Linas Minkevičius[2] and Agnieszka Siemion[1,4]

[1]Faculty of Physics, Warsaw University of Technology, Koszykowa 75, 00-662, Warsaw, Poland
[2]Department of Optoelectronics, Center for Physical Sciences and Technology, Saulėtekio Ave. 3, 10257 Vilnius, Lithuania.
[3]Institute of Photonics and Nanotechnology, Faculty of Physics, Vilnius University, Saulėtekio Ave. 3, 10257 Vilnius, Lithuania
[4]Center for Advanced Materials and Technologies CEZAMAT, Warsaw University of Technology, Poleczki 19, 02-822 Warsaw, Poland
Email: agnieszka.siemion@pw.edu.pl

Terahertz (THz) radiation has emerged as a promising tool for non-invasive medical diagnostics, particularly in the context of skin cancer detection, owing to its sensitivity to water content and tissue composition. Skin tissue phantoms — controlled, repeatable models of biological tissue — provide a practical foundation for developing and validating THz-based diagnostic techniques prior to in vivo testing. Since scattering plays a critical role in the interaction of THz radiation with such heterogeneous biological media, a time domain spectroscopy together with specially designed in-reflection setup was used. Additionally for samples that are scattering not only spectroscopy but also a holographic approach was adopted to examine and characterize these scattering effects with high precision.

In case of in-reflection system diffractive optical elements (DOEs) offer compact and flexible solutions for THz beam shaping, enabling miniaturization of the optical setup [1]. For the holographic method a 4-step phase shifting algorithm was used to extract the phase information properly. The reconstruction methods allow determination of changes in the refractive index and absorption coefficient of the examined samples, supporting the characterization of tissue-mimicking phantoms for future THz diagnostics for dermatological applications.

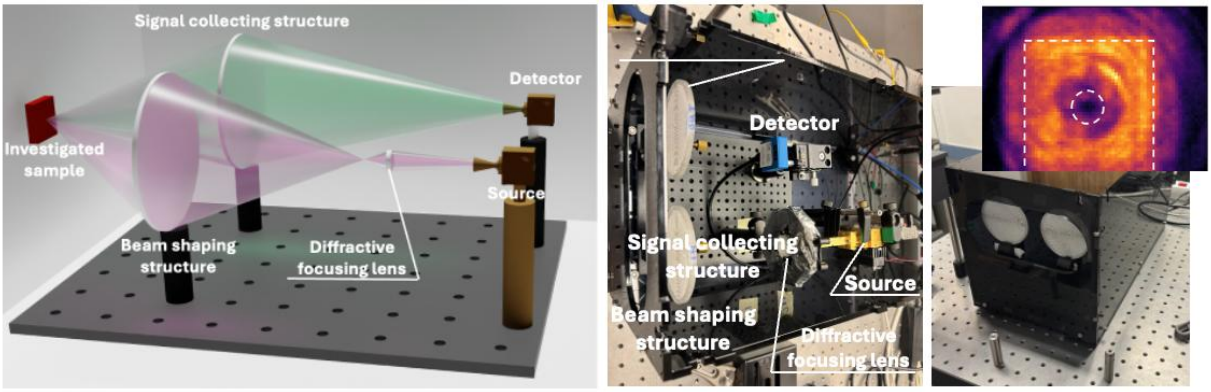


Fig. 1. Scheme of the in-reflection setup with it's photograph inside a demonstrator and exemplary scan.

REFERENCES

[1] A. Siemion; *Journal of Infrared, Millimeter, and Terahertz Waves* **40** (2019) pp. 477–499.

S4-I2

Digital Terahertz Holography Approach to Size-Dependent Scattering in Granular Materials

Rusnė Ivaškevičiūtė-Povilauskienė[1], Lukas Stacevičius[1], Mateusz Kaluza[2], Agnieszka Siemion[2,3], Ignas Grigelionis[1], Gintaras Valušis[4] and Linas Minkevičius[1]

[1]*Department of Optoelectronics, Center for Physical Sciences and Technology, Saulėtekio Ave. 3, 10257 Vilnius, Lithuania.*

[2]*Faculty of Physics, Warsaw University of Technology, Koszykowa 75, 00662 Warsaw, Poland.*

[3]*Center for Advanced Materials and Technologies CEZAMAT, Warsaw University o Technology, Poleczki 19, 02-822 Warsaw, Poland.*

[4]*Institute of Photonics and Nanotechnology, Faculty of Physics, Vilnius University, Saulėtekio Ave. 3, 10257 Vilnius, Lithuania*

Email: rusne.ivaskeviciute@ftmc.lt

Terahertz (THz) radiation exhibits distinctive propagation properties, including penetration through dielectric materials opaque in the visible range [1], while remaining non-ionizing and suitable for biomedical and security applications. However, interaction with nonuniform or granular media induces strong scattering, degrading image quality. This is particularly problematic for optically thin or weakly absorbing samples, where conventional intensity-based imaging provides limited contrast. Coherent methods, such as holography [2], overcome these limitations by enabling phase retrieval, which is essential in highly scattering systems including powders, soils, and biological tissues.

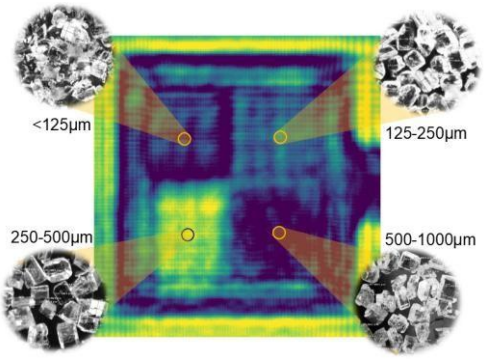


Fig. 1 Holographic reconstruction of amplitude. Insets depict the enlarged microscopic images of investigated grains.

In biological media, intrinsic microstructures and pathological changes (e. g., tumors or burn damage) introduce features often falling within the Mie scattering regime at THz frequencies [3], emphasizing the importance of size-dependent scattering analysis.

Here, THz scattering in granular media is investigated using digital THz holography supported by numerical modeling. The 4-phase-shift (4PS) method reveals a systematic increase in phase with particle size. In contrast to direct imaging, which fails under strong scattering, the 4PS approach reconstructs the complex wavefront via interference with a reference beam. This allows visualization of the transition from smooth effective-index variations in subwavelength structures to localized phase distortions as particle size approaches the wavelength. Experiments with size-classified sugar samples confirm a clear correlation between grain size and scattering behavior, demonstrating the effectiveness of digital THz holography for heterogeneous media characterization.

REFERENCES

[1] S. Sahin, N. K. Nahar and K. Sertel; *J. Infrared Millim. Teraherz Waves* **40** (2019) pp. 557-573.

[2] R. Ivaškevičiūtė-Povilauskienė, I. Grigelionis, A. Siemion, D. Jokubauskis, K. Ikamas, A. Lisauskas, L. Minkevičius and G. Valušis; *IEEE Transactions on Terahertz Science and Technology* **14** (2024) pp. 568-578. [3] K. Xu and M. Hassan Arbab; *Biomed Opt Express* **15** (2024) pp. 2328-2342.

S4-I3

Deep Strong Light-Matter Coupling in Landau-Polaritons

Dmitriy Yavorskiy[1,2], David Hagenmuller[3], Noureddine Charrouj[1], Yurii Ivonyak[1,2], Alexander Kazakov[4], Yanko Todorov[5], Wojciech Knap[1,2], Marcin Białek[1,2]

[1]CENTERA Labs, Institute of High Pressure Physics, Polish Academy of Sciences, Warsaw, 01142, Poland.

[2]CENTERA, CEZAMAT, Warsaw University of Technology, Warsaw, 02-822, Poland.

[3]Institut de Physique et Chimie des Materiaux de Strasbourg, UMR 7504, Universite de Strasbourg and CNRS, Strasbourg, 67000, France.

[4]International Research Centre MagTop, Institute of Physics, Polish Academy of Sciences, Warsaw, 02-668, Poland.

[5]Laboratoire de Physique et d''Etude des Materiaux, LPEM, UMR 8213, ESPCI Paris, Universite PSL, Paris, F-75005, France.

Email: marcin.bialek@unipress.waw.pl

Manipulation of light-matter interactions in the terahertz (THz) spectral range offers new opportunities for developing active photonic and optoelectronic devices. In particular, the strong- and ultra-strong-coupling regimes enable the formation of hybrid light-matter states whose properties can be engineered through cavity design and electronic structure control. Materials hosting relativistic quasiparticles are especially attractive in this context because their low effective masses can significantly enhance the coupling strength.

In this work, we investigate THz light-matter coupling in bulk $Hg_{0.85}Cd_{0.15}Te$, a narrow-gap semiconductor supporting three-dimensional Kane fermions. By integrating the material into a Fabry-Perot resonator and performing magneto-THz spectroscopy, we observe the formation of Landau polaritons over a broad range of magnetic fields and carrier densities. The exceptionally low cyclotron mass of Kane fermions enables coupling strengths that extend from the strong-coupling regime deep into the deep-strong-coupling regime, with a normalized coupling ratio exceeding 1.6. The hybridized polaritonic modes remain clearly observable up to and beyond room temperature, demonstrating the robustness of the phenomenon under technologically relevant operating conditions.

The experimental results are supported by a gauge-invariant microscopic theory that accurately reproduces the observed polariton dispersion and coupling behavior. Beyond the fundamental interest in extreme cavity quantum electrodynamics, our findings establish $Hg_{0.85}Cd_{0.15}Te$ as a promising platform for cavity-engineered THz functionalities. The demonstrated combination of giant coupling strength, tunability, and room-temperature operation opens prospects for next-generation THz photonic components, including tunable modulators, detectors, non-linear devices, and polaritonic architectures based on semiconductor materials with relativistic electronic spectra.

REFERENCES

[1] D. Yavorskiy, D. Hagenmuller, N. Charrouj, Y. Ivonyak, A. Kazakov, Y. Todorov, W. Knap, M. Bialek. arXiv:2604.28042 (2026).

SESSION 5:

Novel Materials 2: Metamaterials

S5-PL
Automated Deep Learning Inverse Design of Artificial Electromagnetic Materials

Willie J. Padilla[1]

[1]*Electrical and Computer Engineering, Duke University, Durham, North Carolina, USA*
Email: willie.padilla@duke.edu

Research on artificial electromagnetic materials (AEMs) including metamaterials, metasurfaces, photonic crystals, and plasmonics has historically utilized computational electromagnetic solvers to obtain optimized designs. More recently, numerical techniques have been augmented by deep learning approaches for AEM design as both forward and inverse processes. [1] We overview the theory and application of artificial intelligence applied to AEM design and research. Special emphasis is placed on recent developments of agentic frameworks capable of automating the design process and permitting these systems to function as digital researchers. [2]

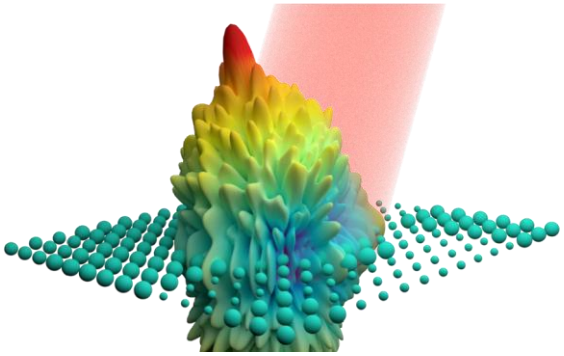


Fig. 1 A deep learning designed metasurface operating in the infrared wavelength regime.

REFERENCES

[1] J. M. Malof, S. Ren, and W. J. Padilla, “Forward and inverse design of artificial electromagnetic materials,” in Advances in Electromagnetics Empowered by Artificial Intelligence and Deep Learning, pp. 345–370 (Wiley, 2023).
[2] D. Lu, J.M. Malof, and W.J. Padilla, An Agentic Framework for Autonomous Metamaterial Modeling and Inverse Design, ACS Photonics **12**, (2025) pp. 6071-6080.

S5-I1
Terahertz Optical-Digital Neural Network Imaging

Shang-Hua Yang[1,2]

[1]*Department of Electrical Engineering, National Tsing Hua University, Hsinchu, Taiwan*
[2]*THz Optics & Photonics Center, National Tsing Hua University, Hsinchu, Taiwan*
Email: shanghua@ee.nthu.edu.tw

Terahertz (THz) band has recently had significant attention due to its exceptional capabilities in non-invasive, non-destructive sensing and imaging applications [1-3]. However, current THz imaging systems face substantial challenges due to hardware limitations, leading to information loss and reduced imaging throughput during data digitization and information extraction. To overcome these challenges, we propose a hybrid compressive optical–digital neural network that enables both real-time THz imaging and precise object information extraction. This approach utilizes a physical encoder, an optical neural network (ONN), to transform and reduce the dimensionality of physical signals, effectively compressing them to fit the physical constraints of THz sensor arrays. After the compressed signals are captured and digitized by the THz sensor array, a jointly trained digital neural network (DNN) reconstructs the signals into their desired or original form. Our proposed THz ONN–DNN computational imaging system demonstrates enhanced imaging quality, an expanded field of view with a lens-free system, diffraction-free imaging, and real-time THz video capture at 2 frames per second without requiring a graphics processing unit. Furthermore, the end-to-end optimization of the hybrid architecture allows the system to maintain high fidelity even under low signal-to-noise ratio (SNR) conditions, a common bottleneck in THz sensing. By offloading the primary computational burden to the passive optical layer, we achieve a significant reduction in digital post-processing latency and power consumption. Experimental results confirm that the system successfully identifies complex spatial features across a variety of material substrates, providing a scalable solution for high-throughput security screening and industrial quality control. This work establishes a new paradigm for THz wave modulation, demonstrating that the synergy of wavefront engineering and deep learning can circumvent traditional hardware boundaries, paving the way for compact, edge-deployable THz intelligent vision systems.

REFERENCES

[1] G. C. Walker, E. Berry, N. N. Zinov’ev, A. J. Fitzgerald, R. E. Miles, J. M. Chamberlain, and M. A. Smith, Medical Imaging 2002: Physics of Medical Imaging, 4682 (SPIE, 2002), p. 683.
[2] E. Berry, J. Biol. Phys. 29, 263 (2003).https://doi.org/10.1023/a:1024461313486 [3] R. H. Clothier and N. Bourne, J. Biol. Phys. 29, 179 (2003).

S5-I2

Recent Advances in Metasurface-based Optics for THz Imaging Systems

Vladislovas Čižas[1], Kasparas Stanaitis[1], Rusnė Ivaškevičiūtė-Povilauskienė[1], Ignas Grigelionis[1] and Linas Minkevičius[1]

[1]*Department of Optoelectronics, Center for Physical Sciences and Technology, Saulėtekio ave. 3, Vilnius, Lithuania.*
Email: linas.minkevicius@ftmc.lt

The terahertz (THz) frequency range is emerging as a key enabler for next-generation wireless communications, sensing, and imaging systems due to its large available bandwidth and unique interaction with matter. However, practical implementation remains challenging due to high propagation losses, atmospheric absorption, alignment sensitivity, and the limited availability of compact, efficient, and “easy to fabricate” beam-control components. Metasurface-based optics have already attracted attention as a promising alternative to conventional refractive and reflective elements, offering ultrathin, lightweight, and customizable wavefront manipulation capabilities [1-4].

This contribution will highlight the current state and the recent achievements of the beam-shaping optics for THz and sub-THz frequencies. Recent developments have demonstrated that carefully engineered metasurfaces can simultaneously manipulate transmitted and reflected wavefronts, enabling beam steering, focusing, and structured beam generation within a single ultrathin device. Experimental studies in the sub-THz frequency range reveal that laser-fabricated metallic metasurfaces can be successfully integrated into various imaging systems, such as single-pixel direct or homodyne imaging, providing enhanced functionality while maintaining performance comparable to systems equipped with classical beam-shaping components. Dual-mode operation (reflection and transmission modes), as well as Gaussian and Bessel-beam-forming structures, will be presented and discussed. Such unique functionality, attributed to metasurface-based structures, is particularly attractive for non-line-of-sight communication links, beam routing, multi-channel architectures, and compact imaging systems. Finally, the potential of higher-order resonant modes to enable operation at increasingly higher THz frequencies without demanding prohibitively small fabrication features will be outlined.

REFERENCES

[1] Ivaškevičiūtė-Povilauskienė, Rusnė, et al. *Light: Science & Applications* 11.1 (2022) p. 326.
[2] Cizas, Vladislovas, et al. *ACS Photonics* 12.2 (2025) pp. 636-647.
[3] Driukas, Simonas, et al. "*Optical Materials Express* 15.5 (2025) pp.1019-1031.
[4] Ivaškevičiūtė-Povilauskienė, Rusnė, et al. *Frontiers in Physics* 11 (2023) pp. 1196726.

S5-O1
Laser micromachining with a large-aperture metalens for a 1064-nm nanosecond laser

Shotaro Kawano[1], Kazuya Motohashi[2], Mizuho Matoba[1], Haruyuki Sakurai[1], and Kuniaki Konishi[1]

[1]*Institute for Photon Science and Technology, The University of Tokyo, Tokyo, 113-0033, Japan*
[2]*KOITO MANUFACTURING CO., LTD., Tokyo, 141-0001, Japan*
Email: kawano@ipst.s.u-tokyo.ac.jp

Laser micromachining with a micrometer-scale focal spot by an ultrashort-pulse laser is a powerful technique for fabricating electronic and optical devices because it combines broad material compatibility with non-contact processing [1-2]. In most implementations, tight focusing is achieved with objective lenses. However, conventional objective lenses are bulky and have short working distances, which constrain the optical layout and limit access to recessed regions or geometrically complex workpieces. Their limited incident pupil diameter further restricts the use of high-intensity ultrashort-pulse lasers under practical damage-threshold constraints.

Metalenses are planar optical elements that control wavefronts through sub-wavelength structures. They have recently been developed and are expected to serve as new functional focusing lenses [3]. Because metalenses can be fabricated lithographically, they can integrate a

thin form and a large aperture within a single optical element. These features have motivated growing interest in their use for ultrashort-pulse laser processing [4]. However, it remains unclear whether they are applicable to 1-μm-band nanosecond laser sources, which are widely used in industrial laser processing. Here, we demonstrate laser micromachining using a large-aperture metalens for a 1064-nm nanosecond laser.

We designed and fabricated a metalens for 1064 nm light by integrating pillar and diffraction-grating structures, as shown in Fig. 1a. The metalens had a 22 mm aperture and an 11.5 mm working distance, corresponding to a numerical aperture of 0.7. Focusing measurement at 1064 nm yielded a focal spot diameter of 1.5 μm (FWHM). Figure 1b shows scanning electron microscope (SEM) images of micro-holes fabricated in silicon using 1064-nm, 10-ns laser pulses focused by the metalens and a commercial objective lens. The results indicate that the morphologies fabricated by the metalens are comparable to those obtained with the commercial objective lens. We also demonstrated logo patterning at recessed locations that are difficult to access with a conventional objective lens by engraving the logo on the camera sensor plane inside a package, as shown in Fig. 1c. These results demonstrate that large-aperture metalenses are promising focusing elements for laser micromachining.

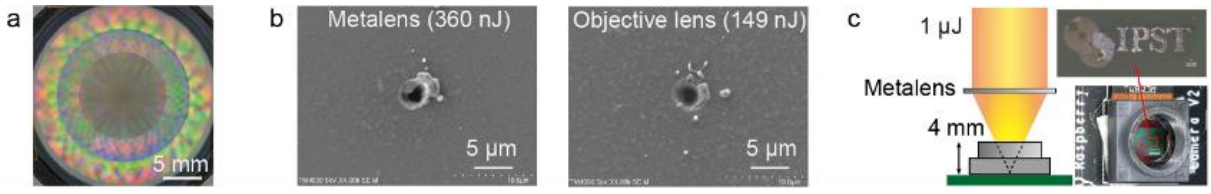


Figure 1: a, Optical microscope image of the fabricated metalens. b, SEM images of fabricated micro-holes. c, Logo patterning on the camera sensor surface inside the package.

REFERENCES

[1] K. Sugioka and Y. Cheng, Light Sci. Appl. **3**, e149 (2014). [2] X. Wang *et al.*, Opt. Laser Technol. **135**, 106687 (2021). [3] M. Khorasaninejad and F. Capasso, Science **358**, eaam8100 (2017). [4] Y. C. Peng *et al.*, Nano Lett. **25**, 3141 (2025).

S5-O2

Control of polarization ellipticity of THz radiation with ultrathin metamaterial.

Aleksandr Saushin[1], Mizuho Matoba[2], Aadya Menon[1], Deborah Adigun[1], Esko Kauppinen [3], Kuniaki Konishi[2], Polina Kuzhir[1] and Georgy Fedorov[1]

[1] *University of Eastern Finland, Yliopistokatu 7, Joensuu, 80101 Finland.*
[2]*University of Tokyo, 7-3-1 Hongo Bunkyo-ku, Tokyo, 113-0033 Japan.*
[2]*Aalto University, Otakaari 1 B, Espoo, 02150 Finland.*
Email: alekssau@uef.fi.

THz radiation has got growing importance for industry last decades because of useful combination of properties especially for biomedical diagnostics and nondestructive testing. Additional data can be extracted from THz imaging due to polarization state of THz beam [1]. Polarization spectroscopy make new demands to optical components of THz setups. In additional to lens and mirrors, THz setup should include components for polarization control which still remains challenging. Ordinary, THz polarization metamaterials work similarly to visible range components where birefringence is provided which helps them to achieve high efficiency.

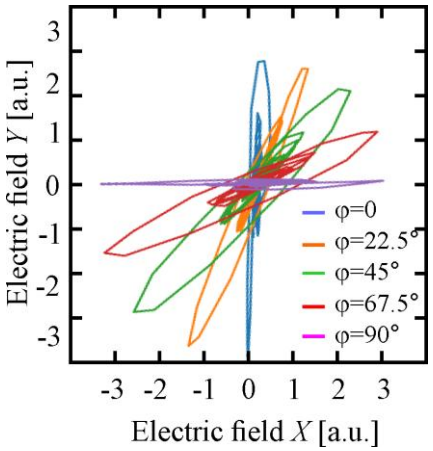


Fig. 1 Polarization state evolution of the radiation passed through a sample.

However, since wavelength of THz radiation starts from 30 μm, for THz range typical metamaterials have requirement to be hundreds of micrometers in thickness to be able change polarization state effectively. It limits their application and fabrication issues to be resolved appears. That is why industry is interested in development ultrathin structures providing polarization control in THz range.

In this work we demonstrate polarization conversion of THz radiation in a broad spectral range. For the demonstration we fabricated THz metamaterial stripe samples with different parameters made of carbon nanotube (CNT) film (100 nm thickness) applied to silicon substrate. For experiments we used time domain spectrometer using electrooptic sampling with polarization modulation of probe pulses which allows highly precise and accurate terahertz polarization measurements [2]. We analyzed the polarization state of THz waves passed through the samples and observed transformation of linearly polarized THz wave into elliptically polarized one at different angles φ between plane of polarization and CNT stripes. Fig. 1 shows polarization state evolution of the radiation passed through a sample demonstrating changing of ellipticity of polarization depending on φ. The results open way for developing of ultrathin THz devices for polarization control in THz spectrometry and THz imaging.

REFERENCES

[1] A. Moriwaki; M. Okano and Sh. Watanabe, *APL Photonics* **2**, (2017) pp. 106101
[2] N. Nemoto, T. Higuchi, N. Kanda, K. Konishi and M. Kuwata-Gonokami, *Optics express* **22**(*15*) (2014) pp. 17915

SESSION 6:

Quantum Materials and Technologies

S6-I1

Ultrafast, low-noise, THz graphene photodetectors and applications in quantum science

Miriam Serena Vitiello

NEST, National Research Council CNR-NANO and Scuola Normale Superiore, Piazza San Silvestro 56127, Pisa, Italy

Bi-dimensional nano-materials and related heterostructures are establishing themselves as intriguing material systems for the development of electronic, photonic and plasmonic quantum devices with properties that can be engineered “from scratch”. Their peculiar band-structure and electron transport characteristics, which can be easily manipulated via layer thickness control, indeed suggest they could also form the basis for a new generation of high-performance devices operating in the Terahertz frequency range (1-10 THz) of the electromagnetic spectrum.

In this talk, I will review recent advances in the design and realization of state-of-the-art THz photothermoelectric high-speed, low noise detectors based on two-dimensional materials and related heterostructures with a focus on the role of material and cavity engineering in optimizing device performance, and the current challenges toward scalable and integrated THz technologies.

Finally, I will discuss emerging perspectives for the use of these platforms in quantum science, with a focus on their potential impact on future quantum sensing and opti communication architectures, where fast, sensitive, and compact THz detection may provide new functionalities and operational regimes.

REFERENCES

[1] L. Shi, et al. Small Methods, e70657 (2026).
[2] L Shi, et al. Small Science 6 (4), e202500654 (2026).
[3] L Viti, et al. Small Methods 9 (11), e70055 (2025).
[4] L Viti, et al. Nano Letters 25 (15), 6005-6012, (2025).
[5] L Viti, et al. Advanced Optical Materials 13 (4), 2402100 (2025).
[6] A Sorgi, et al. Laser & Photonics Reviews 19 (6), 2301082 (2025).

S6-I2

Characterizing the electronic structure of quantum defects in semiconductors using time-resolved spectroscopy

Ronald Ulbricht

Max Planck Institute for Polymer Research, Ackermannweg 10, Mainz, Germany

ulbricht@mpip-mainz.mpg.de

Wide-bandgap semiconductors like diamond and silicon carbide (SiC) are a leading solid-state platform for quantum technologies because they can host optically active point defects ("color centers") whose electronic structure enables optical spin initialization and readout schemes, as well as robust operation across a broad range of environments. Nowadays often called "quantum defects", these color centers have found widespread use cases such as quantum sensing and computing. Among them, the nitrogen-vacancy (NV) center in diamond is the most well-established system that is already utilized by several companies and startups for quantum-technology applications.

The particular spin-optical properties of quantum defects are defined by specific *intrinsic* relaxation channels occurring after photoexcitation that enable methods such as optically detected magnetic resonance (ODMR). In actual devices, defects do not exist in isolation but can interact with the host material and other defects through processes like photoionization and tunneling. These *extrinsic* dynamics lead to intricate interactions that alter important defect parameters such as their charge state.

I will give an overview on how we use time-resolved spectroscopy techniques to characterize bulk ensembles of quantum defects with respect to their intrinsic and extrinsic photodynamics. We use transient absorption (TA) spectroscopy to characterize intrinsic photodynamics by probing localized electronic transitions of the defect and time-resolved Terahertz (THz) spectroscopy as an all-optical probe for charge carrier dynamics in the electronic bands of the host [1]. Examples include quantum defects in diamond, SiC and hexagonal boron nitride [2-4].

References

[1] R. Ulbricht, E. Hendry, J. Shan, T. F. Heinz, and M. Bonn. Carrier dynamics in semiconductors studied with time-resolved terahertz spectroscopy. Reviews of Modern Physics, 83(2):543–586, 2011

[2] A. T. Younesi, M. T. Luu, C. Linderälv, V. Žalandauskas, M. E. Bathen, N. T. Son, T. Ohshima, G. Thiering, L. Razinkovas, and R. Ulbricht, Unraveling the electronic structure of silicon vacancy centers in 4H-SiC, Adv. Funct. Mater., e76183, 2026. https://doi.org/10.1002/adfm.76183

[3] A. Alkauskas, C. G. Van de Walle, L. Razinkovas, and R. Ulbricht. Charge state equilibration of nitrogen-vacancy center ensembles in diamond: The role of electron tunneling. arXiv preprint arXiv:2512.00952, 2025.

[4] M. T. Luu, A. T. Younesi, and R. Ulbricht. Nitrogen-vacancy centers in diamond: discovery of additional electronic states. Materials for Quantum Technology, 4(3):035201, 2024.

S6-O1

Laser-Induced Room-Temperature Single-Photon Emission from Defect Centers in Hexagonal Boron Nitride

Ifra Bibi*, Vakaris Šilys, Viktorija Nargelienė, Julius Janušonis, Edgaras Markauskas, Danielis Rutkauskas, Tadas Paulauskas

Department of Optoelectronics, Center for Physical Sciences and Technology, Sauletekio al 3, Vilnius LT-10257, Lithuania

*Email: ifra.bibi@ftmc.lt

Single-photon emitters (SPEs) have attracted significant attention owing to their central role in quantum photonic technologies, including secure quantum communication, quantum information processing, and advanced sensing applications. Among solid-state platforms, hexagonal boron nitride (hBN) has emerged as a promising host material owing to its wide bandgap, two-dimensional layered structure, and ability to support bright quantum emitters operating at room temperature [1]. Nevertheless, the controlled generation of high-purity single-photon emitters at predefined locations remains a significant challenge for scalable quantum photonic applications.

Here, we investigate the formation of defect-based SPEs in mechanically exfoliated hBN through localized femtosecond laser processing followed by thermal annealing. The highly nonlinear interaction between ultrashort laser pulses and the hBN lattice enables spatially selective defect engineering with minimal impact on the surrounding material. Laser-modified regions exhibit bright and localized fluorescence, indicating the successful formation of optically active defect centers. Spectroscopic analysis reveals narrow emission peaks characteristic of defect-mediated optical transitions in hBN from UV to near IR region. Time-resolved measurements provide insight into the excited-state dynamics of the generated emitters, while Hanbury Brown and Twiss interferometry confirms their quantum nature through pronounced antibunching behavior with $g^2(0) < 0.5$. The influence of laser processing parameters and post-annealing conditions on emitter formation and optical performance was systematically investigated, demonstrating the importance of defect activation and local lattice modification in achieving stable single-photon emission.

The demonstrated approach provides a versatile route toward the deterministic fabrication of roomtemperature SPEs in hBN and offers a scalable pathway for integrating quantum light sources into photonic architectures. These findings advance the understanding of laser-induced defect engineering in two-dimensional materials and support the development of hBN-based platforms for future quantum communication systems and integrated quantum photonic devices.

REFERENCE

[1] Paulauskas, T., Janušonis, J., Markauskas, E., Nargelienė, V., Šilys, V., Bibi, I., ... & Talaikis, M. (2026). Laser direct writing and Raman Stokes contrast screening of quantum emitter sites in hBN. *Discover Nano*, *21*(1), 85.

S6-O2

Temperature-dependent fluorescence of color centers in diamond structures

Paulius Rindzevičius[1], Elena Filonenko[2], Sergei Malykhin[2], Polina Kuzhir[2] and Renata Karpicz[1]

[1]*Department of Molecular Compound Physics, Center for Physical Sciences and Technology, Lithuania.*
[2]*Department of Physics and Mathematics, Faculty of Science, Forestry and Technology, University of Eastern Finland, Finland.*
Email: paulius.rindzevicius@ftmc.lt.

Diamond color centers are promising in quantum and optical biosensing due to diamond's biocompatibility and easy functionalization [1]. NV, SiV and GeV color centers are investigated for their potential in quantum and optical sensing of magnetic fields, electric fields and temperature. However, there are hundreds of other diamond color centers in diamond [2]. They are interesting because of their unknown fundamental properties and potential applications in biosensing. In this work, fluorescence behavior of 389 nm, 468 nm and NV^0 color centers in diamond microneedles was investigated in the biological temperature range (298 K – 338 K).

Conducted experiments revealed 389 nm, 468 nm and NV^0 color centers in diamond microneedles. 468 nm color center was not observed in a bulk diamond sample. 389 nm and 468 nm color centers in diamond microneedles exhibit a linear fluorescence intensity dependence on temperature. However, the 389 nm color center in bulk diamond showed a nonlinear fluorescence quenching behavior. In case of NV^0 color center, the nonlinear fluorescence intensity dependence on temperature was observed. Most investigated color centers did not show a significant fluorescence lifetime temperature dependence, however, lifetimes, measured at 468 nm color center phonon sideband show a linear decrease with increasing temperature. Another parameter that could be useful in optical thermometry and was extracted from the measured spectra is ZPL and PSB intensity ratio, which changes with increasing temperature in case of NV^0 color center.

The observed changes in fluorescence spectra and kinetics (changes in fluorescence intensity, ZPL and PSB intensity ratio, and fluorescence lifetimes) demonstrate the potential for all-optical temperature sensing, while also provide new fundamental insights into 389 nm and 468 nm color centers in diamond.

Acknowledgements: This work was supported by QuantERA project EXTRASENS through Lithuanian Research Council (No. S-QUANTERA-24-1) and Horizon Europe MSCA FLORIN (No. 101086142).

REFERENCES

[1] J. Zhang, L. Ma, Y. Hou et al.; *Advanced Drug Delivery Reviews* **221** (2025) 16 p.
[2] A. M. Zaitsev, *Optical Properties of Diamond: a Data Handbook*, 3rd ed., Bochum: Springer (2000) 486 p.

S6-O3

Ab initio emission lineshape modeling of color centers in semiconductors

Rokas Silkinis and Lukas Razinkovas

Department of Fundamental Research, Center for Physical Sciences and Technology (FTMC), Saulėtekio al. 3, LT-10257, Vilnius, Lithuania

Email: rokas.silkinis@ftmc.lt

Deep-level point defects in semiconductors have emerged as versatile platforms for quantum sensing, communication, and information processing. Identifying and characterizing these centers requires reliable theoretical methods to determine their electronic and optical signatures. In this work, we present high-resolution calculations of the emission lineshapes for a handful of technologically relevant color centers using a force-constant embedding methodology [1]. This approach exploits the short-range nature of interatomic forces to describe the vibrational structure and electron–phonon coupling, enabling the simulation of defects in the dilute limit entirely from first principles.

However, standard density functional theory (DFT) often struggles with defects exhibiting complex electronic structures or non-adiabatic vibronic interactions. By combining the embedding methodology with specialized computational strategies, we demonstrate that it is possible to accurately reproduce experimental spectral fingerprints that fall outside the reach of standard adiabatic frameworks. Our results underscore the need for new methodologies to advance predictive modeling and the discovery of quantum point defects in semiconductor materials.

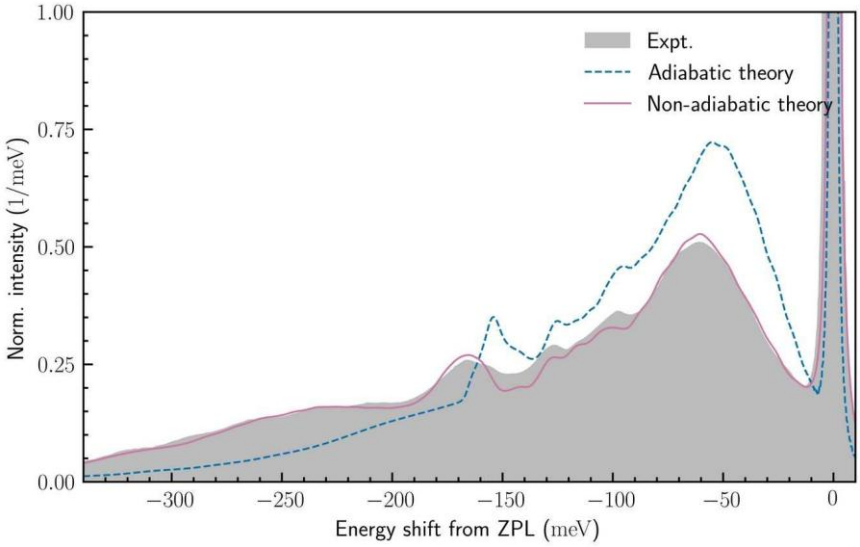


Figure 1. Calculated emission lineshapes of the NiV center in diamond obtained using adiabatic and non-adiabatic theories. Experimental lowtemperature data are taken from [2].

REFERENCES

[1] L. Razinkovas, M. W. Doherty, N. B. Manson, C. G. Van de Walle, and A. Alkauskas, Vibrational and vibronic structure of isolated point defects: The nitrogen-vacancy center in diamond, Phys. Rev. B 104 (2021) pp. 045303. [2] A. T. Collins and P. M. Spear, The 1.40 eV and 2.56 eV centres in synthetic diamond, J. Phys. C: Solid State Phys. 16 (1983) pp. 963-973.

SESSION 7:

Novel Optoelectronic Systems

S7-I1

Terahertz systems and components in industry

Erik Hagen Waller, Raphael Hussung, Shiva Mohammadzadeh, and Maris Bauer

Department of Materials Characterization and Testing, Fraunhofer Institute for Industrial Mathematics ITWM, Fraunhofer-Platz 1, 67663 Kaiserslautern, Germany
Email: erik.waller@itwm.fraunhofer.de

Terahertz technology has reached a level of maturity that enables its successful deployment in industrial environments. Advances in system core components – sources, detectors, and quasi-optical elements – and measurement techniques – time-domain and frequency-domain approaches of signal generation, detection, acquisition and processing – have led to increasingly efficient and compact systems at cost levels that make industrial applications financially viable.



Different systems developed at Fraunhofer ITWM for industrial applications.

At Fraunhofer ITWM, research and development focuses on customized terahertz systems for applications, such as layer thickness measurement, material characterization, and nondestructive testing (NDT) [1]. Both terahertz time-domain spectroscopy (TDS) and all-electronic frequency-modulated continuous wave (FMCW) radar systems are employed for defect detection and quality inspection, complemented by recent optoelectronic frequency-domain approaches [2]. Beyond the measurement hardware itself, system integration at ITWM addresses typical challenges of industrial environments including integration into production lines, matching process speeds, and ensuring system robustness. We present several projects in which terahertz systems have already been successfully deployed in industrial processes.

One key enabler for next-generation customized systems operating in the EHF and THz frequency range are high-performance, compact components. In this context, we introduce results from our TERA-AMP project – a collaboration between Fraunhofer ITWM and Düsenfabrik Leipold GmbH – which pioneers the use of 3D laser microprinting to fabricate interface structures between waveguides, microstrip lines, MMICs, and free space. This additive manufacturing approach enables independent sourcing of MMICs with arbitrary geometry, the integration of additional functionality directly into printed interface components, a massive reduction of manual assembly steps, and rapid progression from design to ready-to-use components.

REFERENCES

[1] F. Ellrich et al., *Journal of Infrared, Millimeter, and Terahertz Waves* (**41**), pp. 470–489, 2019.
[2] S. Mohammadzadeh, M. Bauer, A. Keil, and F. Friederich, in *Optica Sensing Congress 2024 (AIS, LACSEA, Sensors, QSM),* p. AM2A, 2024,.

S7-I2

Fabrication of anti-reflective moth-eye structures using ultrashort-pulse laser processing and their application to radio astronomy observations

Kuniaki Konishi

Institute for Photon Science and Technology, The University of Tokyo, 113-0033, Japan
Email: kkonishi@ipst.s.u-tokyo.ac.jp

In radio astronomy, suppressing surface reflection from optical components such as lenses, windows, and filters is a fundamental yet crucial issue for improving signal detection sensitivity. This is especially important in the sub-terahertz to terahertz frequency range, where typical transparent materials have high refractive indices and suffer from substantial Fresnel reflection. Moth-eye surface structures are promising because they provide a gradual effective refractive-index transition between air and the substrate, enabling broadband anti-reflection without multilayer coatings. However, moth-eye structures for these wavelengths require submillimeter-scale heights and periods, which are difficult to fabricate by conventional lithography or mechanical machining, especially over large areas and on various materials. In this talk, I report the fabrication of such structures using ultrashort-pulse laser processing, a maskless direct-writing technique that enables three-dimensional surface structuring over macroscopic areas.

By controlling the laser irradiation and scanning conditions, we formed moth-eye structures with suitable height, pitch, and arrangement for sub-terahertz and terahertz optics (Fig. 1) [1-3]. The fabricated structures effectively reduced reflection and enhanced transmission over broad frequency ranges relevant to astronomical observations. Importantly, these laser-fabricated moth-eye structures have already been implemented in optical components used at a radio astronomy observatory, demonstrating their practical applicability beyond laboratory-scale experiments [4-5]. We also found that, when combined with a thin absorbing film, the structures can function as ultrabroadband absorbers [6]. Because the anti-reflective function is integrated directly into the substrate surface, moth-eye structures offer high robustness under vacuum and cryogenic environments, avoiding failures associated with multilayer coatings. These results demonstrate that ultrashort-pulse laser processing can overcome a key fabrication bottleneck and provide a promising platform for broadband and durable optical components for next-generation high-sensitivity radio astronomy instruments.

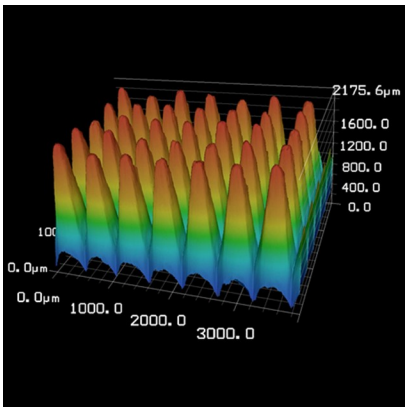


Fig. 1. Laser microscope image of a moth-eye structure fabricated by ultrashort-pulse laser processing.

REFERENCES

[1] H. Sakurai et al.; *OSA Continuum* **2** (2019) pp. 2764-2772.
[2] R. Takaku et al.; *Journal of Applied Physics* **128** (2020) 225302.
[3] R. Koike, M. Matoba, S. Kawano, H. Sakurai, K. Konishi, and N. Mio; *Applied Optics* **63** (2024) pp. 7442-7446.
[4] R. Takaku et al.; *Optics Express* **29** (2021) pp. 41745-41765.
[5] R. Takaku et al.; *Applied Optics* **65** (2026) pp. 4579-4587.
[6] Y. Hakamada et al.; *Advanced Optical Materials* **13** (2025) 2500948.

S7-O1

Charge Carrier and Spin Diffusion in a Polycrystalline and Single Crystal Lead Halide Perovskite Semiconductor

Kazimieras Nomeika[1,2], Justina Jovaišaitė[1], Ramūnas Aleksiejūnas[2], Xinwen Zhang[3], Duong Nguyen Minh[3], Md Azimul Haque[3,4], Matthew C. Beard[3,4], Joseph M. Luther[3,4], Justin C. Johnson[3,4]

[1]*Light Conversion Ltd., Keramikų str. 2B, LT-10233 Vilnius, Lithuania*
[2]*Vilnius University, Faculty of Physics, Institute of Photonics and Nanotechnology, Saulėtekio Ave. 3, LT-10257 Vilnius, Lithuania*
[3]*National Laboratory of the Rockies, 15013 Denver West Pkwy, Golden, CO 8040, USA*
[4]*RASEI, University of Colorado, Boulder, CO 80309, USA*
Email: kazimieras.nomeika@lightcon.com; kazimieras.nomeika@ff.vu.lt

Light-induced transient gratings (LITG) spectroscopy is a powerful technique for probing carrier transport dynamics in semiconductors. Despite its complexity, the non-destructive and contactless nature, along with simultaneous multi-parameter acquisition renders the technique an attractive alternative to others, where magnetic fields, high spatial resolution, or cryogenic conditions may be needed. In this work, we employ the user-friendly HARPIA-TG spectrometer (*Light Conversion*) to investigate both carrier and spin transport in the halide perovskite semiconductor $FA_{0.95}Cs_{0.05}PbI_3$ with varying degrees of crystallinity. Population gratings generated with parallel-polarized excitation pulses probe carrier diffusion and recombination, while cross-polarized excitation produces spin gratings that enable direct observation of spin transport and relaxation dynamics.

Carrier dynamics measurements yield ambipolar diffusion coefficients on the order of 1 cm^2/s (Fig. 1(a)) and diffusion lengths approaching 1.5 μm in single crystals, with strong attenuation in polycrystalline films due to grain boundary barriers (Fig. 1(b)). In contrast, spin grating measurements reveal diffusion coefficients exceeding 100 cm^2/s, indicating spin transport occurring on timescales nearly two orders of magnitude faster than population diffusion at room temperature. The substantial enhancement in spin transport suggests a mechanism involving exchange-mediated interactions and doping-assisted effects that facilitate ultrafast spin propagation prior to picosecond-order relaxation. These results demonstrate the capability of a single experimental setup to probe both carrier and spin dynamics, offering new insight into spin motion in metal–halide perovskites and highlighting their potential for spintronic applications.

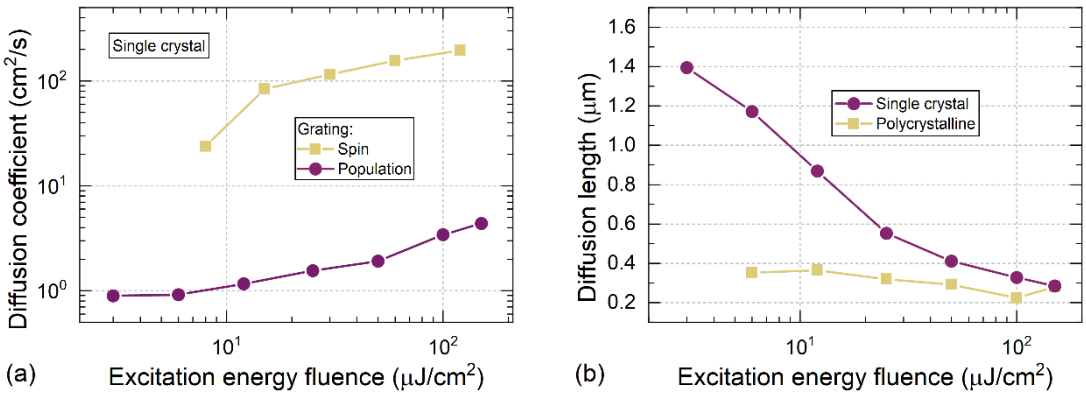


Fig. 1 Diffusion coefficient in a single crystal acquired by probing spin and population gratings (a). Carrier diffusion length in a single crystal and a polycrystalline film (b).

S7-O2

Narrowband picosecond laser light sources for wide infrared spectral range based on nonlinear light conversion

R. Januškevičius, R. Antanavičius, A. Alesenkov, T. Kašponas, M. Grishin, V. Petrauskienė, A. Michailovas, R. Kananavičius, J. Lukošiūnas
Ekspla Ltd., Vilnius, Lithuania

Widely tunable, narrowband mid-infrared coherent sources realised using optical parametric oscillators play an essential role in spectroscopic research. A part of the mid-infrared spectral region represents the “fingerprint range” of solid-state materials; therefore, a narrow bandwidth is a particularly important feature. Typically, a bandwidth of 2–5 cm^{-1} is required to satisfy the necessary resolution for spectroscopy of solids. Only a limited number of laser sources can generate such a narrowband radiation.

The biggest challenge is meeting customer’s needs by providing a set of high-performance parameters from a single device simultaneously: a broad spectral range, high spectral resolution, fast wavelength tuning, a high repetition rate, and a stable beam direction. Ideally, all these features must be maintained throughout the entire spectral range of the laser source. The range of 540–750 cm^{-1} presents a specific challenge in achieving a reasonable output power and other parameters required for practical infrared spectroscopy. These capabilities are relevant for various spectroscopic applications, especially for scanning near-field optical microscopy (SNOM), for example, near-field fingerprint spectroscopy of 2D electron systems [1], near-field imaging of the hybrid plasmon-phonon polaritons [2].

This presentation will describe the architecture and applications of Ekspla broadly tunable commercial ns and ps laser sources operating from 1.4 μm to 18 μm based on Mid-IR nonlinear optical crystals. Ekspla developed Mid-IR laser series guarantee a spectral bandwidth of less than 4 cm^{-1} which is close to the Fourier-transform limit for ~8 ps pulse at 1064 nm. Advantages and limitations of these laser sources in different narrowband OPO setups will be presented.

These lasers can also have a second optically synchronised output channel to support scientific applications which need laser pulses in the different spectral ranges. The second optically synchronised output allows the laser to be used in nonlinear spectroscopy, such as Coherent Anti-Stokes Raman Spectroscopy (CARS), Sum Frequency Generation Spectroscopy (SFG).

REFERENCES

[1] J. Barnett *et al. Nat Commun* **16**, 4417 (2025). https://doi.org/10.1038/s41467-025-59633-1
[2] V. Janonis *et al*. *Materials* **18**, 2849 (2025). https://doi.org/10.3390/ma18122849

S7-O3

Imaging and Spectroscopy at 10nm Spatial Resolution using s-SNOM

Adrian Cernescu[1]

[1]*neaspec – attocube systems GmbH – Haar, Germany*

The performance of the next-generation electronic devices based on plasmonic nanomaterials is strongly influenced by the structure-function relationship. Scattering-type scanning near-field optical microscopy (s-SNOM) is the ideal technology to investigate such material systems at the nanoscale.

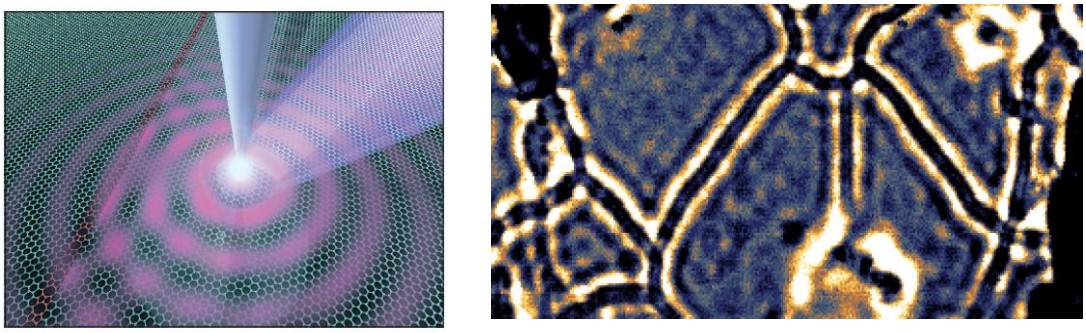


Figure 1 Left: Diagram of the Infrared nano-imaging experiment. Concentric circles illustrate plasmon waves launched by the illuminated tip. Right: Image of infrared amplitude recorded on a graphene 1x2 μm^2 area. This image shows a characteristic plasmon interference pattern close to graphene edges and grain boundaries.

s-SNOM combines the best of two worlds: (i) the high spatial resolution of Atomic Force Microscopy (AFM) and (ii) the analytical power of optical microscopy and spectroscopy. Achieving an unmatched spatial resolution below 10 nanometer this technology opens a new era for modern nano-analytical applications such as chemical identification, free-carrier profiling and plasmonic near-field mapping. Recent research highlights on graphene and other 2D materials include contact-free access to the local conductivity, the electron mobility, and the intrinsic electron doping by resolving propagating phonon- plasmon (Fig 1), exciton-polariton directly in space and time, at RT and cryogenic conditions (5K).

This talk will introduce the basic principles of near-field microscopy for imaging and spectroscopy with 10 nanometer spatial resolution, correlative measurement (optical, photocurrent and AFM) and address heir impact and key applications in the field of plasmonic materials.

SESSION 8:

Spectroscopy and Applications

S8-I1

High-resolution THz spectroscopy of the mesosphere and lower thermosphere of the Earth

Heinz-Wilhelm Hübers[1,2]

[1]*Deutsches Zentrum für Luft- und Raumfahrt, Institute of Space Research, Rutherfordstr. 2, 12489 Berlin, Germany*
[2]*Humboldt University Berlin, department of Physics, Newtonstr. 5, 12489 Berlin, Germany*
Email: heinz-wilhelm.huebers@dlr.de

The mesosphere and lower thermosphere (MLT) at altitudes from about 100 km to 250 km is are largely unexplored. Atomic oxygen is a key species in in this part of the atmosphere. It plays an important role for the chemistry and energy balance in the MLT region as well as for the deceleration of satellites and space debris in Low Earth Orbit (LEO). In particular because of the latter one there is an increasing interest in this part of the atmosphere. However, measurements of atomic oxygen are scarce, despite that is the most abundant species above about 150 km. The fine-structure transitions of atomic oxygen at 2.1 and 4.7 THz are particularly well suited for the observation of atomic oxygen [1, 2, 3]. The radiance of these transitions provides information about the number density, the linewidth provides information about the temperature, and the Doppler shift and line profile provide information about wind speed in the MLT.

Recently, atomic oxygen in the MLT has been measured with OSAS-B (Oxygen Spectrometer for Atmospheric Science on a Balloon), which is dual frequency, balloon-borne THz heterodyne spectrometer developed by DLR [3]. The spectrometer is optimized for measuring the 2.1-THz transition and the 4.7-THz transition of atomic oxygen. Both frequency bands rely on a superconducting hot electron bolometer mixer. At 2.1 THz the local oscillator is an amplifier-multiplier chain while at 4.7 THz it is a quantum-cascade laser. The design and performance of the OSAS-B dual frequency heterodyne spectrometer as well as results from measurement campaigns with OSAS-B flying on a stratospheric balloon at altitudes above 30 km will be presented. Finally, perspectives towards a satellite mission with a THz spectrometer for atomic oxygen will be discussed [4, 5].

REFERENCES

[1] H. Richter et al., “Direct measurements of atomic oxygen in the mesosphere and lower thermosphere using terahertz heterodyne spectroscopy,” Comm. Earth Environ., vol. 2, 19 (2021).
[2] H. Wiesemeyer et al., “First detection of the atomic 18O isotope in the mesosphere and lower thermosphere of Earth,” Phys. Rev. Res., vol. 5, 013072 (2023).
[3] M. Wienold et al., “OSAS-B: A balloon-borne terahertz spectrometer for atomic oxygen in the upper atmosphere,” IEEE THz Science and Technol., vol. 14, 327 (2024).
[4] P. Hansen et al., “Feasibility of a space-borne terahertz heterodyne spectrometer for atomic oxygen and temperature in the mesosphere and lower thermosphere”, Atmos. Meas. Tech., 18, 5749 (2025).
[5] ESA (2026), “Report for Mission Assessment. Earth Explorer 12 Candidate Mission Keystone”, European Space
Agency, Nordwijk, The Netherlands, ESA-EOPSM-KEYS-RP-2026, 142pp., doi:105281/zenodo.20543287

S8-I2

Saturation Spectroscopy of Rotational Transitions Toward the Molecular Clock Application

Koichiro Tanaka[1, 2]

[1] *RIKEN Center for Advanced Photonics, RIKEN, Wako, JAPAN*
[2] *HIKARI-COOL Kyoto, Institute for Advanced Study, Kyoto University, Kyoto, JAPAN*

Rotational transitions of polar molecules give rise to molecule-specific spectra in the terahertz (THz) region and have long been used in chemical analysis and the search for interstellar molecules. Most of these studies rely on linear absorption spectroscopy, where the absorption linewidth is dominated by Doppler broadening resulting from the thermal motion of the molecules. Since the rotational levels of molecules are not equally spaced, specific transitions can be isolated and treated as two-level systems. In addition, their transition frequencies are remarkably stable against external stimuli, such as electromagnetic fields, rendering them suitable candidates for frequency standards known as “molecular clocks.” Recently, the IMRA group demonstrated that employing a dual-wavelength Brillouin laser as the THz source—stabilized to the OCS rotational transition at 316 GHz—yielded a fractional frequency instability of $1.2 \times 10^{-12}/\sqrt{\tau}$ [1]. However, such approaches are fundamentally limited by the inevitable Doppler linewidth. One effective method to overcome this limit is saturation spectroscopy, such as Lamb-dip spectroscopy.

In this study, we quantitatively characterize the absorption saturation effect and determine the saturation parameters for rotational transitions in acetonitrile molecules. Furthermore, we discuss the potential application of Lamb-dip spectroscopy to frequency stabilization and the development of high-precision molecular clocks. Lamb-dip spectroscopy was performed using a frequency-stabilized sub-THz light source [2]. A typical Lamb-dip spectrum is shown in Fig. 1. From the fitting analysis, the transition frequency was determined with an accuracy of 10^{-9}.

Furthermore, we constructed a differential spectroscopy system and attempted to stabilize the frequencies of the free-running diode lasers used for difference-frequency generation in the sub-THz light source by using molecular rotational transitions. In the absence of the Lamb-dip (i.e., using the Doppler-broadened line), we achieved a frequency stability of 1.0×10^{-9} at an integration time of $\tau = 1$ s. We will also discuss the potential of using the Lamb-dip to further enhance frequency stability.

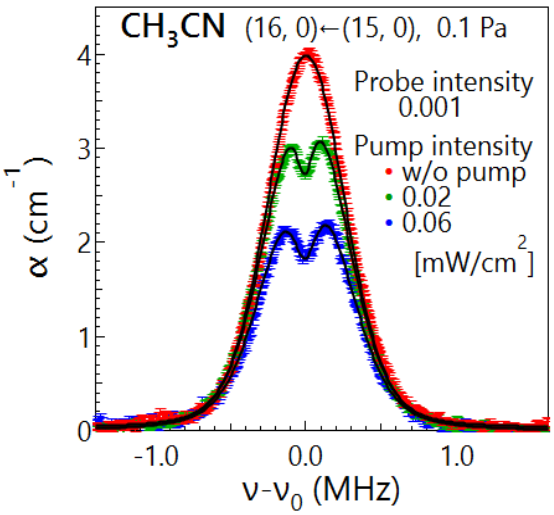


Fig. 1. Pump intensity dependence of Lamb-dip spectra of acetonitrile molecules at 0.1 Pa. υ_0 =294302.389 MHz.

REFERENCES

[1] J. Greenberg, B. M. Heffernan, W. F. McGrew, et al., “Dual wavelength Brillouin laser terahertz source stabilized to carbonyl sulfide rotational transition,” Nat. Commun. 16(1), 2411 (2025).
[2] K. Eguchi, T. Arikawa, H. Ito, and K. Tanaka, “Lamb-dip spectroscopy of rotational levels with photomixing terahertz emitter,” Opt. Express 33(14), 29442-29455 (2025).

S8-O1

Dual-mode Terahertz Time-Domain Spectroscopy for Versatile Characterization of Semiconductors

Chia-Ming Mai[1], Karthickraj Muthamalingum[2], Cheng-Siang Le[1], Zi-Xiang Liao[1], YuLin Yang[3], Chen-Peng Hsu[2], Hungyen Lin[4] and Shang-Hua Yang[1,3]

[1]*Institute of Electronic Engineering, National Tsing Hua University, Hsinchu City, Taiwan*
[2]*Electronics and Optoelectronics Research Laboratories, Industrial Technology Research Institute, Hsinchu County, Taiwan*
[3]*College of Semiconductor Research, National Tsing Hua University, Hsinchu City, Taiwan*
[4]*School of Engineering, University of Warwick, Coventry, United Kingdom*
Email: yms40736@gmail.com

Electrical characterization of semiconductors has long been critical for their quality assurance. Conventionally, these characterizations heavily rely on contact methods, such as Hall effect measurement[1]. Whilst mature, its contact nature greatly hinders the throughput and real-world applicability.

Contactless methods, for instance, terahertz (THz) spectroscopy, has been intensively investigated for electrical characterization of semiconductors. Much literature has demonstrated sensing of a broad variety of semiconductors with THz spectroscopy, including bulk substrates, thin films, stratified structures[2]. However, these measurements utilize single topology, and are dependent on task-specific designs.

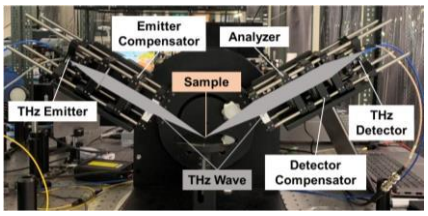


Fig. 1 Photo of the dual-mode THz spectrometer setup, allowing switching between transmission and ellipsometry modes

Thus, in this work, we proposed a dual-mode THz time-domain spectrometer, aiming to cater a greater variety of semiconductors. Attributed to its versatility, this instrument is capable of seamless switching between transmission (T-mode) and ellipsometry (E-mode) modes. In addition, a unified modeling based on optical transfer matrix method is developed, to extract the complex refractive indices of specific layer in given structures under both modes. Moreover, computational and instrumentational robustness of this method is discussed. Results are benchmarked against Hall effect measurement, to showcase its versatility and robustness.

Sample: n-type GaN on sapphire	**Sheet Resistivity** (Ω/sq)	**Concentration** (cm^{-3})	**Mobility** ($cm^2V^{-1}s^{-1}$)
THz Spectroscopy (T-mode)	9.332 ± 0.040	$(2.27 \pm 0.30) \times 10^{20}$	147.5 ± 11.0
Hall Measurement	9.075	2.80×10^{20}	123.3

Sample: ITO on glass	**Sheet Resistivity** (Ω/sq)	**Concentration** (cm^{-3})	**Mobility** ($cm^2V^{-1}s^{-1}$)
THz Spectroscopy (T-mode)	37.40 ± 0.32	$(2.03 \pm 0.39) \times 10^{20}$	53.1 ± 11.1
Hall Measurement	36.61	2.32×10^{20}	46.1

Sample: 2DEG in HEMT	**Sheet Resistivity** (Ω/sq)	**Concentration** (cm^{-2})	**Mobility** ($cm^2V^{-1}s^{-1}$)
THz Spectroscopy (E-mode)	350.5 ± 1.3	$(1.023 \pm 0.003) \times 10^{13}$	1741.7 ± 3.7
Hall Measurement	320.9	1.01×10^{13}	1930.0

REFERENCES

[1] Lindberg, O. Hall effect. Proc. IRE 40, 1414–1419 (1952).
[2] Lloyd-Hughes, J. & Jeon, T.-I. A review of the terahertz conductivity of bulk and nano-materials. J. Infrared Millim. Terahertz Waves 33, 871–925 (2012).

S8-O2

Development of a portable optoelectronic system for terahertz gas spectroscopy

Patricija Ivanauskaitė[1], Dovilė Čibiraitė-Lukenskienė[1,2], Domantas Vizbaras[2], Alvydas Lisauskas[1,2],

[1] *Department of Optoelectronics, Center for Physical Sciences and Technology, LT*
[2] *Institute of Applied Electrodynamics and Telecommunications (IAET), Vilnius University, LT*
Email: patricija.ivanauskaite@ftmc.lt

The terahertz (THz) band (0.1-10 THz) [1] enables high-resolution gas-phase spectroscopy because it coincides with rotational transitions of many polar molecules [2], allowing for precise “fingerprinting”. But current spectroscopic systems are often bulky, expensive and lab bound. To address portability need without losing sensitivity, this work focused on developing a portable optoelectronic spectroscopy system operating near 250 GHz.

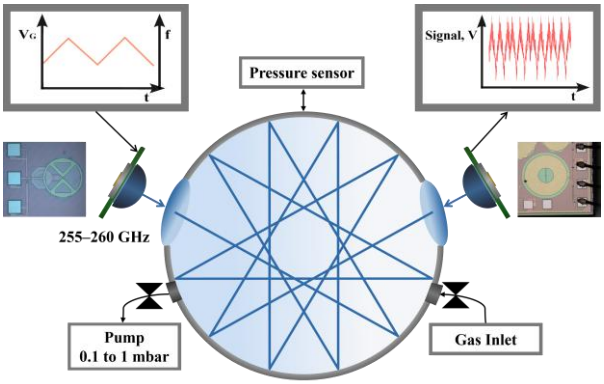


Fig. 1 Experimental spectroscopy setup employing CMOS-based emitter, detector, and a circular multipass gas cell.

The proposed system integrates a commercial complementary-metal-oxide-semiconductor (CMOS) based sub-THz emitter and a TeraFET (THz field-effect-transistor) detector (optopair) with a custom designed multipass gas cell (designed in collaboration with German Aerospace Center (DLR) and based on their design [3]). For optimal beam collimation and coupling into a cell, double-hyperbolic high-density polyethylene (HDPE) aspheric lenses (f=42 mm) were designed, and their focus was experimentally confirmed. The gas cell’s optical path length (OPL) was confirmed via frequency-modulated continuous wave (FMCW) radar technique to be 1.93 m (withing just ~1% of the 1.91 m from the theoretical model), while the cell had only 21.5 cm diameter. Proof-of-concept spectroscopy was conducted using methanol vapor at pressure from 0.1 to 1 mbar. The system successfully resolved multiple transmittance lines in the 255-260 GHz range, aligning well with the JPL spectroscopy database. At 1 mbar, the peak absorption coefficient was ~0.073 m^{-1} for the strongest feature at 255.2 GHz. The system achieved a 600:1 signal-to-noise ratio (SNR) in a rapid 2 second single sweep.

These results successfully validate the feasibility of employing low-cost, room-temperature CMOS electronics with a circular multipass architecture for sensitive trace gas detection. This lays the basis for development of real-time, field-deployable THz gas systems for environmental monitoring, industrial safety, and non-invasive medical diagnostics.

REFERENCES

[1] G. Valušis et al., ”Roadmap of terahertz imaging 2021,” Sensors, vol. 21, no. 12, p. 4092.
[2] N. Rothbart, A. Glück, and H.-W. Hübers, ”Terahertz gas spectroscopy applied to medicine and metrology,” IEEE Trans. Terahertz Sci. Technol. (2024), vol. 14, no. 5, pp. 613–620.
[3] N. Rothbart, K. Schmalz, and H.-W. Hübers, A compact circular multipass cell for millimeter-wave/terahertz gas spectroscopy, IEEE Transactions on Terahertz Science and Technology, 2020, 10, 9–14.

S8-O3
Meta-Atom Photonic Sensor for THz Detection of Organic Molecules

S.R.Ayyagari[1], S.Indrišiūnas[2], V.Janonis[3], J.Macutkevič[1] and I.Kašalynas[1,3]

[1] *Institute of Applied Electrodynamics and Telecommunications (IAET), Vilnius University, Saulėtekio av. 9, Vilnius, LT-10222 Lithuania*

[2]*Laser Microfabrication Laboratory, Center for Physical Sciences and Technology (FTMC), Savanoriu ave. 231, Vilnius, LT-02300 Lithuania*

[3]*Terahertz Photonics Laboratory, Center for Physical Sciences and Technology (FTMC), Saulėtekio av.3, Vilnius, LT-10257 Lithuania*

Email: surya.revanth@ftmc.lt; surya.ayyagari@ff.vu.lt.

The terahertz (THz) spectrum is a highly promising yet one of the least exploited regions of the electromagnetic spectrum, offering spectroscopically rich interactions with materials [1], and strong potential for sensing [2] applications due to its low photon energy, high penetration capability, nondestructive inspection properties. However, the long wavelengths of THz radiation, typically ranging from millimeters to tens of micrometers (0.1–10 THz), fundamentally limit the sensitivity of conventional sensors for detecting small or subwavelength molecules. This limitation has hindered the development of highly sensitive and compact THz functional sensing devices. Understanding and controlling interaction at the subwavelength scale is therefore a key requirement for advancing THz sensing technologies. Metasurfaces, a artifically structured media that are composed of an array of artificial meta-atoms, where each individual meta-atom is capable of confining EM fields to deep subwavelength light–matter volumes, achieving extreme field enhancement [3]. In this work, we demonstrated a photonic sensing platform based on a single planar meta-atom composed of concentric disk- and ring-shaped elements patterned on a freestanding metal film for the THz detection of organic molecules. Coupling the meta-atom to a α-lactose monohydrate layer resulted in enhancment of the resonances amplitudes and significant redshift of the resonances frequencies from 0.35 THz and 0.80 THz to 0.26 THz and 0.53 THz, respectively. Furthermore, the characteristic absorption feature of lactose at 0.53 THz [4] produced a pronounced transmission dip at the second resonance, providing direct evidence of molecule-specific detection. These results demonstrate that the planar meta-atom can serve as a compact and highly sensitive THz sensor, offering a approach for the identification of small volumes of organic and biomolecules promising for future miniaturized THz spectroscopy applications.

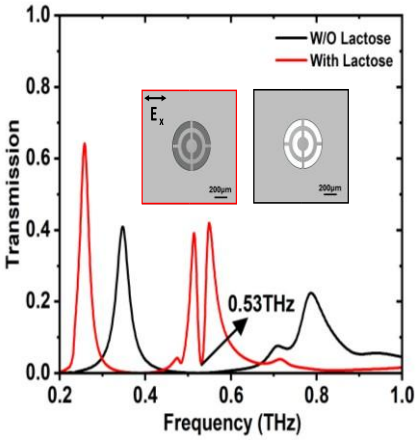


Fig. 1 Transmission spectra of a single planar meta-atom with (red) and without (black) a 60 μm αlactose monohydrate layer using FDTD simulations. Inset: schematics of the corresponding structures.

This work is supported by Lietuvos Mokslo Taryba (LMT) Postdoctoral project under the GA no. SPD-25-44 and THz-Skin project, GA no. 101257203.

REFERENCES

[1] P. U. Jepsen et al., Laser Photonics Rev., vol. 5, no. 1, (2011) pp. 124–166, doi: 10.1002/lpor.201000011.
[2] I. Kašalynas et al., Sensors, vol. 16, no. 4, (2016) p. 432, doi:10.3390/s16040432.
[3] S. R. Ayyagari et al., Appl. Sci., vol. 16, no. 10, (2026) p.4608, doi:10.3390/app16104608.
[4] S. J. Park et al.,Adv. Theory Simulations, vol. 5, no. 3, (2022), doi: 10.1002/adts.202100428

SESSION 9:

Wireless Communication Systems

S9-PL

Terahertz Technologies for Wireless Communications: Achievements and Future Directions

Tadao Nagatsuma[1]

[1]*Graduate School of Science, The University of Tokyo, Japan*
Email: nagatsuma@ipst.s.u-tokyo.ac.jp

Terahertz (THz) technologies have long been driven by advances in materials and device physics, leading to remarkable progress in sources, detectors, and functional components. However, the transition from individual device demonstrations to practical wireless communication systems remains a critical challenge.

In this talk, we review recent progress in THz devices and circuits and discuss their impact on emerging wireless communication applications beyond 6G. System-level integration—scaling, packaging, and co-design—is crucial for maximizing output power, sensitivity, and energy efficiency.

We argue that opto-electronic convergence offers a promising pathway to overcome fundamental limitations of purely electronic or photonic approaches. Figure 1 demonstrates the integration of materials, device physics, and system architectures through heterogeneous approaches, facilitating advanced functionalities and improved performance. This integrated viewpoint clarifies the importance of co-optimizing digital, analog, and photonic domains to achieve scalable THz wireless systems.

Finally, we present a forward-looking perspective on the key challenges and opportunities, and outline how the community can move toward fully integrated THz wireless systems.

Part of this work is supported by a Commissioned Research Project (JPJ012368C09801) from the National Institute of Information and Communications Technology (NICT), Research and Development for Expansion of Radio Resources (JPJ000254) from the Ministry of Internal Affairs and Communications (MIC), JSPS KAKENHI Grant Number JP 24K00887, and the RIKEN TRIP initiative.

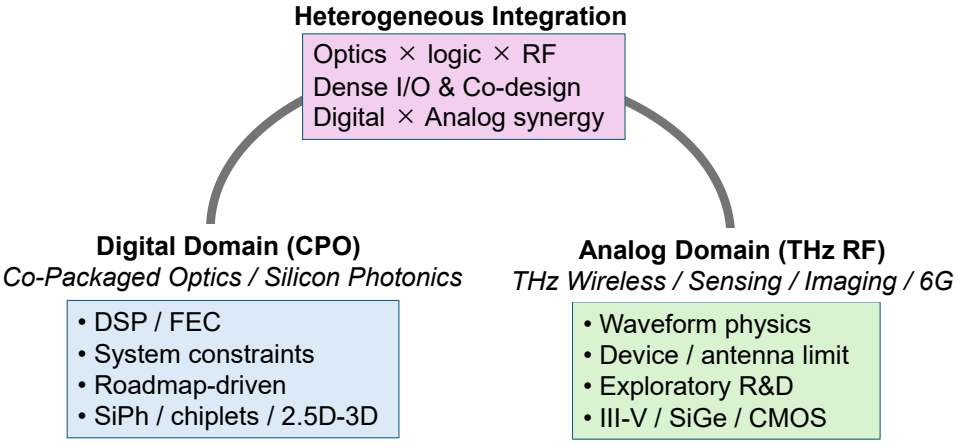


Fig. 1 Conceptual diagram illustrating heterogeneous integration across optics, logic, and RF domains, highlighting the co-design requirements for future THz wireless systems.

S9-I1

Towards the integration of THz antennas in novel communication links: the Hermes project

A. Maffucci[1], G. Fedorov[2], M. Portnoi[3], I. Kašalynas[4], C. Couteau[5], K. Konishi[6], F. Ogrin[7], A. Babusci[8], and A. Urbanovič[9]

[1]*University of Cassino and Southern Lazio - Cassino, Italy*
[2]*University of Eastern Finland - Joensuu, Finland*
[3]*University of Exeter - Exeter, United Kingdom*
[4]*FTMC - Vilnius, Lithuania*
[5]*University of Technology of Troyes - Troyes, France*
[6]*University of Tokyo - Tokyo, Japan*
[7]*MaxLLG ltd - Exeter, United Kingdom*
[8]*Monozukuri Spa - Rome, Italy*
[9]*TeraVil - Vilnius, Lithuania*
Email: maffucci@unicas.it

The HERMES project [1] addresses a key challenge for future 6G and beyond systems: the integration of terahertz (THz) devices into ultra-high-speed communication links. By exploiting graphene and other two-dimensional materials, HERMES aims to develop room-temperature THz emitters, detectors, and transceivers for short-range communications approaching 100 Gbit/s. The project combines nanomaterials, THz electronics, photonics, and system integration to overcome challenges related to efficiency, miniaturization, and infrastructure compatibility.

A key objective of the project is the integration of graphene-based THz devices into communication architectures through two complementary strategies, Fig.1. The first is an electrical integration approach, based on the co-integration of THz devices with silicon electronics and high-speed interface circuits, enabling compact and scalable solutions with reduced interconnection losses. The second is an electro-optical integration approach, where THz signals are directly converted into optical signals through graphene-enabled photonic interfaces operating in the telecom band, allowing seamless connection with existing optical communication networks. By demonstrating both integration paradigms, HERMES will contribute to establish the technological foundations for future THz communication systems.

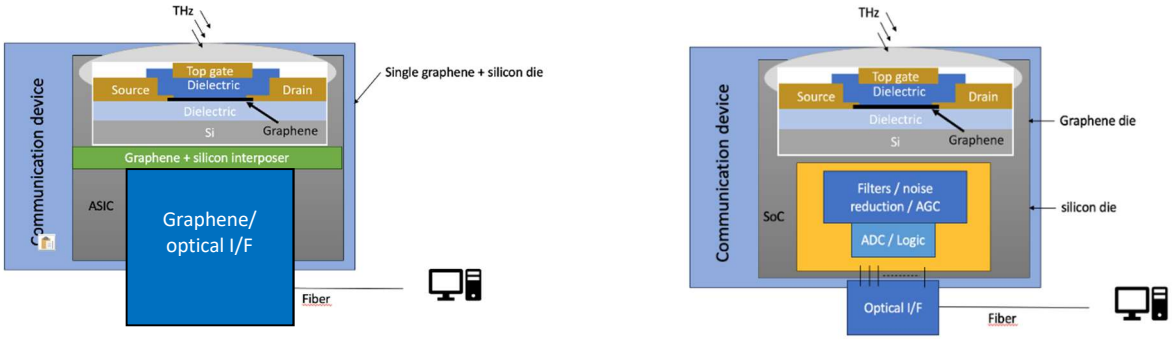


Figure 1: integration of THz devices: (left) all-optical interface; (right) electro-optical interface.

This work is supported by the European Union's Horizon Europe research and innovation programme under the Marie Skłodowska-Curie Actions through the project 101236439 "*Towards a teraHERtz short-range wireless communication system based on graphene devicES*" (HERMES, 2025–2029).

[1] www.hermes-project.eu

S9-O1
High-speed terahertz communication in the W and J bands

Przemysław Zagrajek[1], Paweł Komorowski[1], Marcin Maciejewski[1], Kamil Kamiński[1], Mateusz Karol[1] and Norbert Pałka[1]

[1]*Institute of Optoelectronics, Military University of Technology, gen. S. Kaliskiego 2 00-908 Warsaw, Poland*
Email: pawel.komorowski@wat.edu.pl

Recent years have witnessed a growing interest in the terahertz and sub-terahertz frequency ranges, driven by the increasing demand for higher data rates and reliable wireless connectivity beyond the capabilities of optical, infrared and millimeter wave technologies. This spectral region offers wide available bandwidth while preserving more favorable propagation characteristics than optical systems [1, 2].

Despite significant attenuation due to atmospheric water vapor, transmission windows can be identified in which links spanning several kilometers are feasible [3]. In particular, the W (75–110 GHz) and J (220–330 GHz) bands are highly promising due to a well-balanced combination of wavelength, beam divergence, manageable atmospheric attenuation, and the availability of efficient sources and detectors.



Fig. 1 Outdoor measurement setup for the longrange W-band

In this paper, we report recent progress in high-speed terahertz communication links developed at the Military University of Technology. Targeting specific application niches that benefit from highly directive communication with reduced detectability and increased resistance to eavesdropping and jamming, we investigate several types of THz data links differing in transmission range, data rate, modulation format, and system complexity. Measurements were conducted over various distances, data rates, and attenuation conditions. Error-free communication was achieved over distances up to 750 m between the transmitter and receiver, with data rates reaching 1.5 Gbit/s.

REFERENCES

[1] M. Shehata, et al. "Optical and terahertz wireless technologies: the race to 6G communications." IEEE Wireless Communications 30.5 (2023): 10-18.
[2] L. Zhang, et al. "Beyond 100 Gb/s optoelectronic terahertz communications: Key technologies and directions." IEEE Communications Magazine 58.11 (2020): 34-40.
[3] G. Siles, et al. "Atmospheric Attenuation in Wireless Communication Systems at Millimeter and THz Frequencies [Wireless Corner]," IEEE Antennas and Propagation Magazine, 57.1 (2015): 48-61

S9-O2

Dielectric resonator array rectenna for radio frequency energy harvesting

J. Žemgulytė[1], P. Ragulis[1], R. Simniškis[1], M. Sadauskas[2], A. G. Belous[3], O. I. V'yunov[3], Ž. Kancleris[1]

[1]*Department of Physical Technologies, Center for Physical Sciences and Technology, Vilnius, Lithuania*

[2]*Department of Physical Technologies, Center for Physical Sciences and Technology, Vilnius, Lithuania*

[3]*V. I. Vernadsky Institute of General and Inorganic Chemistry, National Academy of Sciences of Ukraine, Kyiv, Ukraine*

Email: justina.zemgulyte@ftmc.lt

This paper presents a dielectric resonator array rectenna designed for radio frequency (RF) energy harvesting in the 2.4 GHz WiFi band. The rectenna is based on a 2×2 array of horizontally oriented cylindrical dielectric resonator antennas (CDRAs) – a configuration that, unlike conventional vertically placed elements, offers a low-profile structure with broadside radiation and wide angular coverage, making it well suited for harvesting ambient RF energy arriving from multiple directions.

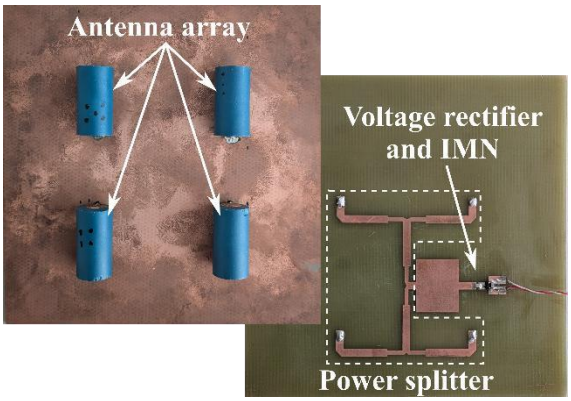


Fig. 1 CDRA antenna array and feeding network with integrated voltage rectifier and impedance matching network (IMN) manufactured using SSAIL.

The array, fed by a corporate microstrip network based on cascaded quarter-wave power dividers, achieves measured realized gains of 5.7 dBi at 2.4 GHz and 10.7 dBi at 5.4 GHz. Building on this array design, two rectenna topologies are proposed and compared: a centralized architecture employing a single rectifier connected after a 4-to-1 power combiner, and a distributed architecture featuring four individual rectifiers, one integrated at each antenna element. Both topologies are realized using SSAIL (selective surface activation induced by laser) fabrication technology, enabling compact, planar integration of the rectifying circuits directly within the feed network [1]. The conductor quality of the fabricated structures was verified through resistance measurements.

The proposed comparison offers insight into the trade-offs between circuit complexity, impedance matching, and RF-to-DC conversion efficiency in multi-element rectenna systems, contributing to the development of compact and scalable energy harvesting solutions for wireless sensor networks and IoT.

REFERENCES

[1] Ratautas, K. "Evaluation and optimisation of the SSAIL method for laser-assisted selective electroless copper deposition on dielectrics" Results Phys. 19, 103432 (2020).

The research was supported by the NATO Science for Peace and Security Program project G6002 "3D Metamaterials for Energy Harvesting and Electromagnetic Sensing."

S9-O3

Laser Communications in Action: Real-World Deployments from the Arctic to the Baltic Sea

Gedminas Elertas

Astrolight, Mokslininkų St. 2, 08412 Vilnius, Lithuania
Email: gedminas.elertas@astrolight.com

Astrolight designs and manufactures laser communication terminals optimised for free-space optical data transfer across low Earth orbit (LEO), space-to-space, space-to-ground, and maritime links. These terminals deliver secure, jam-resistant, high-data-rate connectivity. To date, three first-generation ATLAS-1 body-pointed space terminals have been deployed in LEO. A next-generation gimbaled variant featuring enhanced data rates and compatibility with the Space Development Agency (SDA) standard is currently under development. Astrolight has deployed an optical ground station in Greece and is establishing an additional facility in Greenland in partnership with the European Space Agency (ESA). In the maritime sector, Astrolight, in collaboration with the Lithuanian Navy, has developed shipborne laser communication terminal POLARIS to mitigate vulnerabilities to GPS jamming and provide secure data links. These terminals leverage C-band laser transceivers utilising commercial high-modulation-bandwidth laser diodes coupled with in-house-developed fibre amplifiers. Optical reception relies on high-bandwidth photodiodes, while tracking and acquisition use a combination of detectors, such as focal plane arrays, cameras, quadrant photodiodes, and position-sensitive detectors. Components for space environments are engineered to be vacuum-compatible, radiation-tolerant, and thermally resilient, while ground-segment hardware is ruggedised against equally harsh atmospheric conditions. Ultimately, sustaining the rapid expansion of the free-space optical communication industry depends on pioneering scalable, cost-effective solutions that push the operational boundaries of laser power, detector sensitivity, and modulation bandwidth.

SESSION 10:

Integrated Photonics

S10-I1

Photonic Integrated Circuits: from Pilot Line Access to Product

Timo Aalto[1]

[1]*Silicon photonics, VTT, Tietotie 3, 02150 Espoo, Finland*
Email: Timo.Aalto@vtt.fi

Research and industrialization of photonic integrated circuit (PIC) technology are both gaining momentum around the world. Optical communication in data centers, including high-performance computing (HPC) and artificial intelligence (AI) systems, is clearly the biggest application domain for PICs. Data center transceivers typically operate at ~1.3 or ~1.55 μm wavelengths, while requiring large bandwidth, low-cost mass production and low power consumption. However, there are also many other promising use cases for PICs, such as various optical sensors and imaging systems for healthcare, automotive, civil engineering and defence applications, as well as photonic and quantum computing. Some of these have totally different requirements, such as operation in other wavelength ranges (between ultraviolet and mid-infrared), ultra-broadband operation, ultra-low losses, low noise or very high optical power. Thus, no single PIC technology can cover all application needs and the entire optical spectrum. This presentation will review a variety of complementary PIC technologies and compare their ability to address different application needs. Access to these technologies via PIXEurope pilot line and the PhotonHub innovation hub will then be described and followed by a discussion about potential paths to volume production.

S10-I2

Terahertz range electrodynamics and possible optoelectronic applications of carbon nanotube films.

Aadya Menon[1], Mikhail Gorbun[1], Maria Cojokari[1], Aleksandr Saushin[1], Polina Kuzhir[1], Irmantas Kašalynas[2], Andžej Urbanovič[2], Vytautas Janonis[2], Xu Zhenyu[3], Esko Kaupinen[3] and Georgy Fedorov[1]

[1]Center for Photonics Sciences, University of Eastern Finland, P.O. Box 111. FI-80101, Joensuu 80100, Finland.
[2]Department of Optoelectronics, Center for Physical Sciences and Technology (FTMC), Sauletekio av. 3, Vilnius 10257, Lithuania.
[3]Department of Applied Physics, Aalto University School of Science, Puumiehenkuja 2, Aalto, Espoo 00076, Finland

Email: georgy.fedorov@uef.fi.

The great potential individual carbon nanotubes have for the future nanoelectronics [1,2] has yet to be realized. At the same time carbon nanotube films that contain different types of nanotubes find different applications including, but not limited to transparent electrodes, flexible sensors, energy storage electrodes, and others.

Here we report on our recent results regarding electrodynamics of carbon nanotube films produced by Aerosol chemical vapor deposition (CVD) technique. We show that dynamic conductivity of these film is well described within Drude model with a scattering rate of about 10 THz that results in untrivial behavior of submicron-thick suspended CNT films, including negative phase velocity controllable by optical pumping [3].

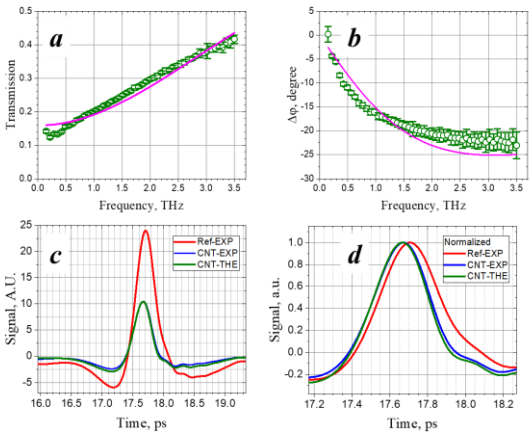


Fig. 1 Upper panel: Power transmission (a) and phase (b) as a function of frequency. Dots show experimental data, olive solid lines are the results of simulations. Lower panel: The as-measured signals (c) and normalized signals (d). Simulations are based on the Drude model for the CNT.

This work was supported by HORIZON-EIC-2025-PATHFINDEROPEN THz-Skin project 101257203 and EU Horizon 2024 MSCA project 101236439 (HERMES)

REFERENCES

[1] E.-X. Ding, et al., High-performance transparent conducting films of long singlewalled carbon nanotubes synthesized from toluene alone, Nano. Res. 13 (2020), 112–120.
[2] Z. Xu, et al., Direct patterning of carbon nanotube aerosols for high-performance flexible electronics, Nano. Today 61 (2025) 102635.
[3] Gorbun, M., et al. "Negative optical phase accumulation in ultrathin conductive films." Carbon Trends (2026): 100641.

S10-O1

Femtosecond Laser-Written Photonic Integrated Circuits for Quantum Applications

Ubaid ur Rehman[1], Vakaris Silys[1], Valdemar Stankevič[2], Eimantas Dermauskas[2], Tadas Paulauskas[1]

[1]*Department of Optoelectronics, FTMC, Vilnius, Lithuania*

[2]*Department of Laser Technologies, FTMC, Vilnius, Lithuania*

Email: ubaid.rehman@ftmc.lt

Femtosecond laser-written waveguides in transparent dielectric materials are attracting significant interest for applications in photonic integrated circuits (PICs) and emerging quantum photonic applications. They offer low-loss three-dimensional routing capability, flexibility in defining waveguide core shapes, rapid prototyping, and suitability for wavelength spanning from visible to infrared [1,2].

In this work, femtosecond laser-written waveguides were developed in aluminoborosilicate glass for integrated photonic applications. The influence of laser writing parameters on waveguide formation, mode propagation, and coupling characteristics was systematically investigated. Detailed studies of the modal field profiles revealed fundamental as well as higher-order mode propagation depending on the writing conditions.

In parallel, beam propagation method (BPM)-based numerical model was developed to simulate light propagation in laser-written refractive index structures. Furthermore, the thermo-optic effect was incorporated into the BPM framework to investigate phase control and tuning mechanisms for interferometric applications. The developed model enables the analysis of integrated thermo-optic phase shifters for reconfigurable quantum photonic circuit applications.

REFERNCES

[1]. Peri, Andrea, et al. "High-performance heterodyne receiver for quantum information processing in a laser-written integrated photonic platform." *Advanced Photonics* 8.1 (2026): 016009-016009.

[2]. Corrielli, et al. "Femtosecond laser micromachining for integrated quantum photonics." *Nanophotonics* 10.15 (2021): 3789-3812.

S10-O2

Near field investigation of GaN surface relief grating coupled plasmon phonon polaritons

V. Janonis[1], A. Cernescu[2], V. Zenin[3], S. Indrišiūnas[1], R. Januškevičius[4], I. Kašalynas[1]

[1] *Center for Physical Sciences and Technology, Vilnius, Lithuania*

[2]*Attocube systems AG, Munich, Germany*

[3]*SDU Nano Optics, The Mads Clausen Institute, University of Southern Denmark, Denmark*

[4]*Ekspla Ltd., Vilnius, Lithuania;*

Semiconductor based thermal radiation sources based on hybrid Surface Plasmon-Phonon Polariton (SPPhP) excitation in n-GaN gratings were recently developed demonstrating emission of high spatial quality in a far-field with high coherence in the vicinity of transfer optical (TO) phonons frequency, namely at wavelengths near 570 cm^{-1}[1]. While far-field results show promising macro-scopic behavior of the SPPhPs, an understanding of underlying physics and extended applicability of the emitters can be obtained by performing near-field studies of the SPPhP characteristics. Initial studies with clasical Scanning Near-field Optical Microscopy (SNOM) geometry of top-side far field illumination at a certain excitation beam incidence angle have shown the technique limitations observing the propagation distance values of up to 30 μm only.[2] In this work we implemented a novel SPPhP excitation scheme, where back-side laser excitation beam is used to excite SPPhPs in the center of a circular n-GaN surface relief grating through a laser-milled via with diameter of around 25 μm . The electric field of the propagating SPPhPs was then recorded using pseudo-heterodyne SNOM scheme with decoupled excitation – probe regime. The grating topography map and SNOM signal phase results are shown in Figure 1, obtained in a wide measurement window reaching size of up to 250 μm. Moreover we observed SPPhP propagation in distances over 250 μm by SNOM measurements of evanecent electic field components and direct comparison with the numerical FDTD modelling results. Modelling also revealed possibility of longer propagating polaritons achievable by optimazation of the gratingf illing factor.

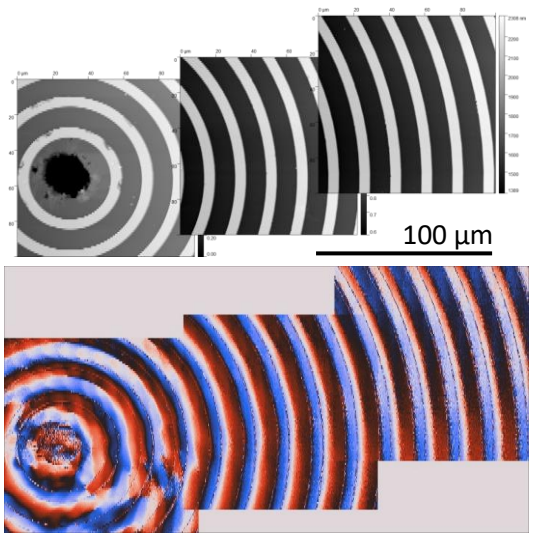


Fig. 1 Measured sample topography (Top) and Phase (Bottom) of the investigated surface relief grating at the laser excitation frequency of 570cm^{-1}.

REFERENCES

[1] V. Janonis et al. Opt. Mater. Express **13**(9), 2662 (2023); https://doi.org/10.1364/OME.494777.
[2] V. Janonis et al. Materials 2025, 18, 2849 (2025); https://doi.org/10.3390/ma18122849.

S10-O3

Engineering Thin-Film Lithium Niobate Cavities for On-Chip Frequency-Space Lattices

Armandas Balčytis[1,2] Hiep X. Dinh[1,2], Guanghui Ren[1,2], Mei Xian Low[1,2], Arnan Mitchell[1,2], and Thach G. Nguyen[1,2]

[1]*Integrated Photonics and Applications Centre, RMIT University, Melbourne, VIC 3000 Australia*
[2]*ARC Centre of Excellence in Optical Microcombs for Breakthrough Science (COMBS), Australia*
Email: armandas.balcytis@ftmc.lt

The synthetic dimension approach offers a powerful means of probing high-dimensional physical models in comparatively simple devices, by treating non-spatial degrees of freedom as additional independent coordinates. In photonics, the discrete equidistantly spaced frequency modes of a ring resonator are a natural synthetic lattice, straightforwardly coupled and partitioned by dynamic modulation. While early demonstrations of this concept relied on macroscopic fiber loop setups, miniaturization and on-chip integration have been identified as essential steps toward scalable and environmentally stable implementations.

Thin-film lithium niobate on insulator (LNOI) is particularly well suited to this task. Its combination of efficient broadband electro-optic response, low propagation loss, high optical power handling, and strong optical nonlinearity makes it useful for demanding electro-optic applications. Realizing synthetic frequency dimension devices in this setting compresses the optical path length by three orders of magnitude relative to fiber predecessors, shifting the relevant operating frequencies from the megahertz into the gigahertz range.

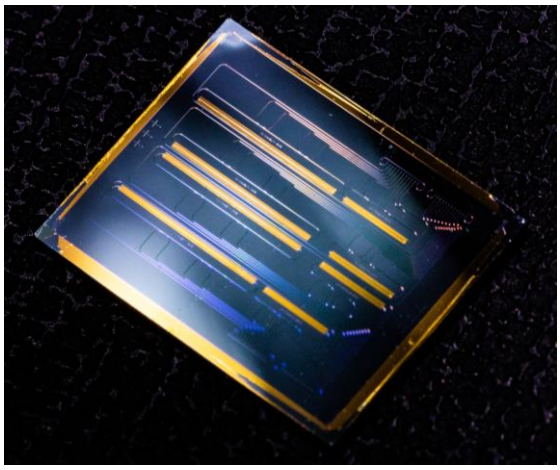


Fig. 1 LNOI photonic chip (14 mm × 11 mm) for synthetic frequency dimension lattice realization.

Within this platform we explore how lattice properties - connectivity, geometry, gauge potential, and boundary conditions - can be controlled through drive signal design and cavity architecture rather than fixed at fabrication. Electro-optic modulation and inter-cavity coupling emerge as complementary tools, together enabling a range of reconfigurable tight-binding lattice configurations of increasing complexity to be realized on the same device.

We present a series of experiments spanning single and coupled LNOI ring cavity configurations. Band structure spectroscopy is used throughout as a direct probe of tight-binding lattice dynamics, connecting experimental observables to the underlying physical models.

REFERENCES

[1] H. X. Dinh, A. Balčytis, T. Ozawa, Y. Ota, G. Ren, T. Baba, S. Iwamoto, A. Mitchell and T. G. Nguyen; *Communications Physics* **7** (2024) pp. 185.
[2] H. X. Dinh, A. Balčytis, G. Ren, M. X. Low, A. Mitchell and T. G. Nguyen; *Laser & Photonics Reviews* (2026) pp. e71745.

POSTER SESSION:

All sections contributions as poster presentations

P01

Estimation of electromagnetic pulse power during magnetic microcumulation in a thin superconducting film

Oleg Kiprijanovič and Linas Ardaravičius

Center for Physical Sciences and Technology, Saulėtekio al.3, LT-10257, Vilnius, Lithuania,
oleg.kiprijanovic@ftmc.lt

The operation of a magnetocumulative generator is accompanied by the appearance of parasitic electromagnetic radiation. It is presumed that the compressed coil acts as a loop antenna [1]. The article [2] considers the case of microscopic cumulation of a trapped magnetic field in a thin YBaCuO film of a type II superconductor. As a result of microcumulation, superconducting properties locally disappear, leading to the fast decay of the accumulated field. According to Maxwell's equations, the process of fast magnetic field vanishing should be accompanied by the appearance of an electromagnetic pulse. This raises the question: can this pulse be detected?

The difficulty in estimating the pulse power of a decaying magnetic dipole $\boldsymbol{m}$ is a negligible coefficient $\mu_0/(6\pi \cdot c^3)$ before $|\ddot{\boldsymbol{m}}|^2$, where μ_0 is the magnetic constant and c is the light velocity. In models for the power estimation, functions describing the vanishing moment should be chosen such that the second derivative approaches infinity at a certain point. The microcumulation parameters λ_{eff}, j_{1S} for the film with the highest critical current density are taken from paper [2]. The time of complete decay of $\boldsymbol{m}$ depends on the dynamics of microcumulation and the subsequent increase in temperature. The beginning of the decay process is determined by the Fermi time, which is about 10^{-15} s. Under such conditions, $\boldsymbol{m}$ is estimated to vanish over a time interval between 0÷1.5 ps and 0÷6.5 ps. The value of the $\boldsymbol{m}$ before the decay is $11.8 \cdot 10^{-12}$ A·m^2. The decay process was modeled using the function arcsech(kt) on the interval [0,1] in its logarithmic representation, where k is the scaling factor. Its second derivative tends to infinity at zero. We estimate the average value of $\ddot{\boldsymbol{m}}$ where it is steepest over the [0, 0.25] segment of the boundary time intervals. The results obtained are presented in Table 1.

Table 1. Characterization of magnetic dipole radiation during the microcumulation

$\boldsymbol{m}$ decay time, s	irradiation time, s	$\lvert\ddot{\boldsymbol{m}}\rvert$, A·m^2/s^2	frequency band, Hz	power, W
$1.5 \cdot 10^{-12}$	$0.375 \cdot 10^{-12}$	$1.73 \cdot 10^{16}$	$2.66 \cdot 10^{12}$	$0.74 \cdot 10^{-3}$
$6.5 \cdot 10^{-12}$	$1.625 \cdot 10^{-12}$	$4 \cdot 10^{15}$	$0.615 \cdot 10^{12}$	$0.04 \cdot 10^{-3}$

Detection of repetitive picosecond pulses of electric dipole radiation, whose coefficient is c^2 times greater, is a rather difficult problem [3]. Potentially, to detect randomly generated picosecond milliwatt pulses, it is possible to apply the technology used to detect single photons with a superconducting device [4].

REFERENCES

[1] H. Li, L. Xiao, Y. Zhang, J. Qiu; Proc. of Inter. Conf. on Electronics and Information Engineering, Kyoto, Japan, **2** (2010) pp. 255-258, doi:10.1109/iceie.2010.5559776
[2] O. Kiprijanovič, L. Ardaravičius; Coatings, **15** (2025) 134, doi.org/10.3390/coatings15020134
[3] H. Aggrawal, et al.; IEEE Microwave Magazine **17 (**2016) pp. 24-38, doi**:**10.1109/MMM.2016.2608764
[4] R. Sobolewski et al.; Appl. Phys. Lett. **79** (2001) pp. 705–707, doi.org/10.1063/1.1388868

P02

Dual Planar Inverted-F Antenna Resonant-Tunneling-Diode Oscillator

Petr Ourednik[1] and Michael Feiginov[1]

[1]*Institute of Electrodynamics, Microwave and Circuit Engineering, TU Wien, Gusshausstrasse 25, 1040 Vienna, Austria*
Email: petr.ourednik@tuwien.ac.at

Resonant-tunneling diodes (RTDs) are among the fastest electronic devices capable of generating electromagnetic radiation up to 2 THz [1,2]. Operating at room temperature, RTDs enable truly compact THz sources with significant potential for bringing THz technology into real-world applications [3,4].

Compact RTD oscillators that radiate above the semiconductor substrate are particularly advantageous, as they do not require bulky Si lenses (which are large relative to the oscillator itself) thereby enabling integration of THz sources into larger systems. While lenses can improve beam collimation, a comparable effect can be achieved through the use of RTD oscillator arrays.

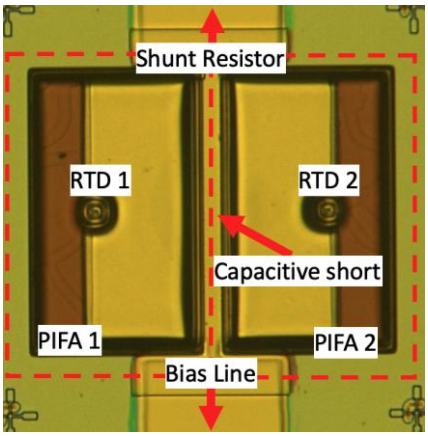


Fig. 1 Micrograph of the dual PIFA RTD oscillator.

We present a novel RTD oscillator geometry that achieves above-substrate radiation based on a planar inverted-F antenna (PIFA). PIFAs inherently exhibit tilted radiation patterns; however, by introducing a second RTD oscillator mirrored across the (capacitive) PIFA short, the combined radiation pattern becomes symmetrical above the substrate. This geometry is closely related to the double-RTD patch antenna [5], with the key distinction that the central section of the patch has a narrow dip, bringing it close to the ground plane. This effectively acts as a capacitive short circuit at high frequencies, transforming the structure into two back-to-back PIFAs. As with double-RTD patch antennas, two resonant modes can exist in this structure: a symmetric mode and an antisymmetric mode. The poorly radiating symmetric mode is shifted to lower frequencies by the capacitive short and suppressed by connecting a resistive shunt at the patch center, making the desired antisymmetric mode dominant. The resulting structure is shown in Fig. 1.

We fabricated and characterized these devices. The RTD oscillators operated at approximately 700 GHz with an output power of ~30 μW. Their emission spectra were free of parasitic spectral lines, confirming single-mode operation. The radiated power pattern was symmetric, with a maximum directed perpendicularly to the substrate. These devices represent a promising foundation for compact RTD oscillator arrays, enabling large-scale integration of THz sources.

REFERENCES

[1] S. Suzuki and M. Asada; Appl. Phys. Express **17** (2024) 070101.
[2] D. Tuan Nguyen, P. Ourednik, M. Feiginov; Appl. Phys. Lett. **123** (4) (2023) 043508.
[3] A. Dobroiu, K. Asama, S. Suzuki, et al.; J Infrared Milli Terahz Waves **43** (2022), 464–478.
[4] P. Ourednik, G. Picco and M. Feiginov, 2022 47th International Conference on Infrared, Millimeter and Terahertz Waves (IRMMW-THz), 2022.
[5] P. Ourednik, M. Feiginov; Appl. Phys. Lett. **120** (18) 2022 183501.

P03

Electromagnetic Design of Integrated CMOS Frequency Multiplier Chains for Sub-THz Frontend Architectures

Maksimas Anbinderis[1,2], Alvydas Lisauskas[1,2], Kęstutis Ikamas[1,2] and Raul Aliyev[1]

[11]*Institute of Applied Electrodynamics and Telecommunications, Vilnius University, Vilnius, 10257 Lithuania*

[2] *Center for Physical Science and Technology, Vilnius, 10257, Lithuania* Email: maksimas.anbinderis@ff.vu.lt

The realization of compact signal generation circuits above 100 GHz remains one of the key technological challenges limiting the broader deployment of sub-terahertz systems for communication, sensing, imaging, and radar applications [1]. While III-V and SiGe technologies dominate high-performance implementations, CMOS provides a scalable and cost-effective platform for compact sub-THz frontend integration [2]. However, efficient frequency multiplication in standard CMOS technologies becomes increasingly challenging due to passive losses, parasitic coupling, impedance matching constraints, and limited transistor performance at elevated frequencies.

This work presents the design and electromagnetic modeling of integrated frequency multiplier chains implemented in a 65 nm CMOS technology for sub-THz applications. The investigated architectures include a Ka-to-W-band frequency tripler and a subsequent multiplication stage targeting D-band as well as operation in the 220-300 GHz frequency range. In contrast to studies focused solely on multiplier cores, the proposed approach considers the complete frontend circuitry, including integrated amplification stages intended to compensate conversion losses between multiplication stages, together with baluns, matching networks, filtering structures, transmission lines, and antenna interfaces. The complete multiplier-chain frontend occupies only 1 × 0.5 mm², including RF pads.

At sub-THz frequencies, circuit performance is strongly influenced by electromagnetic coupling and parasitic effects from integrated passive structures. Therefore, particular attention was devoted to the co-design and optimization of passive components and their interaction with active multiplier cores. Full-wave electromagnetic and circuit-level co-simulations were used to evaluate harmonic generation, impedance matching, signal propagation, and passive loss effects on frontend performance.

Simulation results demonstrate the feasibility of integrated CMOS-based multiplier chains operating toward the sub-THz frequency range while maintaining compact implementation and suitable signal propagation characteristics. The presented study highlights the importance of accurate passive component co-design for efficient operation above 100 GHz and provides insight into practical challenges associated with highly integrated CMOS sub-THz frontend realization.

REFERENCES

[1] G. Wang et al.; *Terahertz integrated sensing and mobile communications empowered by a 220-GHz-band portable device*, Nature Communications, 16 (2025), 11719.

[2] R. Chen, B. Yan and M. F. Chang; *A Review of Circuits and Systems for Advanced Sub-THz Transceivers in Wireless Communication*, MDPI Electronics, 14 (2025), 861.

P04

Investigating the angular characteristics of sensors based on complementary metal-oxide-semiconductor field-effect transistors at 2.52 THz.

Ričardas Petkus[1], Domantas Vizbaras[2], Ignas Grigelionis[1], Linas Minkevičius[1], Alvydas Lisauskas[1;2], Dovilė Čibiraitė-Lukenskienė[1;2]

[1]*Center for Physical Sciences and Technology, Department of Optoelectronics, Lithuania.*
[2]*Vilnius University, Institute of Applied Electrodynamics and Telecommunications, Lithuania*
Email: ricardas.petkus@ftmc.lt.

Terahertz radiation, which is defined as the frequency range of the electromagnetic spectrum between 100 GHz and 10 THz [1], can penetrate non-conductive materials. It is non-ionising in nature and resonates with the rotational and vibrational modes of complex biomolecules. The development of high-power THz sources and high-sensitivity THz detectors is made possible by these properties. Field-effect transistors (FETs) with integrated antennas are being used in the development of such THz radiation detectors [2]. The compatibility of FET technology with commercial complementary metal–oxide–semiconductor manufacturing processes, and its ability to operate efficiently at room temperature, are key advantages.

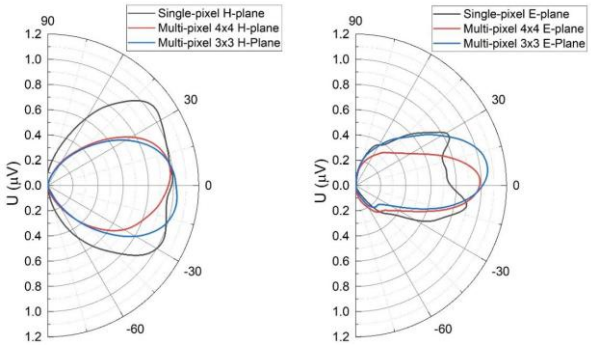


Fig. 1 Normalised angular dependence plots of different antenna configurations. H and E planes are separated.

This work outlines the development of terahertz sensors based on FET technology, as well as studying their angular characteristics while operating at 2.52 THz. The study involved several stages of detector development, including investigating suitable low-noise amplifier components, modelling the amplifier circuit to validate the expected behaviour, soldering the components, and assembling the complete sensor device. Measurements were then carried out to determine the angular dependency of the detected power, with the antenna area scanned using a mirror system that guided the THz wave from a 2.52 THz source.

Figure 1 illustrates the improved beam focusing and symmetry with multi-pixel array in relation to angular dependence. The single-pixel configuration has a broad H-plane lobe and asymmetric, double-peaked E-plane response showing non-uniform sensitivity. Multi-pixel arrays effectively eliminate spatial distortions and increase directivity.

REFERENCES

[1] R. Köhler et al., “Terahertz semiconductor-heterostructure laser,” Nature, vol. 417, no. 6885, pp. 156–159, 2002.
[2] S. Boppel et al., “CMOS Integrated Antenna-Coupled Field-Effect Transistors for the Detection of Radiation From 0.2 to 4.3 THz,” IEEE Transactions on Microwave Theory and Techniques, vol. 60, no. 12, pp. 3834–3843, 2012.

P05

Hole transport in graphene field-effect transistor structures on SiO_2

Linas Ardaravičius[1], Oleg Kiprijanovič[1], Emilis Šermukšnis[1], Artur Šimukovič[1], Nerija Žurauskienė[1], and Joon Young Kwak[2]

[1]*Center for Physical Sciences and Technology, Saulėtekio av. 3, LT–10257, Vilnius, Lithuania*
[2]*Ewha Womans University, 52, Ewhayeodae-gil, Seodaemun-gu, Seoul 03760, Republic of Korea*
Email: linas.ardaravicius@ftmc.lt

Since the discovery of graphene in 2004, there have been intensive studies in two-dimensional materials research [1,2]. Various properties, including optical, magnetic and electrical were explored. The goal of this work is to investigate carrier transport in back-gated graphene field-effect transistor structures. The samples were prepared using CVD monolayer graphene on Cu foil. The graphene film was then transferred to 300 nm SiO_2/p-Si wafers using the wet transfer method [3]. Graphene channels were formed as transmision line method (TLM) patterns with various lengths (L = 5, 10, 15, 20, 30 μm) and a width w = 75 μm. Ti/Au (3/45 μm) contact metals were deposited by an e-beam evaporator. The graphene DC current transfer and output characteristics showed the presence of p-type type graphene channel. Graphene field-effect mobility was estimated to be 1030 cm^2/Vs and hole density was 2-2.2x10^{12} cm^{-2}.

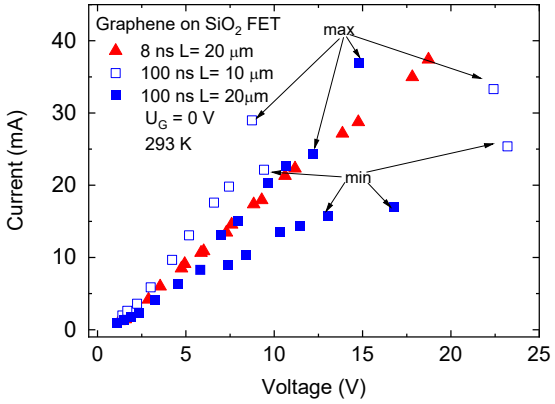


Fig. 1. Pulsed current-voltage characteristics in graphene FETs at U_G = 0 V. Pulse duration: 100ns (squares), 8 ns (triangles). Current curves with maximum (max) and minimum (min) values. Channel length 10 μm (empty squares), 20 μm (triangles, full squares).

Current-voltage characteristics were measured both in DC and pulsed (8 ns, 100 ns) regimes. Pulsed current values up to 40 mA and voltages up to 23 V were reached at a gate voltage U_G = 0 V (Fig. 1). Current oscillations were observed within the certain amplitude interval what corresponds to the max and min current curves [4]. The hole drift velocity was estimated from non-oscillating measured pulsed current density and constant carrier density. The highest drift velocity of ~1.5x10^7 cm/s was estimated at ~18 kV/cm electric field. This value of the hole drift velocity is in agreement with that for graphene grown on SiC and dry transferred on SiO_2 [5]. It can be associated with the influence of non-equilibrium (hot) optical phonons launched by hot-carriers present at moderate-high electric field.

REFERENCES

[1] K. S. Novoselov et al., Nature **490** (2012) pp. 192–200.
[2] C. Backes et al., 2D Mater. **7** (2020) pp. 022001.
[3] J. W. Suk et al., ACS Nano **5** (2011) pp. 6916-6924.
[4] O. Kiprijanovič, E. Park, J. Y. Kwak, L. Ardaravičius, AIP Adv. **13** (2023) pp. 065205.
[5] L. Ardaravičius, O. Kiprijanovič, H. Alsalman, J. Y. Kwak, J. Phys. D: Appl. Phys. **54** (2021) pp.185101.

P06

Near-Infrared Emission Properties of GaAsBi-Based Devices under Electrical Injection

Justas Žuvelis[1], Andrius Bičiūnas[1], Aivaras Špokas[1], Mindaugas Kamarauskas[2], Andrea Zelioli[1], Evelina Dudutienė[1], Renata Butkutė[1]

[1]Department of Optoelectronics, Center for Physical Sciences and Technology, Saulėtekio av. 3, Vilnius

[2]Department of Physical Technologies, Center for Physical Sciences and Technology, Saulėtekio av. 3, Vilnius

Email: justas.zuvelis@ftmc.lt

GaAsBi is a promising material for near-infrared (NIR) emitters due to the large bandgap reduction with the incorporation of Bi, reduced temperature-induced emission wavelength shifts, and the possibility to suppress the non-radiative CHSH Auger recombination channel [1]. These properties make GaAsBi-based light emitting diodes (LED) and laser diodes (LD) attractive for NIR optoelectronic systems, including biomedical sensing, optical telecommunications, and LiDAR ranging. Therefore, it is important to evaluate device performance under electrical injection, as well as the possibility of transferring these structures onto other semiconductor platforms.

In this study, various GaAsBi-based LED and LD structures, incorporating an AlAs sacrificial layer, were grown by molecular beam epitaxy and investigated using electroluminescence (EL) spectroscopy. For the studied GaAsBi/GaAs multiple-quantum-well (MQW) LD structure, room-temperature emission at 1.26 μm was achieved, with the central emission energy shifting by −68 meV over the temperature range from 4 to 300 K. The flipped GaAsBi/GaAs MQW p-i-n LED structure, developed for flip-chip bonding [2], exhibited broader emission spectra and lower radiative efficiency than the standard n-i-p design. Photoluminescence measurements revealed that the lower-energy side of the EL spectrum in the p-i-n structure is broadened due to recombination through defect states, which may be associated with active-region deposition on low temperature growth p-type GaAs. In contrast, electronic-structure modelling with *nextnano* indicated that the high-energy tail likely originates from the first-electron–second-heavy-hole transition, enabled by hole concentration gradients formed through Be diffusion [3].

ACKNOWLEDGEMENTS

This work has received funding from LMTLT, agreement No. S-ST-25-88 and S-LT-TW-24-8.

REFERENCES

[1] S. J. Sweeney, Z. Batool, K. Hild, S. R. Jin and T. J. C. Hosea; 2011 13th International Conference on Transparent Optical Networks (2011) pp. 1-4

[2] D.-M. Geum, M.-S. Park, J. Y. Lim, H.-D. Yang, J. D. Song, C. Z. Kim, E. Yoon, S. Kim, and W. J. Choi; Scientific Reports 6 (2016) pp. 20610.

[3] E. F. Schubert, J. M. Kuo, R. F. Kopf, H. S. Luftman, L. C. Hopkins, and N. J. Sauer; Journal of Applied Physics 67 (1990) pp. 1969–1979.

P07
Terahertz emission from Bi/GaAs heterostructures

Benas Stanionis, Ričardas Norkus, Arūnas Krotkus, Vaidas Pačebutas

Center for Physical Sciences and Technology, Saulėtekio3, 1057 Vilnius, Lithuania
Email: benas.stanionis@ftmc.lt

Two-dimensional (2D) materials exhibit unique properties due to quantum confinement and high surface-to-volume ratios. Thin bismuth (Bi) layers are promising for topological insulators, sensors, thermoelectric devices, and ultrafast optoelectronics. Although bulk Bi is a semimetal, films thinner than ~30 nm become semiconducting, with bandgaps tunable up to 0.8 eV [1]. Bi thin films have mainly been grown on InAs, InP, and Si (111), with promising monolayer structures also shown on GaAs (111) [2–4]. Here, Bi layers were grown by molecular beam epitaxy on GaAs (100), a previously unreported substrate orientation, and their terahertz (THz) emission was investigated using THz excitation spectroscopy (TES).

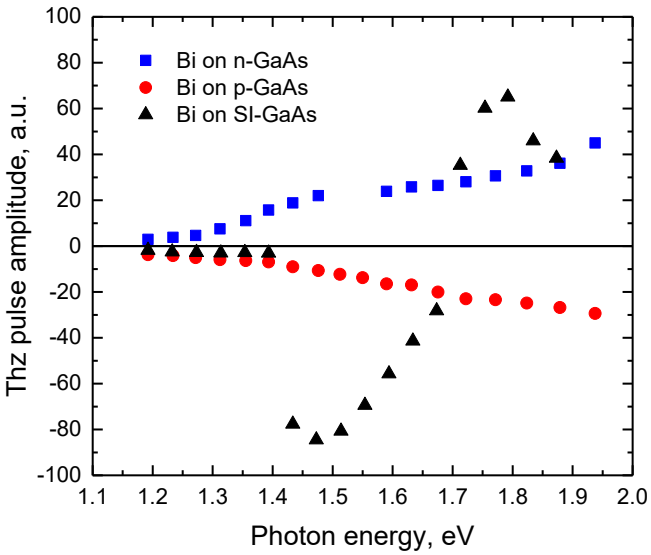


Fig. 1 THz excitation spectra of the heterostructures containing 9 nm thick Bi layers deposited on SI-GaAs, p-GaAs, and n-GaAs substrates..

Heterostructures with 9 nm Bi layers on semi-insulating (SI), n-type, and p-type GaAs (100) substrates were studied in reflection geometry. Excitation photon energy was varied while keeping the average laser power at 20 mW. Strong THz emission appeared only above the GaAs bandgap (1.42 eV), indicating that emission mainly originates from substrate-related processes. Below this threshold, measurable emission was observed only for Bi/n-GaAs. Opposite THz pulse polarities from n- and p-type samples were attributed to reversed internal electric fields at the Bi/GaAs interface. Comparison with bare substrates gave a Bi absorption coefficient of (3–4)×10⁵ cm⁻¹ in the 1.5–1.7 eV range, over an order of magnitude higher than GaAs [5].

Bi/SI-GaAs showed reduced THz amplitude and polarity reversal near 1.7 eV, suggesting an additional interface-related emission mechanism. Bi/p-GaAs exhibited enhanced THz emission, attributed to hole drift velocity overshoot in strong internal fields. These results highlight Bi/p-GaAs heterostructures as promising efficient surface THz emitters.

REFERENCES

[1] Reis, F., Li, G., Dudy, L., Bauernfeind, M., Glass, S., Hanke, W., Thomale, R., Schaefer, J. and Claessen, R., 2017. Bismuthene on a SiC substrate: A candidate for a high-temperature quantum spin Hall material. Science, 357(6348), pp.287-290.

[2] Inbar, H.S., Zubair, M., Dong, J.T., Engel, A.N., Dempsey, C.P., Chang, Y.H., Nishihaya, S., Khalid, S., Fedorov, A.V., Janotti, A. and Palmstrøm, C.J., 2023. Inversion symmetry breaking in epitaxial ultrathin bi (111) films. arXiv preprint arXiv:2302.00803.

[3] Jalil, A.R., Hou, X., Schüffelgen, P., Bae, J.H., Neumann, E., Mussler, G., Plucinski, L. and Grützmacher, D., 2023. Phase-Selective Epitaxy of Trigonal and Orthorhombic Bismuth Thin Films on Si (111). Nanomaterials, 13(14), p.2143.

[4] Liu, Y., Benter, S., Ong, C.S., Maciel, R.P., Bjork, L., Irish, A., Eriksson, O., Mikkelsen, A. and Timm, R., 2023. A 2D bismuth-induced honeycomb surface structure on GaAs (111). ACS nano, 17(5), pp.5047-5058.

[5] Aspens, D.E., Kelso, S.M., Logan, R.A. and Bhat, R., 1986. Optical properties of Al x Ga 1-x As. J. Appl. Phys, 60, pp.754-767.

P08

Terahertz Pulse Excitation Spectroscopy of Thin Bismuth Layers and Their Heterostructures

Ričardas Norkus[1], Benas Stanionis[1], Vaidas Pačebutas[1] and Arūnas Krotkus[1]

[1]*Optoelectronics department, Center for Physical Sciences and Technology, Sauletekio av. 3 Vilnius, Lithuania.*

Email: ricardas.norkus@ftmc.lt

Ultra-short electric pulses generated by femtosecond laser beams are widely used to investigate the physical properties of various materials, including semiconductors. Terahertz excitation spectroscopy (TES) is a powerful non-contact characterization technique that enables the investigation of electronic properties and heterojunction band structure in semiconductors. TES provides fundamental insight into a material's internal electric field, carrier dynamics, and electronic structure. It has been shown that, by examining the dependence of THz emission on the excitation wavelength, important band-structure parameters can be determined, including the direct bandgap, subsidiary valley position, and heterostructure offset value [1]. Recently, this technique has been applied to determine the electronic parameters of thin layers such as bismuth [2]. While investigation of GaSb azimuthal angle dependencies revealed novel way to characterize conduction band valley positions [3].

Bismuth undergoes a semimetal-to-semiconductor transition when confined to nanometer-scale thicknesses (~30 nm), with quantum size effects inducing bandgap opening and tunable optical properties. Ultrathin 9 nm Bi films were grown on (100)-oriented GaAs and GaSb substrates. The Bi/semi-insulating GaAs heterostructure exhibited a unique spectral response, characterized by an onset at 1.41 eV, a peak at 1.5 eV, and a pronounced polarity reversal of the emitted terahertz pulses at 1.67 eV. Band-structure modeling has attributed this reversal to two competing photocurrent-generation mechanisms. At lower energies, intrinsic heterojunction electric fields dominate, whereas at higher energies the photo-Dember effect, arising from ballistically propagating carriers, becomes dominant [3]. A significant enhancement of the THz pulse amplitude was observed for Bi layers on p-GaAs and p-GaSb samples compared with the bare substrates. This phenomenon can be attributed to the stronger electric field at the Bi/GaAs interface, thereby demonstrating the overshoot effect of photoexcited holes. This enhancement mechanism appears to be universally applicable to Bi thin films on p-type semiconductors and is considered a promising candidate for efficient surface THz pulse emission.

REFERENCES

[1] A. Krotkus, I. Nevinskas, and R. Norkus, "Semiconductor characterization by terahertz excitation spectroscopy", Materials 16, 2859 (2023);

[2] I. Nevinskas, S. Stanionytė, J. Devenson, A. Krotkus; "Direct bandgap dependence of bismuth films on their thickness". Journal of Applied Physics; 132 055301 (2022);

[3] R. Norkus, V. Pačebutas, and A.Krotkus, "Spectral dependencies of THz pulse emission from GaSb," Optics Letters 51, 2640-2643 (2026);

[4] Pačebutas, V.; Norkus, R.; Tamulaitis, G.; Stanionis, B.; Krotkus, A. "Terahertz excitation spectroscopy of Bi/GaAs heterostructures", Journal of Applied Physics, 138 085102 (2025).

P09

Dry-etched facets for InAs/AlSb quantum cascade lasers compatible with monolithic integration

Algimantas Lukša[1], Mindaugas Kamarauskas[1], Virginijus Bukauskas[1], Viktorija Nargelienė[1], Karina Pokaliuk[1], Ramūnas Levinas[2] and Jan Devenson[3]

[1]*Department of Physical Technologies, Center for Physical Sciences and Technology, Sauletekis av. 3, Vilnius, Lithuania*
[2]*Department of Catalysis, Center for Physical Sciences and Technology, Sauletekis av. 3, Vilnius, Lithuania*
[3]*Department of Optoelectronics, Center for Physical Sciences and Technology, Sauletekis av. 3, Vilnius, Lithuania*
Email: algimantas.lukša@ftmc.lt

Quantum cascade lasers (QCLs) are compact, electrically-pumped semiconductor sources of mid-infrared (MIR) radiation, uniquely suited for applications spanning trace-gas spectroscopy, chemical sensing, and free-space optical communications [1]. Conventional QCL fabrication relies on wafer cleaving to form laser mirror facets. While cleaving yields optically smooth surfaces, it is fundamentally incompatible with monolithic photonic integration. Replacing cleaved mirrors with lithographically defined, dry-etched facets enables the realization of fully monolithic mid-infrared photonic integrated circuits. Such platforms are especially compelling for surface plasmon polariton (SPP) integrated gas sensors, where QCL sources, plasmonic waveguides, and detectors must be co-integrated on a single substrate to exploit the strong evanescent field overlap between SPP modes and the molecular absorption fingerprints of target analytes [2, 3].

In this work we demonstrate InAs/AlSb QCLs emitting near 9.5 μm in which the mirror facets are formed entirely by inductively coupled plasma reactive ion etching using a BCl_3-Cl_2-Ar-based process chemistry. Scanning electron microscopy (SEM) image (Fig. 1) confirms that the etched sidewalls are smooth and nearly vertical, with a measured etch angle below 2° from the normal to the wafer surface. Atomic force microscopy characterization of the etched floor reveals a surface roughness below 2.5 nm RMS. This level of smoothness is compatible with direct metal deposition for SPP waveguide fabrication, where interface roughness between the metal film and the semiconductor surface is critical for minimizing plasmonic propagation losses.

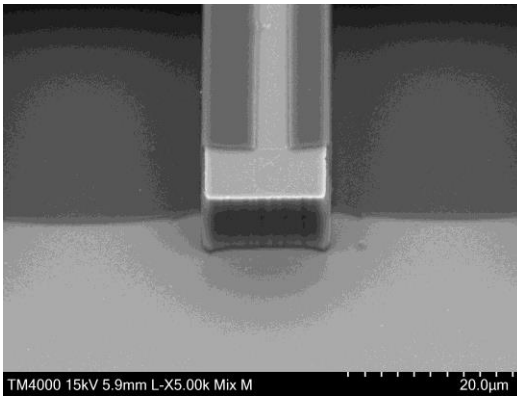


Fig. 1 SEM image of dry-etched QCL mirror facet

REFERENCES

[1] Yao, Y., Hoffman, A. & Gmachl, C. Mid-infrared quantum cascade lasers. Nature Photon 6, 432–439 (2012).
[2] Schwarz, B., Reininger, P., Ristanić, D. et al. Monolithically integrated mid-infrared lab-on-a-chip using plasmonics and quantum cascade structures. Nat Commun 5, 4085 (2014).
[3] Qiangqiang Guo, Jinchuan Zhang, Ke Yang, Yixuan Zhu, Quanyong Lu, Ning Zhuo, Shenqiang Zhai, Junqi Liu, Lijun Wang, Shuman Liu, and Fengqi Liu, "Monolithically integrated mid-infrared sensor with a millimeter-scale sensing range," Opt. Express 30, 40657-40665 (2022)

P10

Peculiarities of power- and temperature-dependent photoluminescence of MBE grown GaAsBi layer.

Aurimas Čerškus[1], Aivaras Špokas[1], Andrea Zelioli[1], Evelina Dudutienė[1] and Renata Butkutė[1]

[1]*Center for Physical Sciences and Technology, Saulėtekio av. 3, Vilnius, LT-10257, Lithuania.*
Email: aurimas.cerskus@ftmc.lt.

Bismuth (Bi) incorporation in GaAs induces band-gap reduction, increase in spin-orbit splitting energy, changes in effective mass, and all of this makes GaAsBi an attractive material in optoelectronics for applications in the near-infrared and terahertz range [1]. Both nondestructive methods, such as power-dependent and temperature-dependent photoluminescence (PL), give valuable information. Analysis of thermal quenching of the PL signal by fitting it with the expression of the Arrhenius type shows activation energies E_{ai} of processes in the material [2]:

$$I_{\mathrm{PL}}(T) = \frac{I_{\mathrm{PL}}(0)}{1+C_1\exp(-E_{\mathrm{a1}}/kT)+C_2\exp(-E_{\mathrm{a2}}/kT)} \dots . \quad (1)$$

Here, C_i are the fitting parameters; k is a Boltzmann constant.

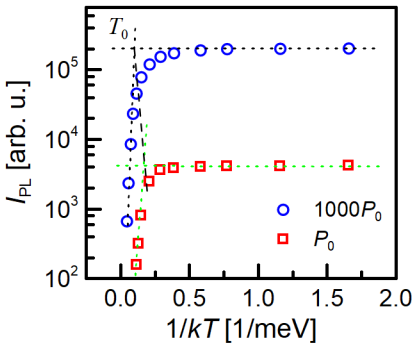


Fig. 1 Arrhenius plots of the temperature-dependent PL intensity from GaAsBi layer at two excitation intensities. Lines are as guidelines.

However, the drop in PL intensity near critical temperature T_0 (see Fig. 1, point where the largest slope crosses the extrapolated low-temperature part) may be very abrupt (nearly vertical in the Arrhenius plot), so that the 'activation energy' or the measured slope could have no physical meaning. Nevertheless, the ionization energy E_a of the acceptor can be found from the fit of the T_0 dependence on the G generation rate (or excitation intensity P) using Equation (2) [3]:

$$T_0 = \frac{E_{\mathrm{a}}}{k\ln(B/G)} \dots . \quad (2)$$

Here, B is a constant for the acceptor. The parameter C_i in (1) can formally be changed as $C_i = B_i/G$.

We will discuss about the energy values extracted using Equations (1) and (2), check their correlation with the values of the mobility edge extracted from time resolved PL measurements and the energy scale of disorder extracted from the temperature-dependent PL peak energy.

REFERENCES

[1] L. Wang, L. Zhang, L. Yue, D. Liang, X. Chen, Y. Li, P. Lu, J., Shao, and S. Wang; *Crystals* **7** (2017) pp. 63.
[2] T. Wilson, N.P, Hylton, Y, Harada, P. Pearce, D. Alonso-Alvarez, A. Mellor, R.D. Richards, J.P.R. David and N.J. Ekins-Daukes; *Sci Rep* **8** (2018) pp. 6457.
[3] M.A. Reshchikov; *Phys. Status Solidi A* **218** (2021) pp. 20000101.

P11

Sustainable Thin-Film Transistor Platform with Integrated Opto-acoustic Anticounterfeiting Features for Smart Electronics

Nisha Naik[a], Ashok Rao[a], Joydeep Biswas[b], Dhanya Sunil[a],

[a]*Manipal Institute of Technology, Manipal Academy of Higher Education, Manipal, India.*

[b]*Department of Chemistry, Sikkim Manipal Institute of Technology, Sikkim Manipal University, Majitar, 737136, Sikkim, India*

Email: a.rao@manipal.edu

Abstract: Thin-Film Transistors (TFTs) have developed from display backplanes to printed, transparent, and conformal forms, flooring the way for next-generation wearable, smart, and secure electronics [1]. TFT-based anticounterfeiting architecture promises significant impact on secure electronics, offering scalable, flexible, and cost-effective protection against product forgery. In the present study, graphene oxide (GO) was prepared by the modified Hummers' method and reduced using ascorbic acid. Furthermore, a NiO/rGO composite was synthesized through microwave irradiation, and its structure was established by XRD, FTIR, XPS, FESEM, and EDX. Commercial phosphor embedded NiO/rGO-based TFT displayed an n-channel behavior with a high on/off current ratio of 1.95×10^6, a field-effect mobility of 0.16 $cm^2/V \cdot s$, and a low subthreshold swing of 0.075 V/decade, highlighting the device's potential for low-voltage, high-performance electronic applications. Furthermore, the TFT integrates built-in optical and acoustic security features, exhibiting blue emission at 475 nm and an audible response under 980 nm laser excitation, as established through visual and audio recordings, corroborates the device's potential as a multifunctional smart, sustainable and secure platform for advanced anticounterfeiting applications [2].

REFERENCES

[1] A. Fei, "A review of the development of transistor technology and its application in electronic devices," *Applied and Computational Engineering*, vol. 56, no. 1, pp. 141–145, Apr. 2024, doi: 10.54254/2755-2721/56/20240642.
[2] I. Boukhoubza *et al.*, "Graphene oxide concentration effect on the optoelectronic properties of ZnO/GO nanocomposites," *Nanomaterials*, vol. 10, no. 8, pp. 1–16, Aug. 2020, doi: 10.3390/nano10081532.

P12

Redirecting of THz beams using flat optical elements dependent on polarization

Adrianna Nieradka[1], Paweł Komorowski[2], Mateusz Kaluza[1] and Agnieszka Siemion[1,3]

[1]*Faculty of Physics, Warsaw University of Technology, 00-662, Warsaw, Poland*
[2]*Institute of Optoelectronics, Military University of Technology, 00-908 Warsaw, Poland*
[3]*Center for Advanced Materials and Technologies CEZAMAT, Warsaw University of Technology, Poleczki 19, 02-822 Warsaw, Poland*
Email: adrianna.nieradka.dokt@pw.edu.pl

Terahertz (THz) radiation has attracted significant attention due to its potential applications in communication, imaging, and sensing systems. In this work, flat optical elements with subwavelength details, fabricated using additive manufacturing, were investigated as compact components for THz beam redirecting and focusing. The structures are based on cyclic olefin copolymer (COC), a material characterized by low absorption coefficient and low refractive index in the THz range. Particular attention is devoted to the structures with different infill geometries, enabling the control of the effective refractive index and the realization of constant-thickness optical elements. Measurements were performed for structures introducing phase delay either through the fill factor (FF) of subwavelength geometries or through geometrical thickness variation. An example of a measurement for variable thickness conical [1] lens designed for a 10° beam deflection angle is presented in Fig. 1, demonstrating simultaneous beam redirection and focusing into an elongated half-line formed just after the structure.

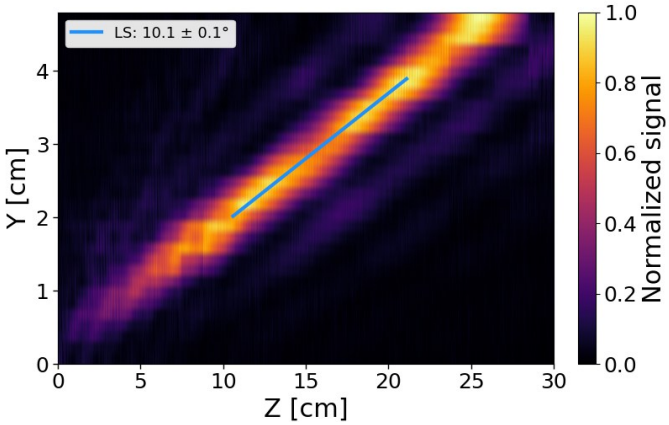


Fig. 1. Normalized signal distributions (Y-Z plane) measured at 96 GHz for the conical 10° element, illustrating beam redirecting and focusing into elongated half-line.

The proposed structures can be applied in compact systems dedicated to the characterization of subwavelength samples in the sub-THz regime. In liquid-crystal-based wedge systems, proper matching of the source polarization is essential for efficient refractive index modulation [2] and controlled beam deflection. Moreover, constant-thickness gradient-index (GRIN) optical elements also exhibit polarization-dependent behavior resulting from their subwavelength internal geometry. Consequently, the efficiency of beam steering depends not only on the operating frequency and infill parameters, but also on the polarization orientation of the THz source.

REFERENCES

[1] A. Siemion, A. Siemion, J. Suszek, A. Kowalczyk, J. Bomba, A. Sobczyk, N. Palka, P. Zagrajek, A. Kolodziejczyk, and M. Sypek, “THz beam shaping based on paper diffractive optics,” IEEE Trans. Terahertz Sci. Technol. 6(4), pp. 568–575 (2016).
[2] U. Chodorow, E. Mavrona, N. Palka, O. Strzezysz, K. Garbat, S. Saitzek, J. F. Blach, V. Apostolopoulos, M. Kaczmarek, and J. Parka, “Terahertz properties of liquid crystals doped with ferroelectric BaTiO3 nanoparticles,” Liquid Crystals 44(8), pp. 1207–1215 (2017).

P13

Surface current phase governing Fano type resonance in metasurface

P.Ragulis[1], D.Seliuta[2] and Ž. Kancleris[1]

[1]Department of Physical Technologies and [2]Department of Optoelectronics, Centre for Physical Sciences and Technology, Saulėtekio av, 3, Vilnius, Lithuania.

Email: paulius.ragulis@ftmc.lt

We consider the simplest inverse periodic metasurface (MS) composed of two parallel slits of different lengths, oriented perpendicular to the applied microwave electric field and cut in a copper foil. It will be shown that the Fano effect appears as a consequence of the phase shift of the current flowing in the inner ends of the strips, parallel to the E-field.

The measured and calculated dependencies of the transmittance on frequency are shown in Fig. 1. In the inset, the elementary cell of the investigated structure is depicted. At a lower frequency, a sharp change from near-complete transparency to almost total suppression within a 150 MHz frequency range is seen, which is characteristic of the Fano effect [1]. It is worth mentioning that in this frequency range, currents in the shorter and longer slits flow in opposite directions, whereas at a higher frequency, where the second, much wider maximum is noticed and is ascribed to plasmonic resonance, they flow in phase.

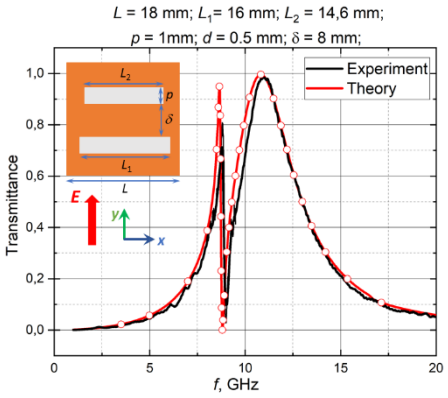


Fig. 1. Dependence of transmittance on frequency. In the inset - unit cell of MS.

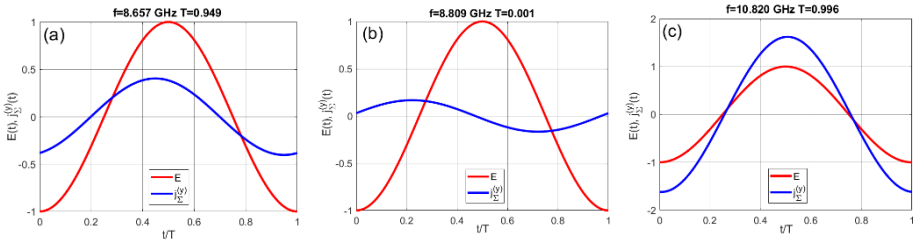


FIG. 2. Calculated electric field and summed average current j_y dependences on time at the Fano interference maximum f = 8.657 GHz, (a); at minimum f = 8.809 GHz (b), and at the maximum of plasmonic resonance f = 10.82 GHz (c).

Calculated waveforms of summed current $j_{\Sigma y}$ and the electric field within one period at characteristic frequencies of Fano interference and plasmonic resonance are shown in Fig. 2. It is seen that at transmittance maxima (a) & (c), the phases of the electric field and current approximately coincide, whereas at the minimum, the shift of the phase by $\pi/2$ appears. This suggests that the current phase in the slits is a primary factor determining the observed sharp transition from total transparency to opacity that is characteristic of Fano resonance. It is worth mentioning that the same peculiarities we observe in an inverse metasurface designed according to Babinet's principle and consisting of conductive strips oriented parallel to the external electric field. The only difference is that in the MS made from strips, the minimum of transmittance appears at lower frequency followed by its maximum.

REFERENCES

[1]. M. F. Limonov, Advances in Optics and Photonics, vol. 13, no. 3, pp. 703–771, 2021.

P14

Extinction engineering in graphene plasmonic resonators for terahertz applications.

Mohammad Esmaeil Daraei[1], Mehdi Abedi-Varaki[2] and Ignas Nevinskas[1]

[1]*Department of Optoelectronics, Center for Physical Sciences and Technology, Saulėtekio ave. 3, LT-10257 Vilnius, Lithuania.*

[2]*Department of Laser Technologies, Center for Physical Sciences and Technology, Savanoriu ave. 231, LT-02300 Vilnius, Lithuania.*

Email: esmaeil.daraei@ftmc.lt.

Graphene plasmonics [1, 2] enables actively tunable terahertz (THz) devices through electrically controllable carrier concentration and strong electromagnetic confinement. In this work, a graphene plasmonic resonator composed of concentric circular sectors and partial rings is investigated using finite-element method simulations. Unlike conventional studies focused on absorption, the analysis is based on the extinction cross section [3], which includes both absorption and scattering. The structure supports localized plasmonic resonances with strong coupling to incident THz radiation. Increasing the graphene chemical potential shifts the dominant resonance from approximately 2.3 to 5 THz, demonstrating efficient electrostatic tunability. Relaxation time mainly affects resonance amplitude and linewidth, while geometry and dielectric environment provide additional spectral control. Normalized extinction values that approach or exceed unity are achieved, indicating highly efficient interaction between incident radiation and localized graphene plasmons. These results highlight extinction as a useful metric for the design of tunable THz graphene plasmonic devices and sensing platforms.

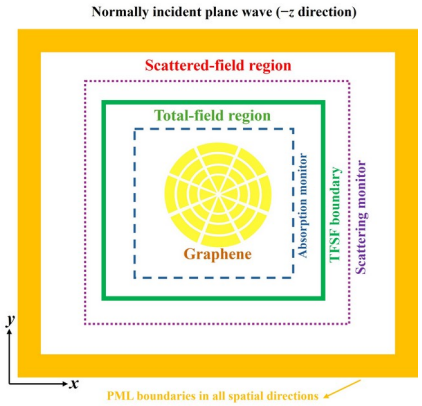


Fig. 1 Simulation configuration for the single graphene resonator, including the TFSF regions, absorption and scattering monitors, incident plane-wave excitation, and PML boundaries.

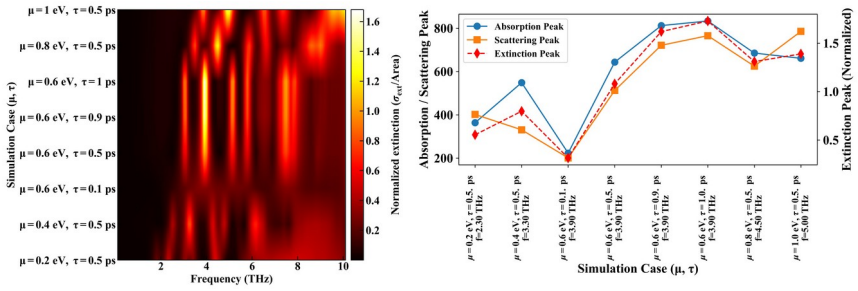


Fig. 2 Normalized extinction of the graphene plasmonic resonator for different chemical potentials and relaxation times: (a) extinction heatmap summarizing the combined dependence on μ and τ, (b) comparison of peak absorption, scattering, and extinction amplitudes.

REFERENCES

[1] Q. Bao and K. P. Loh, ACS nano 6 (5), 3677–3694 (2012).

[2] F. J. Garcia de Abajo, ACS photonics 1 (3), 135–152 (2014).

[3] J. D. Jackson, Classical electrodynamics. (John Wiley & Sons, 2021).

P15

Operator-based exciton–vibrational (OBEV) modelling of *Rhodobacter sphaeroides* bacterial reaction centre using mean-field and one-quantum closures

Arunjyoti Baidya[1], Darius Abramavicius[1], Vytautas Bubilaitis[1]
[1]*Institute of Chemical Physics, Vilnius University, Saulėtekio al. 3, Vilnius, 10257*
arunjyoti.baidya@ff.vu.lt

Bacterial reaction centres (BRC) exhibit strongly coupled electronic excitations embedded in a structured vibrational environment, where exciton delocalisation, vibronic fluctuations, and relaxation jointly shape optical observables. To connect microscopic Hamiltonian models with measurable spectra while retaining explicit bath degrees of freedom, we implement a Heisenberg-picture operator-based formulation. The electronic subsystem is represented by excitonic projection operators, while the vibrational environment is modelled as independent harmonic oscillators linearly coupled to site populations. This operator framework naturally yields a hierarchy of coupled equations for electronic populations/coherences and mixed exciton–phonon correlators [1]. To obtain scalable and tractable dynamics for a complex multi-site BRC model, we implement two complementary closures of the OBEV hierarchy. In the mean-field approximation (MFA), mixed exciton–phonon correlators are factorized, yielding a self-consistent set of equations that captures bath-induced fluctuations and reorganization efficiently. In the one-quantum approximation (1QA), the leading mixed correlators are propagated explicitly, incorporating quantum corrections responsible for vibrational sidebands and asymmetric broadening beyond MFA. Temperature effects are included through thermal ensemble sampling of initial bath configurations, and spectra are obtained from the Fourier transform of the ensemble-averaged time-dependent polarization. We present BRC simulations highlighting how (i) MFA, (ii) pure 1QA, and (iii) hybrid MFA+1QA partitions across frequency windows affect lineshapes and vibronic features, and we discuss the parameter regimes in which quantum corrections are essential. This workflow provides an efficient route for spectroscopy-oriented modelling of *R. sphaeroides* BRC [2] and establishes a foundation for extensions to multidimensional signals and comparison with experiment.

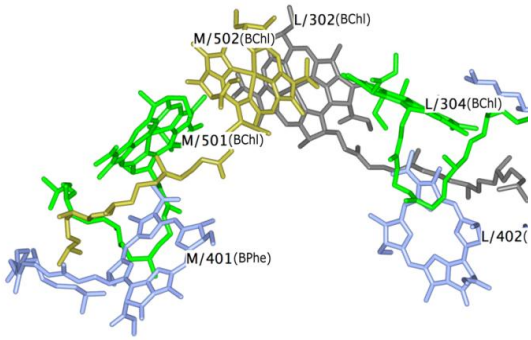


Fig. 1 The arrangement of the chlorophyll-type pigments of Rb. Sphaeroides. (PDB ID 2J8C).

REFERENCES

[1] Bubilaitis V, Rancova O, Abramavicius D. J. Chem. Phys. **154**, 214115 (2021)
[2] Bubilaitis V, Abramavicius D. Chemical Physics **588**, 112445 (2025)

P16

Terahertz Beam Shaping with Diffractive Optics

Mateusz Kaluza[1], Joanna Starobrat[1], Marta Kurowska[1], Dmytro B. But[2] and Agnieszka Siemion[1,2]

[1]*Faculty of Physics, Warsaw University of Technology, Koszykowa 75, 00-662, Warsaw, Poland*
[2]*CENTERA, CEZAMAT, Warsaw University of Technology, Poleczki 19, 02-822 Warsaw, Poland*
Email: mateusz.kaluza@pw.edu.pl

Diffractive optical elements (DOEs) provide compact and flexible solutions for beam shaping applications across different spectral ranges, including the terahertz (THz) domain [1]. In this study, an iterative holographic approach for designing THz diffractive structures dedicated to tailored beam shaping applications is presented. The proposed method is based on iterative wavefront propagation between the DOE plane and the target plane with enforced amplitude corresponding to a Gaussian THz source distribution and a predefined target intensity profile.

The designed structure operates at 267 GHz and transforms the incident beam into two separated focal line segments at a distance of 100 mm from the element. Numerical simulations were performed to evaluate different target intensity profiles and improve the uniformity of the generated line segments. Figure 1a presents the phase delay map of the designed diffractive structure, while Fig. 1b shows the simulated intensity distribution obtained at a propagation distance of 100 mm behind the DOE. The optimized DOE was fabricated via 3D printing using cyclic olefin copolymer, a material with low absorption in the THz radiation range [2]. Experimental measurements confirmed the formation of the designed two-segment intensity distribution, showing good qualitative agreement with numerical results.

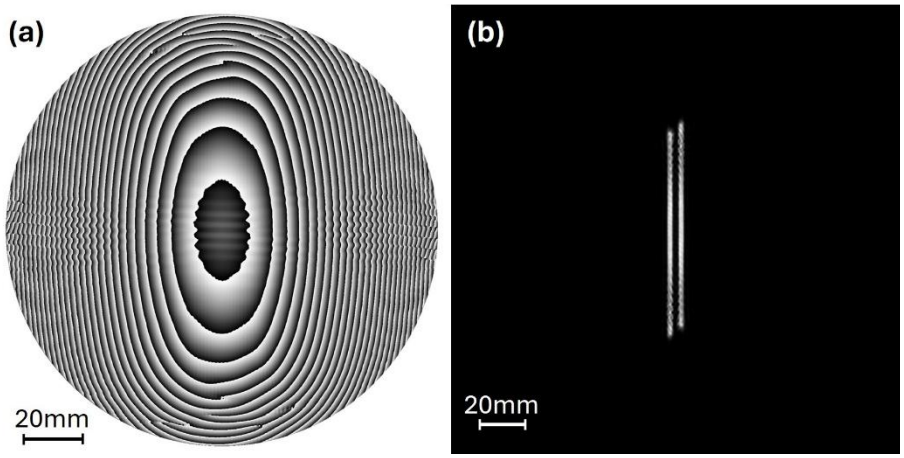


Fig. 1. (a) Phase delay map of the designed diffractive optical element and (b) simulated intensity distribution obtained at a propagation distance of 100 mm behind the structure.

These results demonstrate the potential of iterative holographic design combined with additive manufacturing for developing application-specific THz diffractive optics, particularly for beam shaping in scanning and imaging systems.

REFERENCES

[1] A. Siemion; *Journal of Infrared, Millimeter, and Terahertz Waves* **40** (2019) pp. 477–499.
[2] M. Kaluza, M. Walczakowski, and A. Siemion; *Materials* **17** (2024) p. 5104.

P17

Cell cultured in 3D scaffolds analyzed by second harmonic images

Elisabetta Sieni[1], Danielis Rutkauskas[2], Renata Karpicz[2], Monica Dettin[3], Annj Zamuner[3], Maria Teresa Conconi[3], and Patrizia Lamberti[4]

[1]*University of Insubria, via O. Rossi, 9, Varese, Italy*
[2]*Center for Physical Sciences and Technology (FTMC), Address – Vilnius, Lituania.*
[3]*Padova university, via Marzolo, 9, Padova, Italy*
[4]*Salerno university, Fisciano (SA), Italy*

Email: elisabetta.sieni@uninsubria.it

In this proposal we introduce a functionalized Hyaluronic Acid (HA) scaffold for 3D cell growth. The functionalization of the HA scaffolds was made using self-assembly peptides with laminin adhesion sequence. The resulting scaffold is named HA-EAbuK-IKVAV scaffold and it was used to seed cells of different cell lines. From preliminary results it shown Extra-Cellular-Matrix (ECM) with collagen fibers deposition [1]. The ECM at Masson trichrome histological staining showed collagen area depositions depending on the seeded cell type (e.g. breast cancer, melanoma, cervical cancer, etc.). Cells were seeded in the scaffolds after scaffold hydration with cell medium and cultured three days before analysis.

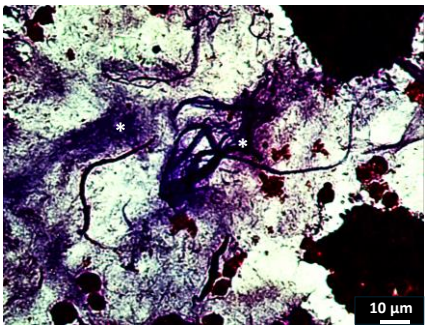
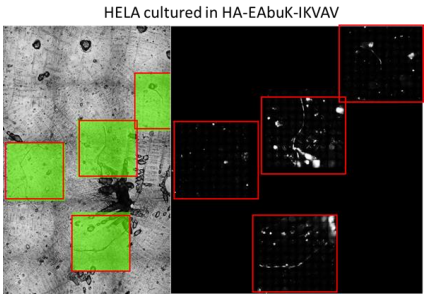


Fig. 1 Example of Masson trichrome staining. Blue area with white stars is collagen.



ig. 2 Example of second harmonic

After three days from the seeding the cultured scaffolds were verified for cell viability and collected for further analysis. They were positioned on a microscope slide with formalin for cell preservation and air dried for histological staining and analysis at biphoton. Fig. 1 shows an example of Masson trichrome staining of Hela cells cultured in HA-EAbuK-IKVAV scaffold where blue area represents the collagen.

Collagen fiber network was imaged using custom-built wide-field second-harmonic generation (SHG) microscopy system [2]. Exemplary tiled SHG image is presented in Figure 2 (right). Corresponding brightfield image is presented in Figure 2 (left).

ACKNOWDLEGEMENT

This work was supported by the THz-Skin project, which has received funding from the European Union

REFERENCES

[1] A. Zamuner A., et Al., Bioelectrochemistry (2024), 156, art. no. 108624,
[2] Padrez, Y., et Al., (2024). *Computerized Medical Imaging and Graphics*, 117:102440

P18
Hybrid Terahertz Imaging with Different Arrangements of 3D-Printed Beam-Shaping Components

Kasparas Stanaitis[1,2], Linas Minkevičius[1], Sergej Orlov[1], Gintaras Valušis[2]

[1]*Center for Physical Sciences and Technology, Department of Optoelectronics, Vilnius, Lithuania*
[2]*Vilnius University, Institute of Photonics and Nanotechnology, Vilnius, Lithuania*
Email: kasparas.stanaitis@ftmc.lt

Optical imaging systems play a critical role across scientific and industrial fields, including non-destructive material inspection, security screening, and industrial quality control. While traditional imaging solutions usually depend on high-energy radiation like X-rays, which show clear drawbacks regarding operational safety, system cost, and potential sample degradation, terahertz (THz) imaging offers a safer alternative by utilizing non-ionizing radiation that can easily penetrate various dielectric materials [1].

This research investigates thin, 3D-printed diffractive optical elements engineered to shape different THz beam profiles, specifically Gaussian, Bessel, and Airy distributions [2]. These elements are incorporated into a hybrid THz imaging architecture capable of performing both amplitude-based and interferometric measurements. Fabricated using extrusion 3D printing, these diffractive components are utilized for beam focusing, and signal collection from the target. The imaging performance is evaluated by testing different combinations of these beam-shaping elements at various positions in the optical system. Different imaging targets such as low-absorbing and thick ones are investigated. The overall system capabilities are assessed by quantitatively comparing image quality between the direct amplitude and interferometric imaging modes. Finally, the impact of these various component configurations on spatial resolution and image contrast are evaluated to identify the optimal lens combinations for THz imaging applications.

The results show, that there is no single best optical component arrangement. The Bessel-Gaussian combination was shown to be the most verstile, while Gaussian-Bessel combination yields the highest numerical resolution. Upon thick object imaging evaluation, it was concluded that Bessel-Gaussian combination performs the best in direct imaging arangement while Airy-based combinations are superior for interferometric imaging applications.

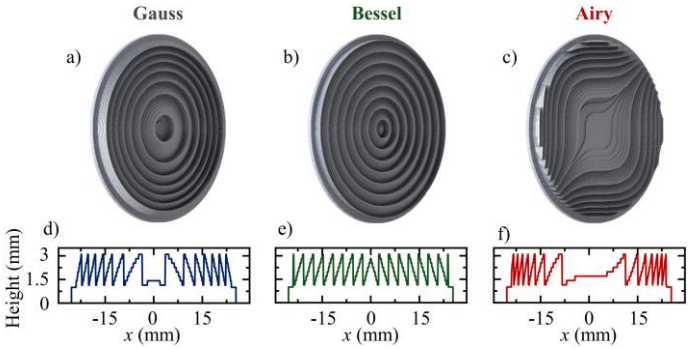


Fig. 1 (a) – (c) Models of THz optical components evaluated in the system, (d) – (f) height profiles along the x-axis

REFERENCES

[1] G. Valušis, A. Lisauskas, H. Yuan, W. Knap, and H. G. Roskos; Sensors 21(12) (2021) p. 4092.

[2] S. Orlov, R. Ivaškevičiūtė-Povilauskienė et al., Laser & Photonics Reviews 18(5) (2024) p. 2301197.

P19
Comparative Benchmarking of ML Models for Magnetic Field Prediction from Simulated ODMR Spectra

Mantas Skaržinskas[1], Tadas Paulauskas[1]
[1]*Center for Physical Sciences and Technology, Saulėtekio av. 3, LT-10257, Vilnius, Lithuania.*
Email: mantas.skarzinskas@ftmc.lt.

Nitrogen-vacancy (NV) centers in diamond are promising room temperature quantum sensors because optically detected magnetic resonance (ODMR) encode magnetic field information through Zeeman shifts and the projection of the applied field onto the four crystallographic NV orientations [1]. Fast and data efficient extraction of secondary information contained through magnetic fields in ODMR is important for practical magnetometry. This work benchmarks machine learning models for magnetic field prediction from simulated hyperfine resolved four orientation NV-ensemble ODMR [2]. Each sample is an ODMR spectrum and the prediction target is the magnetic field magnitude in the range 0-10 mT.

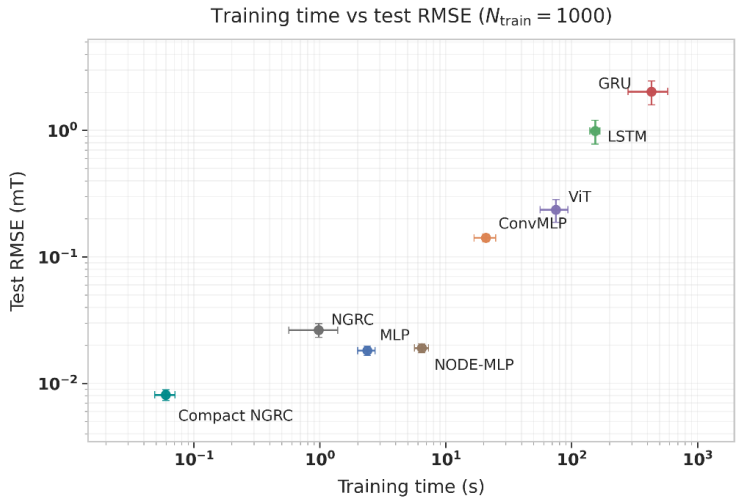


Fig. 1. Accuracy and time tradeoff for magnetic field prediction from simulated ODMR spectra.

We compared Next-Generation Reservoir Computing (NG-RC) and Compact (NG-RC) [3] with common neural network baselines, including Multilayer Perceptron (MLP), Neural Ordinary Differential Equation based Multilayer Perceptron (NODE-MLP), Convolutional Multilayer Perceptron (ConvMLP), Vision Transformer (ViT), Long Short-Term Memory (LSTM) and Gated Recurrent Unit (GRU). We tested training set sizes from 10 to 1000 samples using six repeated splits. With very small training sets (up to 50 samples), the error bars overlap, from 100 samples Compact NGRC gives the best test accuracy and smallest training time. With 1000 training spectra, Compact NGRC reaches an average error of 0.0081 ± 0.0008 mT and a near perfect coefficient of determination (0.999992 ± 0.000001), while training in 0.0597 ± 0.0109 seconds. At this setting it is about 40 times faster than MLP, 108 times faster than NODE-MLP and more than 7000 times faster than GRU.

REFERENCES

[1] M. W. Doherty, N. B. Manson, P. Delaney, F. Jelezko, J. Wrachtrup, and L. C. L. Hollenberg, “The nitrogen-vacancy colour centre in diamond,” Physics Reports, vol. 528, no. 1, pp. 1–45, Jul. 2013.
[2] Y. Zhu, E. Losero, C. Galland, and V. Goblot, “Simulation of ODMR Spectra from Nitrogen-Vacancy Ensembles in Diamond for Electric Field Sensing,” Jan. 2023.
[3] D. J. Gauthier, E. Bollt, A. Griffith, and W. A. S. Barbosa, “Next generation reservoir computing,” Nat Commun, vol. 12, no. 1, p. 5564, Sep. 2021.
[4] A. Afshar, A. H. Proppe, N. Lupu-Gladstein, L. Childress, A. Z. Goldberg, and K. Heshami, “Magnetometry with Broadband Microwave Fields in Nitrogen-Vacancy Centers in Diamond,” Sep. 2025.

P20

Quantum cutting in lead halide perovskites

Simona Streckaite[1], Daniel Rodz[1], Lukas Razinkovas[1], Vitalii Boiko[2], Mariusz Stefanski[2], Dariusz Hreniak[2], Vidmantas Gulbinas[1]

[1]Center for Physical Sciences and Technology, Sauletekio Ave. 3, Vilnius 10257, Lithuania
[2]Institute of Low Temperature and Structure Research, Polish Academy of Sciences, Okolna 2, Wroclaw 50-422, Poland

Ytterbium-doped lead halide perovskites are promising materials for optical and optoelectronic applications due to the stable near-infrared (NIR) emission (~1000 nm) of Yb^{3+} ions and their low nonradiative losses. In these materials, Yb^{3+} ions can enable quantum cutting (QC), where one high-energy photon absorbed by the perovskite host is converted into two NIR photons, emitted by the dopant. This process offers a potential route to improve the efficiency of silicon solar cells [1]. QC in Yb^{3+}-doped perovskites is associated with the $^2F_{5/2} \rightarrow {}^2F_{7/2}$ transition of Yb^{3+}. Although this transition is parity-forbidden for free Yb^{3+} ions, it becomes partially allowed in the perovskite lattice due to crystal-field interactions. Previous studies have shown that both QC-active and inactive Yb^{3+} species can coexist in the $CsPb(Cl_xBr_{1-x})_3$ lattice [2,3].

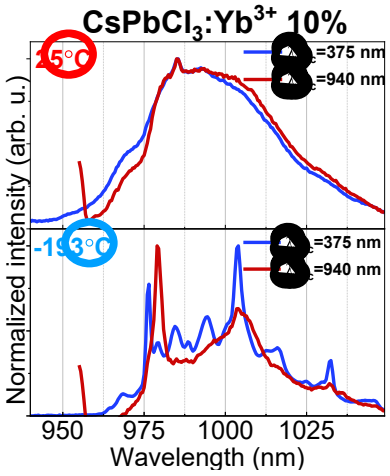


Fig. 1. PL spectra in NIR region at different temperatures of Yb-doped $CsPbCl_3$ upon 375 nm (blue) and 940 nm (red) excitation.

Here, we investigate the photoluminescence (PL) dynamics and oscillator strength of the $^2F_{5/2} \rightarrow {}^2F_{7/2}$ radiative transition for different Yb^{3+} species in $CsPb(Cl_xBr_{1-x})_3$ polycrystalline powders. Time-resolved PL measurements were performed under selective excitation of the perovskite host across its band gap and direct intra-4f excitation of Yb^{3+} ions. This approach allows us to distinguish the dynamics of Yb^{3+} species that are active and inactive in QC across different perovskite matrices.

We show that increasing temperature accelerates the PL decay and enhances the oscillator strength of Yb^{3+} ions, independently of the anion composition. However, the temperature dependence of the decay rate differs for QC-active and inactive Yb^{3+} species, indicating that their local environments and relaxation pathways are distinct. In $CsPbBr_3$ powders, where QC is strongly suppressed, the PL intensity and decay rate are governed by temperature-dependent host-to-Yb^{3+} energy transfer together with nonradiative relaxation. These results clarify the role of different Yb^{3+} centers in lead halide perovskites and provide guidelines for optimizing lanthanoid-doped materials for NIR emission and solar spectral conversion.

REFERENCES

[1] D. Zhou et al., *Nano Lett* 19 (2019) 6904.
[2] S. Streckaitė et al., *J. Mat. Chem. C* 12 (2024) 11995.
[3] S.M. Loh et al., *J. Phys. Chem. Lett.* 16 (2025) 2295.

This research has received funding from the Research Council of Lithuania (LMT) under Polish-Lithuanian project DAINA-3, agreement No [S-LL-24-11].

P21

Zinc gallium oxide nanocrystals doped with Cr^{3+} and Yb^{3+} for persistent luminescence bioimaging

Vilius Čirgelis[1], Simona Streckaitė[1], Vidas Pakštas[1], Vitalli Boiko[2], Lena Golubewa[1], Mariusz Stefanski[2], Dariusz Hreniak[2] and Vidmantas Gulbinas[1]

[1]Center for Physical Sciences and Technology, Sauletekio Ave. 3, 10257 Vilnius, Lithuania.
[2]Polish Academy of Sciences, Institute of Low Temperature and Structure Research, Okolna 2, 5-422 Wroclaw, Poland
Email: vilius.cirgelis@ftmc.lt

Zinc gallium oxide ($ZnGa_2O_4$, ZGO) is a cubic spinel-structured oxide that has recently attracted considerable interest for various photonic applications [1]. Owing to its chemical stability, resistance to oxidation and humidity, and biocompatibility, ZGO is a promising phosphor material for bioimaging applications [2]. In the ZGO lattice, Zn^{2+} ions occupy tetrahedral sites, while Ga^{3+} ions occupy octahedral sites. During the synthesis, partial cation inversion may occur. In this case, a fraction of Zn^{2+} ions occupy octahedral sites, while a fraction of Ga^{3+} ions occupy tetrahedral sites, leading to the formation of antisite defects [3]. Antisite defects act as charge traps, storing excitation energy from hours to days and enabling delayed emission known as persistent luminescence (PersL). Persistent luminescence is particularly advantageous for *in vivo* bioimaging because the material can be pre-charged *ex vivo* and subsequently injected into an organism. This allows imaging without continuous laser excitation, reducing tissue autofluorescence, minimizing phototoxicity and thermal damage. Additional doping with Cr^{3+} and Yb^{3+} can tune ZGO emission to the first (700-900 nm) and second (1000-1700 nm) biological windows, which are characterized by low tissue absorption and scattering, enabling deep-tissue imaging.

In the current study, Cr^{3+}- and Yb^{3+}-doped and Cr^{3+}/Yb^{3+} co-doped $ZnGa_2O_4$ nanoparticles (NPs) were synthesized hydrothermally from metal nitrate precursors at pH 8 and 200 °C for 24 h. The NPs were collected via ultracentrifugation, washed, dried, and annealed at 200–900 °C for 3 h. The structural and optical properties of ZGO:Cr^{3+} were investigated using X-ray diffraction (XRD), steady-state and time-resolved photoluminescence (PL), thermoluminescence, and diffuse reflectance spectroscopy.

XRD analysis confirmed the formation of the cubic spinel structure in the synthesized $ZnGa_2O_4$ materials. With increasing annealing temperature, the diffraction peaks became narrower, indicating improved crystallinity, crystallite growth, and reduced microstrain or defect-related broadening up to 800 °C. At 800 °C, the XRD pattern closely matched that of the pre-annealed sample, suggesting a structural phase transformation or significant crystallinity improvement. The highest steady-state PL intensity was observed for the 1.00 mol% Cr^{3+}-doped ZGO. In contrast, the longest persistent-luminescence decay was obtained for the 0.25 mol% Cr^{3+}-doped sample, indicating that the optimal Cr^{3+} concentration for steady-state emission intensity does not necessarily coincide with the optimal concentration for persistent luminescence.

REFERENCES

[1] E. Chikoidze, et al. *Cryst. Growth and Design.* **2020** 20 (4) 2535-2546.
[2] M. N da Silva, et al. *ACS App. Nano Mat*. **2019** 2(11) 6918-6927.
[3] A. De Vos, et al. *Inorg. Chem.* **2016** 55(5), 2402-2412.

P22

Graded AlGaAs barriers for near-infrared emission enhancement in InGaAs and GaAsBi quantum wells

Denis Goldobin, Aistė Štaupienė, Aivaras Špokas, Andrea Zelioli, Martynas Skapas, Aurimas Čerškus, Evelina Dudutienė and Renata Butkutė

SRI Center for Physical Sciences and Technology, Saulėtekio ave. 3, LT-10257, Vilnius, Lithuania
Email: denis.goldobin@ftmc.lt

III-V semiconductor quantum well (QW) heterostructures are widely employed in near-infrared photonic devices, yet radiative efficiency is often limited by non-radiative losses, which graded-barrier design directly addresses. InGaAs and GaAsBi occupy complementary roles in this study: the former serves as a mature, well-studied reference system, while GaAsBi offers a temperature-insensitive bandgap and spin-orbit splitting sufficient to suppress Auger recombination [1], though its adoption is constrained by challenging growth conditions. Graded barrier profiles enhance carrier trapping in both systems [2,3], improving radiative efficiency and thermal stability.

Three barrier profiles were investigated: parabolic (PQW) and linear (TrQW) AlGaAs barriers with Al content varying from 30% to 0% at the QW interface, and references with rectangular GaAs barriers (RQW). Structures were grown by molecular beam epitaxy on semi-insulating GaAs(100) substrates. Characterisation techniques employed temperature-dependent photoluminescence (PL), photoreflectance, time-resolved PL, transmission electron microscopy, and *nextnano* simulations. In InGaAs QWs, PQW sample sustains the highest PL intensity up to 300 K. Similarly, in GaAsBi QWs, the sample with parabolic grading yields more than three times the room-temperature PL intensity of the linear barrier sample, while both graded profiles achieve greatly enhanced carrier localization relative to RQWs.

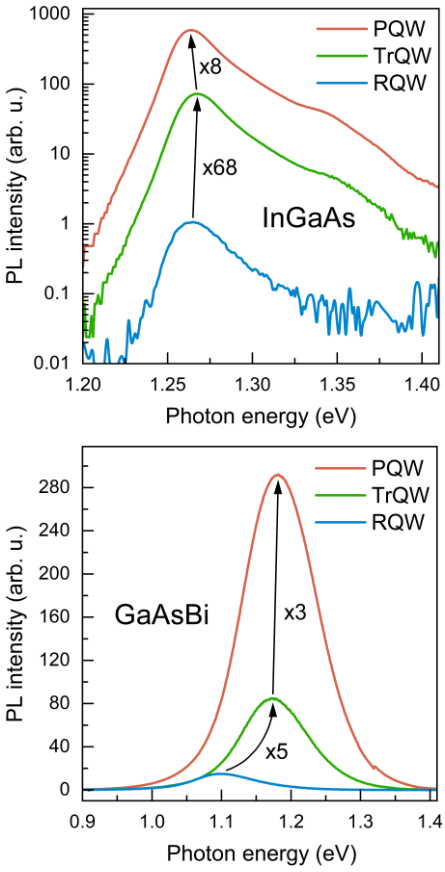


Fig. 1 Room-temperature PL spectra of InGaAs (top) and GaAsBi (bottom) QW heterostructures.

While the underlying mechanisms differ (suppressed thermal escape in InGaAs versus enhanced localization across a blurred well-barrier interface in GaAsBi), parabolic grading consistently improves QW emission performance. Low-temperature PL excitation confirms more efficient trapping in GaAsBi PQW structures, establishing parabolic barrier grading as a broadly applicable strategy for near-infrared QW emitters and laser diode structures.

REFERENCES

[1] B. Fluegel et al., *Phys. Rev. Lett.*, **97**, 067205 (2006).
[2] D. Feldmann et al., *Appl. Phys. Lett.*, **51**, 226 (1987).
[3] S. Pūkienė et al., *Nanotechnology*, **30**, 455001 (2019).

P23

Topological particles in spherically polarized Bessel-X pulses

S. Savitski[1], J. Beršky[1] and S. Orlov[1]

[1]*Department of Optoelectronics, State research institute Center for Physical Sciences and Technology, Sauletekio av. 3, Vilnius, Lithuania*
Email: stanislau.savitski@ftmc.lt

Bessel beams exhibit non-diffracting behavior, making them of considerable interest for short-pulse applications [1]. For small cone angles, they are typically described within the scalar approximation. However, when the cone angle becomes sufficiently large, scalar theory no longer provides an accurate description, and a vectorial treatment of the electromagnetic field is required [2].

Skyrmions are topologically stable quasiparticles that have been predicted and demonstrated in quantum fields, solid-state physics and magnetic materials, but have only recently been observed in electromagnetic fields. In optics, skyrmions and other topological quasiparticles can be constructed with various three-dimensional vector fields, such as the electric field, spin angular momentum, and polarization Stokes vector [3].

In this work, we investigate the topological structure of spherically polarized Bessel-X pulses in different domains, including the Poynting vector, Stokes vector, and spin angular momentum.

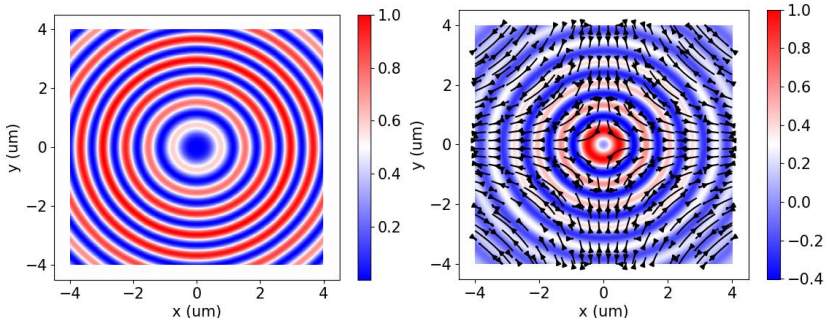


Fig. 1 Normalized total intensity of the transverse electric mode of the Bessel-X pulse (a) and the magnitude of the longitudinal component of the spin angular momentum (b), where the black streamlines with arrows show the orientation of the transverse field. The parameters of the simulation: the cone angle = 45 deg, the pulse duration α = 1.06e-14 s, frequency ω = 1.885e15 Hz, the topological charge m = 2, distance z = 0, time t = 0.

REFERENCES

[1] P. Saari, H. Sõnajalg, Pulsed Bessel beams, Laser Phys. 7 (1) (1997) 32–39.
[2] J. A. Stratton, Electromagnetic Theory (John Wiley & Sons, 2007), Vol. 33.
[3] Shen, Y., Zhang, Q., Shi, P., Du, L., Yuan, X., & Zayats, A. V. (2024). Optical skyrmions and other topological quasiparticles of light. Nature Photonics, 18(1), 15-25.

P24

Charge State Equilibration of Nitrogen-Vacancy Center Ensembles in Diamond: The Role of Electron Tunneling

Lukas Razinkovas
Center for Physical Sciences and Technologyab

Abstract

Authors: Lukas Razinkovas[1], Chris G. Van de Walle[2], and Ronald Ulbricht[3]
1. Department of Fundamental Research, Center for Physical Sciences and Technology, Vilnius, Lithuania.
2. Materials Department, University of California, Santa Barbara, CA, United States.
3. Max Planck Institute for Polymer Research, Mainz, Germany.

The nitrogen-vacancy (NV) center in diamond is a well-established solid-state defect with promising applications ranging from quantum sensing of physical properties to room-temperature quantum computing. NV centers possess two charge states with well-established optical transitions: the neutral NV^0 state and the negatively charged NV^- state. The negatively charged state exhibits spin-optical properties that give the NV center its unique capabilities. In diamond crystals, single-substitutional nitrogen defects (N) are usually more abundant than NV centers and function as donors, providing NV centers with the additional electron required to attain their preferred charge state. During optical excitation of NV^-, photoionization can occur, promoting an electron to the conduction band and converting NV^- to NV^0. While optical protocols can restore NV^-, recovery is also observed in the absence of illumination, indicating a charge-transfer process from donors to NV centers.

Despite the central role of charge transfer in establishing and restoring the NV^- charge state, the microscopic mechanism enabling charge transfer between deep-level defects such as NV and N remains unresolved. In diamond, the high ionization energies of these defects rule out thermally activated carrier emission and capture as likely explanations. To address this long-standing issue, we use pump-probe spectroscopy to monitor the relaxation dynamics of NV^0 back to NV^- following photoionization. We find that following photoconversion of NV^- to NV^0, NV^- recovery strongly depends on the N donor concentration, with no discernible temperature dependence. These observations, supported by first-principles-based theoretical modeling, identify phonon-assisted electron tunneling between localized defect states as the dominant mechanism governing charge equilibration in NV center ensembles.

P25

Sustainable management of electronic and semiconductor waste in the era of advanced photonic technologies

Abdullah Jan Frogh[1]

Department of Business & Industrial Management, Veer Narmad South Gujarat University (VNSGU), Surat, Gujarat 395007, India
Email: abdullahfrogh.dmgphd22@vnsgu.ac.in

The rapid advancement of advanced photonic technologies has accelerated the production of semiconductor devices used in artificial intelligence, optical communication, quantum computing, biomedical imaging, renewable energy systems, and integrated photonic circuits. While these technologies have significantly improved industrial innovation and digital transformation, they have also increased the generation of complex electronic and semiconductor waste containing hazardous substances, critical raw materials, and rare earth elements. Existing electronic waste management frameworks primarily address conventional electronic products and provide limited attention to the distinctive waste streams generated by photonic and semiconductor technologies. This research therefore investigates sustainable management strategies for electronic and semiconductor waste generated by advanced photonic technologies from the perspective of environmental sustainability and circular economy. The study has three objectives: **(**1) to identify the environmental challenges associated with semiconductor waste generated by advanced photonic technologies; **(2)** to examine the relationship between photonic technology development, waste generation, recycling practices, and circular economy adoption; and (3) to propose an integrated framework for sustainable semiconductor waste management. The research is guided by two questions: How do advanced photonic technologies influence the generation and management of electronic and semiconductor waste? and Which sustainable management strategies can improve resource recovery and environmental performance within photonic manufacturing systems? The research adopts a mixed-method design integrating quantitative and qualitative approaches. Primary data will be collected from approximately 150 respondents, including researchers, academic experts, environmental specialists, and professionals from the electronics and semiconductor sectors using structured questionnaires and semi-structured interviews. Participants will be selected through purposive and stratified sampling techniques to ensure representation of key stakeholder groups. Secondary data will be obtained from peerreviewed journals, international reports, semiconductor industry publications, and sustainability databases. Quantitative data will be analysed using descriptive statistics, correlation analysis, and multiple regression analysis in SPSS, while qualitative data will be examined using thematic analysis. The conceptual framework analyses the relationships among photonic technology advancement, semiconductor waste generation, recycling technologies, circular economy practices, and environmental sustainability. The study is currently in progress; therefore, no final empirical results

are reported. However, preliminary analysis of recent literature indicates that the rapid expansion of photonic integrated circuits, compound semiconductors, and optoelectronic devices is expected to substantially increase complex semiconductor waste, while existing recycling infrastructure remains insufficient to recover high-value materials efficiently. These observations emphasise the need for specialised recycling technologies, environmentally responsible manufacturing practices, and circular economy policies specifically designed for photonic industries. The expected outcomes will provide an integrated sustainable management framework linking advanced photonic technologies with semiconductor waste management, resource efficiency, and environmental governance. The study aims to contribute to the development of practical strategies for researchers, industry practitioners, and policymakers to improve the sustainability of nextgeneration photonic technologies while reducing the environmental impacts associated with semiconductor waste.

REFERENCES

[1] J. Wang, F. Sciarrino, A. Laing, and M. G. Thompson; *Integrated Photonic Quantum Technologies*, arXiv preprint arXiv:2005.01948 (2020).

[2] Y. Yin and Y. Yang; *Sustainable Transition of the Global Semiconductor Industry: Challenges, Strategies, and Future Directions*, Sustainability 17 (2025) p. 3160.

[3] P. Sun, Z. Zeng, X. Pan et al.; *Recycling Power Semiconductor Devices*, Nature Reviews Electrical Engineering 3 (2026) pp. 111–122.

[4] V. Forti, C. P. Baldé, R. Kuehr, and G. Bel; *The Global E-waste Monitor 2020*, United Nations University (2020).

P26

Broadband Radiation Sensor Based on a Hot Carrier Ratchet Structure

Ihor Zharchenko[1,2], Oleksandr Masalskyi[1,2], Jonas Gradauskas[1,2], Steponas Ašmontas[1], Aldis Šilėnas[1], Aurimas Čerškus[1,2], Jonas Petrokas[1]

[1]*Laboratory of Electronic Processes, Center for Physical Sciences and Technology, Lithuania*
[2]*Vilnius Gediminas Technical University, Lithuania*
Email: oleksandr.masalskyi@ftmc.lt

Broadband radiation sensors are in high demand in optoelectronics, particularly in the infrared region, where conventional semiconductor detectors are limited by their bandgap and often require cryogenic cooling for effective operation. In this work, a GaAs/$Al_xGa_{1-x}As$ ratchet-based sensor operating on the hot carrier effect is presented, enabling detection from the visible to long-wavelength spectral range without cryogenic cooling or complex fabrication. The sensor is built on a periodic asymmetric potential of a MBE-grown GaAs/$Al_xGa_{1-x}As$ structure, with the AlAs mole fraction gradually changing from x = 0.3 to 0. In the dark, electrons are localized in potential wells (Fig. 1a). Under illumination, they become hot carriers and diffuse between neighboring wells (Fig. 1b). Their asymmetric relaxation and transport generate an electromotive force at the device terminals, producing a direct current in a closed circuit (Fig. 1c).

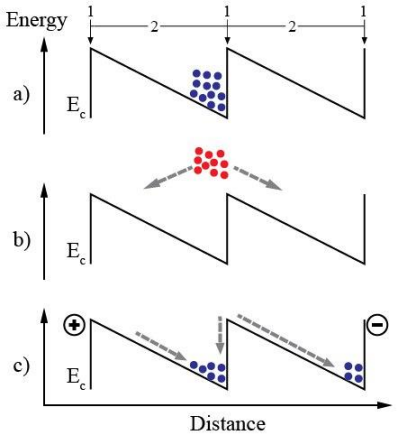


Fig. 1 Photovoltage formation across the sensor: (a) absence of irradiation; (b) heating of free electrons and their diffusion in both directions; (c) electron relaxation and redistribution between potential wells [1].

The sensor shows a linear photocurrent response under both inter- and intraband excitation in the studied intensity range. The photocurrent magnitude follows the strong spectral variation of the GaAs absorption coefficient. Temperature measurements show that at 0.532 μm the response is higher at room temperature due to stronger interband absorption and greater excess energy left for carrier heating, whereas at 1.064 μm the temperature influence is weak since the response is governed mainly by the free carrier absorption.

To conclude, the GaAs/$Al_xGa_{1-x}As$ ratchet-based sensor offers a promising approach for broadband radiation detection based on hot carrier effects. Its room-temperature operation and response to both high and low photon energy laser radiation make it a potential alternative to existing detectors requiring cryogenic cooling, particularly in the infrared region.

REFERENCES

[1] Gradauskas J., Ašmontas S., Sužiedėlis A., Masalskyi O., Zharchenko I. „Reketinis plataus spektro spinduliuotės jutiklis“ („Ratchet-based sensor of broad radiation spectrum“). Lietuvos Respublikos patentas Nr. LT 7030B (2023/02/17).

P27

Terahertz images quality enhancement by means of multichannel processing.

Viktoriia Abramova[1], Sergiy Abramov[2], Ignas Grigelionis[1], Linas Minkevičius[1] and Volodymyr Lukin[3]

[1]Department of Optoelectronics, Center for Physical Sciences and Technology, Saulėtekio 3, 10257 Vilnius, Lithuania.
[2]Department of Functional Materials and Electronics, Center for Physical Sciences and Technology, Saulėtekio 3, 10257 Vilnius, Lithuania.
[3]Department of Information-Communication Technologies, National Aerospace University, Vadym Manko 17, 61070 Kharkiv, Ukraine
Email: viktoriia.abramova@ftmc.lt.

A typical problem for terahertz (THz) images obtained by raster-scanning imaging systems is the possible presence of impulse noise that might take a compact form localizing as strips extending in the direction of detector movement. The noise significantly degrades the visual quality of images and makes identification of studied objects problematic, so its elimination is highly desirable. In [1], it was shown that such noise can be reduced by using a digital median filter with a rectangular sliding window oriented perpendicular to the noise strips. However, to ensure an acceptable level of introduced distortion, the processed image or its region of interest must be at least 100x100 pixels in size, which is not always feasible in practice.

In this study, the possibility of increasing the processing efficiency of THz images distorted by compact impulse noise through the simultaneous processing of multiple channel images [2] was investigated. During the system's focus search, it is often necessary to obtain multiple images at different distances from the source. Among such "service" images there are the ones with luminance patterns formed due to the standing wave interference at similar phases. These images can be used as channels and the datasets for joint processing can be formed based on the analysis of linearity parameters of the abovementioned luminance patterns.

It is shown that joint processing of three channels allows to decrease the recommended in [1] sliding window sizes from 9x1…15x1 to 3x1…5x1, increasing the filtering efficiency by an average of 5...7 dB in accordance with the PSNRHVSM metric. Even for the images of size 20x20 pixels, for which at impulse noise probability about 0.5 in one-channel processing mode quality improvement was virtually impossible [1], multichannel processing provides up to 16 dB increase in quality by PSNRHVSM, while under favorable circumstances (e.g. low probability of noise and its loose localization), even noise elimination without introducing distortions into the object is possible.

REFERENCES

[1] V. Abramova, S. Abramov, L. Minkevičius, and I. Grigelionis, Radioelectronic and Computer Systems 1(117) (2026) pp. 192-206.
[2] V. Lukin, S. Abramov, V. Abramova, J. Astola, and K. Egiazarian, Telecommunications and Radioengineering 76(19) (2018) pp. 1719-1748.

P28

Hot Carrier Impact on Photovoltage Formation in Solar Cells

S. Ašmontas, J. Gradauskas, A. Čerškus, A.Sužiedėlis, E. Širmulis, and O. Žalys

Laboratory of Electronic Processes, Center for Physical Science and Technology,

Saulėtekio av. 3, 10257, Vilnius, Lithuania.

Email: ovidijus.zalys@ftmc.lt

Global electricity demands are fueling fast growth in the renewable energy industry, and along with it the technological advances that make these sustainable alternatives more dependable, efficient, and cost effective. Solar cells are among the most promising and environmentally friendly sources of electricity.

Here, the results of investigation of photovoltage formation in perovskite and inorganic solar cells under pulsed laser excitation are presented. Transient photovoltage measurements reveal the photoresponse composed of two components with opposite polarities, $U = U_f + U_{ph}$ (see Fig. 1) The fast component follows the laser pulse shape and is attributed to carrier heating, whereas the slow component corresponds to the conventional photovoltage arising from electron-hole pair generation. The latter can be expressed as [1]

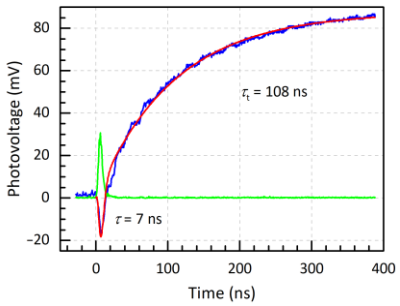


Fig. 1. Temporal shapes of the 0.53 μm laser pulse (green) and photovoltage (blue) across the perovskite solar cell. The excitation laser power density is 0.8 MW/cm^2. The red curve is theoretical calculation.

$$U_{ph}(t) = U_0[(\exp(-t/\tau) - \exp(-t/\tau_{rec})] / (1/\tau_{rec} - 1/\tau), \quad (1)$$

where U_0 represents the initial voltage, τ denotes the time constant associated with carrier transport within the absorber layer, and τ_{rec} refers to the time of carrier recombination. The calculated dependence of U_{ph} on time is depicted in Fig. 1. The same figure shows the measured photovoltage. The measured photovoltage as a function of time can be well described by Eq. (1). This enables us to determine the charge carrier transit time through the perovskite layer.

To conclude. the photoresponse of the solar cells under pulsed laser excitation is found to consist of two components: a thermoelectric force generated by hot carriers and a conventional photovoltage arising from light-induced electron–hole pair generation. Carrier heating reduces the conversion efficiency of the solar cells, as the polarity of the hot-carrier thermoelectric force is opposite to that of the conventional photovoltage. The adverse effect of carrier heating on conversion efficiency can be mitigated by employing multi-junction solar cells [2].

REFERENCES

[1] R. Hidayat, A.A. Nurunnizar, A. Fariz, Herman, E.S. Rosa, Shobih, T. Oizumi, A. Fuji, and M. Ozaki; *Scien.Rep*. **10** (2020) pp.19197.

[2] S. Ašmontas, J. Gradauskas, A. Čerškus, A.Sužiedėlis, E. Širmulis, and O. Žalys; *Lith.J. Phys*. **65** (2025) pp. 248-257.

P29

Hybrid conductive ink printed RFID antennas and printed heaters with secure optical features

Anand P J, Dhanya Sunil, Ashok Rao

Manipal Institute of Technology, Manipal Academy of Higher Education, Manipal, Karnataka, India.

Email: dhanyadss3@gmail.com

A multifunctional conductive ink incorporating integrated optoelectronic security features is presented for anticounterfeiting applications in printed electronics [1]. The formulation combines conductive fillers and a polymeric binder with multimodal luminescent taggants, creating a unique authentication signature intrinsically embedded within the electrically functional material. Unlike conventional security labels, the optical features are inseparable from the conductive matrix required for device operation, significantly enhancing resistance to unauthorized replication [2].

The ink was screen-printed on flexible polyethylene terephthalate (PET) substrates to fabricate functional electronic devices, including a 2.1 GHz rectangular microstrip patch antenna for RFID applications and resistive heater circuits. Under 365 nm ultraviolet excitation, the printed patterns exhibit a distinct green downconversion emission, while 980 nm near-infrared excitation generates a characteristic purple upconversion luminescence.

This multi-modal verification platform provides rapid, non-destructive authentication through visible photoluminescence and near infrared upconversion emission. The developed conductive ink demonstrates excellent adhesion, environmental stability, and printability on diverse substrates. By integrating optical security functions directly into conductive device architectures, this work offers a robust strategy for safeguarding RFID systems and printed electronic circuits while providing reliable authentication for manufacturers, regulators, and end users.

REFERENCES

[1] E. Glogic *et al.*, *ACS Sustain. Chem. Eng.*, 9 (2021) pp. 11691–11704.
[2] I. Boukhoubza *et al.*, “Graphene oxide concentration effect on the optoelectronic properties of ZnO/GO nanocomposites,” *Nanomaterials*, vol. 10, no. 8, pp. 1–16, Aug. 2020, doi: 10.3390/nano10081532.

P30

Oil contamination detection using THz spectroscopy and imaging

Mindaugas Karaliūnas

Terahertz Photonics Laboratory, Department of Optoelectronics, Center for Physical Sciences and Technology, Saulėtekio Ave. 3, 10257 Vilnius, Lithuania
Email: mindaugas.karaliunas@ftmc.lt

Crude oil production, although criticized in the context of global warming, remains high compared to previous decades and is growing [1]. Renewable energy and material sources are replacing crude oil products, but the industry is not going away anytime soon. The aim of this research is to find and propose new ways to detect, identify, quality control and monitor crude oil and its products using new optoelectronic tools to make the use of crude oil products safer for the environment and effective for the people. It has been previously established that the refractive index and absorption coefficient depend on the length of hydrocarbon molecules, and the presence of such bonds as esters fundamentally changes the trends in the dependence of optical properties [2]. In this regard, crude oil is the most complex medium for research in the class of petroleum products, since its chemical composition is extremely rich and diverse.

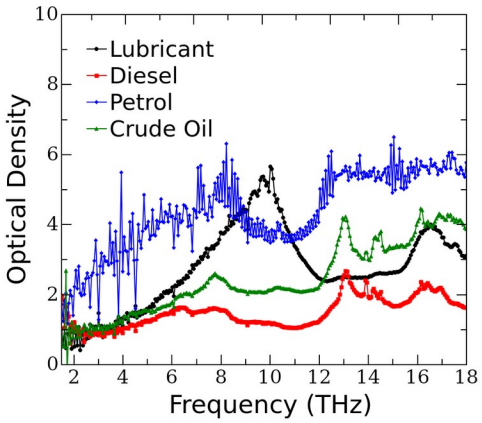


Fig. 1 The spectra of crude oil and its products, lubricant, diesel and petrol, were measured by Fourier transform infrared spectroscopy in the 1.5–18 THz.

Five different viscosities of engine lubricant oils were purchased from local suppliers, as were 2 types of diesel from 2 different suppliers, and 1 type of petrol from 2 different suppliers. In the fuel study, pure fuels, both petrol and diesel, were mixed with a specified amount of contaminants commonly found in crude oil, namely water, methanol, isopropanol, and sulfur. Each type of fuel was separately mixed with 5% to 0.5% of contaminants.

Figure 1 shows the characteristic spectra for the sample groups, i.e. lubricant, diesel, petrol and crude oil. This work presents the spectra of crude oil and its products measured using Fourier transform THz spectroscopy in order to identify unique spectral features that could be used in complex characterization studies of oils. The work focus on the THz imaging at frequency of 253 GHz capabilities for fast and reliable detection of contaminants in crude oil and its products.

REFERENCES

[1] IEA, World crude oil production by region, 1971-2020, IEA, Paris, IEA.
[2] M. Karaliūnas *et al.*, Sci. Rep. **8**, 18025 (2018).

P31

Phase-Sensitive THz Heterodyne Imaging Using Nonparaxial Structured Illumination

Domantas Vizbaras[1], Kęstutis Ikamas[1,2], Alvydas Lisauskas[1,2], Rusnė Ivaškevičiūtė-Povilauskienė[2], Sergej Orlov[2], Ignas Grigelionis[2] and Linas Minkevičius[2]

[1]*Vilnius University, Institute of Applied Electrodynamics and Telecommunications, Lithuania*
[2]*Center for Physical Sciences and Technology, Department of Optoelectronics, Lithuania*
Email: domantas.vizbaras@ff.vu.lt

Direct-power terahertz (THz) imaging offers poor contrast for weakly absorbing dielectric samples. Heterodyne detection overcomes this by preserving both amplitude and phase of the transmitted field, providing up to 43 dB higher dynamic range [1] and enabling phase-resolved imaging and computational refocusing [2]. Combined with nonparaxial structured illumination – Airy and Gaussian beams generated by compact silicon diffractive elements – this approach delivers simultaneously enhanced sensitivity, resolution, and phase contrast.

The demonstrated imaging system uses compact silicon nonparaxial diffractive optical elements and a broadband (0.3–2.2 THz) silicon CMOS FET detector with dual-substrate-lens coupling, routing the local-oscillator and RF beams to opposite sides of the chip and eliminating the beam-splitter [3]. Harmonic mixing (600 GHz – 600 GHz) achieves 57.8 dB SNR – 34 dB above direct detection – while sub-harmonic mixing (600 GHz – 300 GHz) yields 54.8 dB.

A multi-material sample (one to five layers of paper sheets, metallic foil, fabric, plastic, gauze) was raster-scanned in all three modes. Direct-power and heterodyne amplitude images show similar few-dB contrast; heterodyne phase images reveal sharp boundaries between all material zones invisible in amplitude data, with a phase range of 0.77π across the paper stack (Fig. 1). Modulation transfer function analysis on a Siemens star target confirms that heterodyne imaging reaches 2.55 cycles/mm – exceeding the 1.45–1.69 cycles/mm of direct detection – with mean squared error reduced from 0.19–0.21 to 0.11. Nonparaxial Airy-beam illumination [4] further enhances SNR and phase sensitivity beyond conventional Gaussian beams [5].

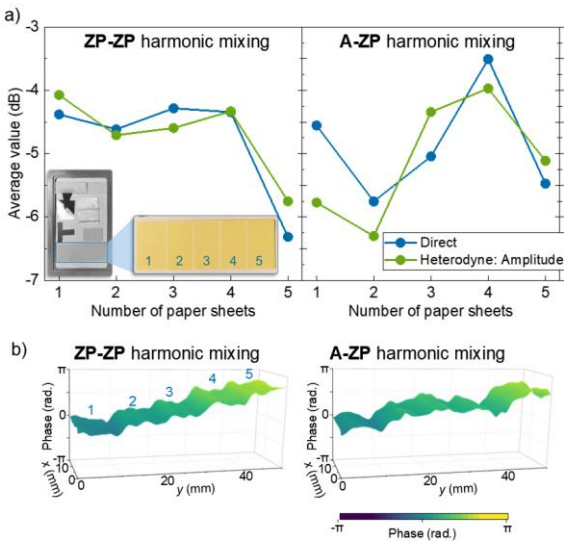


Fig. 1 Comparison of direct and heterodyne imaging results: amplitude (top) and phase (bottom) distributions for the zone plate–zone plate (a) and Airy lens–zone plate (b) configurations. The imaged sample consists of one to five layers of paper sheets.

REFERENCES

[1] L. Minkevičius et al., Appl. Phys. Lett. 99, 131101 (2011).
[2] H. Yuan et al., Opt. Express 31, 40856–40870 (2023).
[3] K. Ikamas et al., IEEE Electron Device Lett. 39, 1416 (2018).
[4] S. Orlov et al., Laser & Photonics Reviews 18, 2301197 (2024).
[5] P. Kizevičius et al., Lith. J. Phys. 63, 210–217 (2023).

P32

Investigation of transient processes in magnetic pulse welding system using CMR B-scalar sensors.

Pavel Piatrou[1], Voitech Stankevic[1,2], Skirmantas Kersulis[1] and Nerija Zurauskiene[1,2]

[1]Department of Functional Materials and Electronics, Center for Physical Sciences and Technology, LT-10257 Vilnius, Lithuania;
[2]Faculty of Electronics, Vilnius Gediminas Technical University, LT-10105 Vilnius, Lithuania
Email: pavel.piatrou@ftmc.lt.

Magnetic pulse welding (MPW) is an advanced solid-state joining technique that uses transient electromagnetic forces to accelerate a flyer workpiece toward a parent workpiece, enabling high-velocity impact and metallurgical bonding between them. MPW is widely recognized for its ability to join dissimilar materials [1].

Direct experimental identification of transient process stages remains a significant challenge. The onset of flyer deformation and the precise moment of collision between workpieces occur on a microsecond time scale, while the process itself is accompanied by intense electromagnetic interference. Therefore, high-speed in-situ measurements of deformation, collision, and magnetic-field dynamics are difficult to perform using conventional diagnostic techniques.

This study presents an experimental and numerical investigation of transient magnetic field evolution during MPW of an AA6063 aluminum tube onto an AISI 304 stainless-steel rod. The main objective is to measure the magnetic field directly in the narrow 1 mm gap between the field shaper and the flyer tube and to correlate its dynamics with flyer deformation and impact. For this purpose, a non-invasive technique based on thin CMR B-scalar sensors was developed. In combination with the measurement module, these sensors enable orientation-independent real-time measurement of high-amplitude, microsecond-duration magnetic field pulses up to several tens of tesla, while suppressing parasitic electromotive forces.

To support the experimental findings and interpret the measured magnetic field dynamics, a coupled electromagnetic–mechanical model was developed in COMSOL Multiphysics. The mechanical performance of the welded joints was evaluated by tensile testing.

Overall, the results demonstrate that CMR B-scalar sensors with the measurement module provide an effective tool for direct measurement of transient magnetic fields in MPW. These measurements enable the identification of deformation and collision stages and can support further optimization of the process for industrial applications.

REFERENCES

[1] A. Kapil, A. Sharma; *J. Clean. Prod* **100** (2015) pp. 35-58.
[2] V. Stankevic et al., *Sensors*, **20** (2020) p.5925.

P33

Controlled Generation of Bessel Beam Braids with Complex Topological Structure

Klemensas Laurinavičius[1]

[1]*State Research Institute Center for Physical Sciences and Technology. Saulėtekio al. 3, Vilnius, Lithuania.*

Email: Klemensas.laurinavicius@ftmc.lt

The controlled generation of structured light fields with complex topologies has become an important frontier in modern optics. Bessel beams provide a versatile platform due to their nondiffracting behavior and well-defined transverse structure [1]. In this work, we investigate the formation of Bessel beam braids - field configurations created through the superposition of multiple Bessel beams with carefully engineered cone angles and topological charge relationships. We develop a theoretical framework that describes how interference between constituent beams gives rise to braided intensity channels with robust propagation invariance. The influence of parameters such as topological charge combinations and cone angles is analyzed to determine their role in braid formation and controllability. Numerical simulations reveal a wide range of braid geometries, including helical, multi-strand, and dynamically evolving topologies, all maintaining nondiffracting characteristics over extended propagation distances. Our results demonstrate a practical route for generating and tailoring optical braids, opening opportunities for advanced optical manipulation, robust information encoding, and the study of topological phenomena in structured light fields [2].

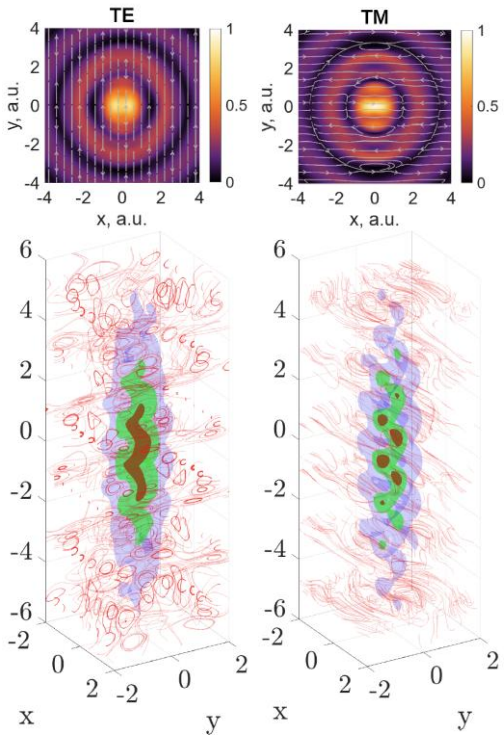


Fig. 1 Field distributions of transverse electric (TE, left) and transverse magnetic (TM, right) polarizations for a topological-charge pair $m_1 = 0$ and $m_2 = 1$.

From a theoretical standpoint, the rotation frequency is governed by the difference between the longitudinal propagation constants of the two contributing beams and by the number of strands composing the braid. The resulting axial phase difference grows linearly with propagation distance, producing a constant azimuthal rotation rate of the interference pattern. This rotation is distributed among the $N_{braids} = \Delta m$ intensity strands, yielding a characteristic braid rotation speed that depends only on the cone angle difference $\Delta\theta$ and the topological charge difference Δm.

REFERENCES

[1] P. Saari and H. Sonajalg. Pulsed bessel beams. Laser Physics, 7(1):32–39, 1997.

[2] Gabrielius Kontenis, Darius Gailevičius, Vytautas Jukna, and Kestutis Staliūnas. Terahertz rate rotating helical intensity beams. Optics & Laser Technology, 182:112036, 2025.

P34

Development of Artificial Birefringence for Phase and Polarization Control at 253 GHz

Ernestas Nacius, Vytautas Jukna and Linas Minkevičius

Department of Optoelectronics, Center for Physical Sciences and Technology, Saulėtekio ave.3, Vilnius LT-10257, Lithuania

.

Email: ernestas.nacius@ftmc.lt

Terahertz radiation is widely employed in imaging of optically opaque materials, spectroscopy, and communication, and it also holds potential for applications in security and defense. However, most elements used for radiation control typically modulate amplitude or phase. To enable simultaneous polarization control, artificial birefringence can be exploited. This physical phenomenon can be realized in isotropic materials by introducing subwavelength periodic structures that interact with transmitted radiation [1]. The resulting anisotropy expands wavefront control capabilities, allowing simultaneous manipulation of phase and polarization and thereby increasing the available degrees of freedom [2,3].

In this study, we investigate birefringence and the fabrication of functional elements operating at 253 GHz. Specifically, we examine the feasibility of manufacturing half-wave plates and Pancharatnam–Berry (geometric phase) elements using three materials: high-impact polystyrene, fused silica, and high-resistivity silicon (see Fig. 1). Each material entails distinct fabrication techniques and associated constraints. Therefore, a comparative analysis of these processes will be presented. In addition, numerical modeling of birefringent structures will be conducted to identify optimized designs, followed by experimental validation.

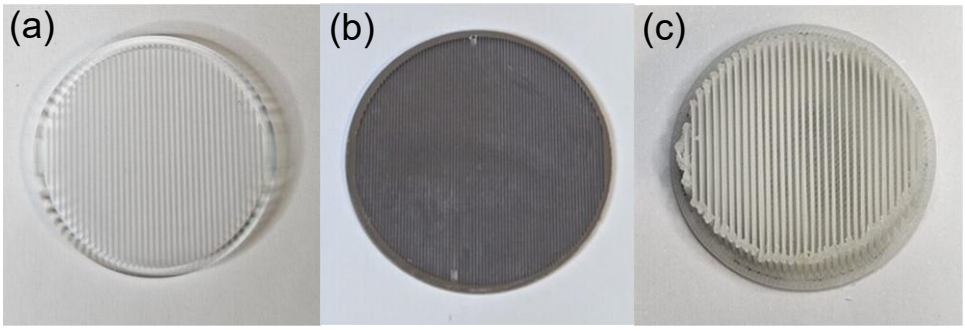


Fig. 1 Pictures of manufactured 1-inch diameter half-wave plates designed at 253 GHz made of (a) fused silica, (b) highly resistive silicon, and (c) high-impact polystyrene.

REFERENCES

[1] M. Scheller, *et al*, "Terahertz form birefringence", Opt. Express 18, 10137-10142 (2010).

[2] B. Piccirillo *et al*, “Flat polarization-controlled cylindrical lens based on the Pancharatnam–Berry geometric phase”, Eur. J. Phys. 38 034007, (2017)

[3] E. Hasman, *at al*, "Polarization dependent focusing lens by use of quantized Pancharatnam–Berry phase diffractive optics", Appl. Phys. Lett., 82 (3): 328–330, (2003).

P35

Lensless formation and turbulence response of Airy-type beams generated by direct Fresnel propagation.

Justas Berškys[1], Klemensas Laurinavičius[1], Sergej Orlov[1]

[1]*State Research Institute Center for Physical Sciences and Technology, Savanorių st. 231, LT-02300 Vilnius.*
Email: justas.berskys@ftmc.lt.

We investigate a lensless Airy-type beam generated by direct Fresnel propagation of a Gaussian-apodized cubic phase. Unlike the conventional finite-energy Airy beam, which is formed by a Fourier-transforming lens system [1], the lensless field is not an Airy beam at the input plane. Starting from the Fresnel diffraction integral, we show analytically that an Airy-type structure forms during propagation, but with a different Airy argument and therefore different transverse dynamics.

The conventional beam follows the familiar parabolic main-lobe trajectory, while the lensless field undergoes a formation stage before developing an Airy-like profile. The two beams are compared using propagation maps, transverse profiles, and two-dimensional and three-dimensional intensity distributions. We then examine their behaviour in atmospheric turbulence [2] using a phase-screen model. The comparison is performed at a matched free-space plane where both beams have the same normalized transverse intensity distribution. The results show that, despite this free-space intensity matching, the two fields exhibit different scintillation behaviour, indicating that turbulence response depends not only on the receiver-plane intensity profile but also on the beam's complex-field evolution during propagation.

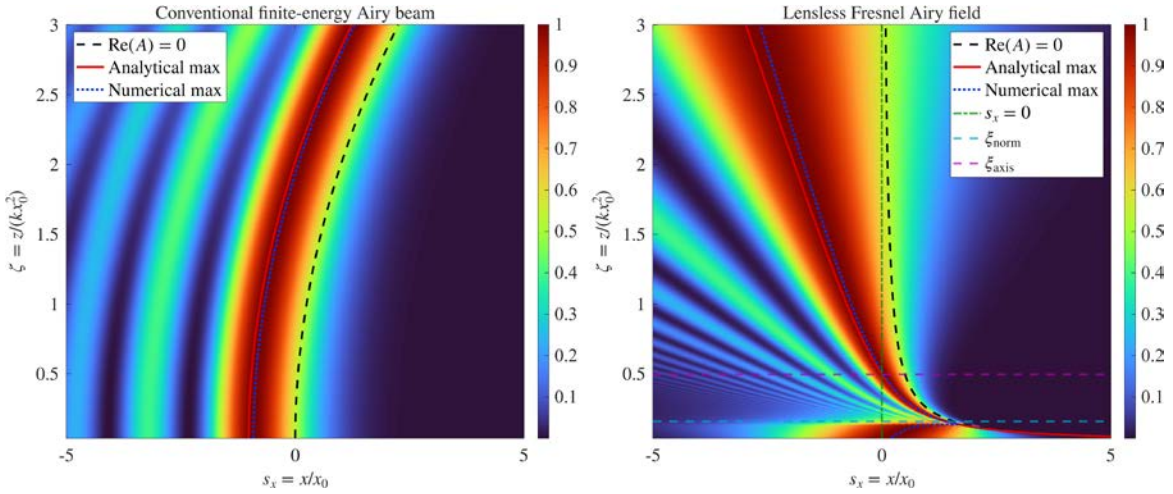


Fig. 1 Short and clear caption, revealing the message of the figure.

REFERENCES

[1] G. A. Siviloglou, J. Broky, A. Dogariu, and D. N. Christodoulides; Phys. Rev. Lett. 99 (2007) 213901.
[2] L. C. Andrews and R. L. Phillips; Laser Beam Propagation through Random Media, 2nd ed., Bellingham: SPIE Press (2005).

TCAD Simulation Study of Avalanche Operation in GaN LGAD Structures

Dominykas Augulis[1,*] and Tadas Malinauskas[1]

[1]*Institute of Photonics and Nanotechnology, Faculty of Physics, Vilnius University, Saulėtekio al. 3, LT-10257 Vilnius, Lithuania*

*E-mail: dominykas.augulis@ff.vu.lt

Low-gain avalanche detectors (LGADs) improve timing resolution by using a high-field gain layer that provides moderate impact-ionization multiplication below breakdown [1]. Silicon LGADs already provide excellent timing performance, but radiation damage, cooling demands, and the relatively low critical field of Si motivate detector concepts based on wider-bandgap materials. GaN is a promising candidate because of its high breakdown field, wide bandgap, and radiation tolerance, which are attractive for high-luminosity and harsh-environment measurements [2,3].

Here, the operation of GaN LGADs was studied using Sentaurus TCAD simulations. The model solved the Poisson and carrier-continuity equations in a two-dimensional axisymmetric geometry and included Fermi statistics, incomplete dopant ionization, field- and doping-dependent mobility, SRH, radiative and Auger recombination, impact ionization, and trap-assisted tunneling.

Reverse bias I-V curves, electric-field profiles, avalanche generation, excitation response, and gain were calculated. The IV comparison in Fig. 1 shows that the LGAD gain layer moves the rapid current increase to a lower voltage than in the PiN structure, indicating earlier avalanche onset. Sweeping the gain-layer thickness from 50 to 200 nm and the Si doping from 5 x 10^{16} to 6 x 10^{17} cm^{-3} shifted the onset and breakdown behavior, demonstrating that epitaxial thickness and doping can tune the operating window. Optical and alpha-particle-like excitation simulations further indicate that TCAD can identify GaN LGAD detector designs with a controlled low multiplication gain before breakdown, reducing trial-and-error growth and fabrication steps.

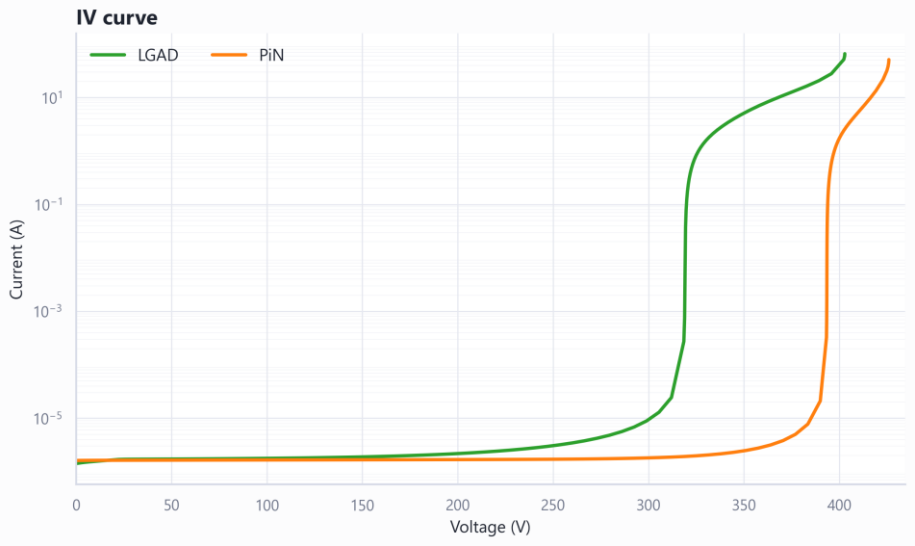


Fig. 1. TCAD-simulated reverse bias I-V characteristics of the reference GaN LGAD and PiN structures.

REFERENCES

[1] N. Cartiglia et al., Nucl. Instrum. Methods Phys. Res. A 796, 141-148 (2015).
[2] D. Ji and S. Chowdhury, Front. Mater. 9, 846418 (2022).
[3] H. Okumura et al., Jpn. J. Appl. Phys. 65, 016501 (2026).

P37

Modified Keplerian lens system for efficient signal coupling in sub-THz free-space communication

Marta Kurowska[1], Paweł Komorowski[2], Mateusz Kaluza[1] and Agnieszka Siemion[1,3]

[1]*Faculty of Physics, Warsaw University of Technology, 00-662, Warsaw, Poland*
[2]*Institute of Optoelectronics, Military University of Technology, 00-908 Warsaw, Poland*
[3] *Center for Advanced Materials and Technologies CEZAMAT, Warsaw University of Technology, Poleczki 19, 02-822 Warsaw, Poland*
Email: marta.kurowska2.dokt@pw.edu.pl

As global communication networks transition toward the 6G standard, exploiting the sub-terahertz (sub-THz) spectrum has become essential to meet the demand for ultra-high data rates. Within this regime, particularly around 100 GHz, free-space communication (FSC) links suffer from significant beam divergence caused by diffraction, making efficient energy collection a primary challenge [1]. In this work, we present a compact quasi-optical dual-lens system based on a modified Keplerian beam reducer, tailored for 95.75 GHz FSC links.

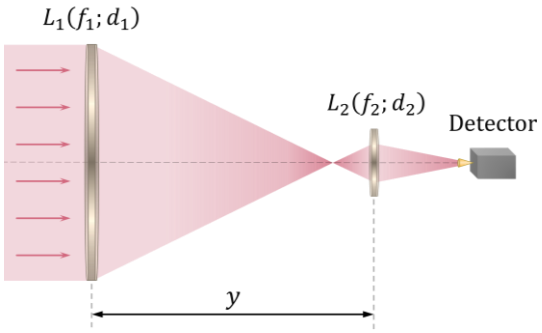


Fig. 1 Schematic of the proposed Keplerian dual-lens system.

The system comprises a primary diffractive lens L_1 with a focal length f_1=150 mm and a diameter d_1=187 mm, and a secondary diffractive lens L_2 with f_2=21.65 mm and d_2=76 mm, separated by a distance of y=175 mm, as illustrated in the schematic layout (Fig. 1). The lenses are designed to collect and shape the radiation into a converging cone that matches the WR-10 horn antenna of the receiver. To minimize absorption losses and reduce weight, the diffractive optical elements were fabricated using Fused Deposition Modeling (FDM) 3D printing technology with Cyclic Olefin Copolymer (COC) [2].

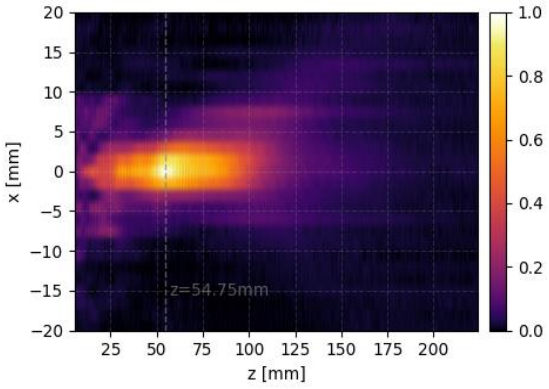


Fig. 2 Experimental xz-plane intensity scan.

Experimental verification of the fabricated structure was conducted using a 95.75 GHz IMPATT diode source and a THz camera mounted on a motorized 3-axis scanning stage. The laboratory measurements successfully confirmed the operation of the beam-shaping system and the formation of the intended focal spot. However, the experimental evaluation also revealed the system's high sensitivity to even minor levels of convergence in the incident wavefront. Ultimately, these results demonstrate that maximizing coupling efficiency in such systems requires rigorous control over the incident wavefront.

REFERENCES

[1] H.-J. Song and N. Lee; *IEEE Transactions on Terahertz Science and Technology* **12** (2022) pp. 105–117
[2] S. F. Busch, M. Weidenbach, J. C. Balzer, and M. Koch; *Journal of Infrared, Millimeter, and Terahertz Waves* **37** (2015) pp. 303–307

P38

Effect of Charge Transport Layers on Charge Extraction Kinetics in Perovskite Solar Cells Investigated by Kinetic Photoconductivity.

[1]Ernestas Kasparavičius, [1]Dovilė Vasiliauskaitė, Lauryna M. Svirskaitė[2],

[1]Vidmantas Gulbinas

[1]Center for Physical Sciences and Technology.
[2]Kaunas University of Technology, Faculty of Chemical Technology.
Email: ernestas.kasparavicius@ftmc.lt

Perovskite solar cells (PSCs) are among the most rapidly developing photovoltaic technologies, with power conversion efficiencies increasing from 3.8% to 27.2% in less than two decades [1–3]. Further improvements require a better understanding of charge extraction and transport processes, particularly at interfaces with charge transport layers.

In this work, the effect of different charge transport layers (CTLs) on charge extraction kinetics in perovskite solar cells was investigated using the kinetic photoconductivity method. The measurements revealed pronounced differences in charge extraction kinetics depending on the materials employed as charge transport layers. Comparison of novel CTLs with established high-performing materials, such as SnO_2 and MeO-2PACz, provided insight into charge extraction efficiency, interfacial energetics, and band bending within the investigated semiconductor systems.

Based on the obtained kinetic data, schematic band-bending profiles were constructed for the investigated CTLs. These profiles enabled a comparative assessment of their charge extraction properties and their suitability as charge transport layers in perovskite solar cells.

REFERENCES

[1] Organometal Halide Perovskites as Visible-Light Sensitizers for Photovoltaic Cells | Journal of the American Chemical Society
[2] Perovskitoids as Functional Materials | Accounts of Chemical Research
[3] https://doi.org/10.1038/s41566-025-01827-6 , Photostable donor–acceptor interface for minimizing energy loss in inverted perovskite solar cells

After Deadline Contribution

P39

Study of the Interactions Between Carbazole-Based Quaternary Ammonium Salts and Lead-Based Perovskite.

Matas Steponaitis[1], Vidmantas Gulbinas[1], Marius Franckevičius[1]

[1] *Department of Molecular Compounds Physics, State Research Institute Center for Physical Sciences and Technology, Savanorių st. 231, LT-02300 Vilnius, Lithuania*

Perovskite solar cells (PSCs) have undergone a remarkable increase in power conversion efficiency, rising from 3.8% to 27% within a relatively short period [1;2]. However, limited operational stability remains a major obstacle to their widespread commercialization. Surface defect passivation has therefore become an important strategy for improving both device performance and long-term stability [3;4]. Despite numerous reported approaches, the mechanisms governing the effectiveness of different passivating agents are still not fully understood.

In this work, we systematically investigated quaternary ammonium and thiouronium organic salts as surface passivating agents for triple-cation PSCs and compare their behavior with the commercially available sulfonium-based salt DMPESI. A combination of steady-state photoluminescence (PL), time-resolved photoluminescence (trPL), X-ray photoelectron spectroscopy (XPS), liquid-state nuclear magnetic resonance (NMR), and photovoltaic device measurements were used to evaluate organic–perovskite interactions and their influence on device properties.

The results demonstrated that different characterization techniques probe distinct aspects of the passivation process. While several surface treatments enhance radiative recombination, as indicated by PL and trPL measurements, these improvements do not necessarily translate into enhanced photovoltaic performance. Among the investigated compounds, only the iodide-containing quaternary ammonium salt CzEAI produces a clear improvement in device performance, consistent with the interactions observed by XPS.

These findings highlight the complex relationship between molecular interactions, defect passivation, and photovoltaic performance, emphasizing the importance of combining complementary characterization techniques when evaluating surface passivation strategies for PSCs.

REFERENCES

[1] Kojima, A. et al. *J. Am. Chem. Soc*. **131** (2009), pp. 6050–6051.
[2] Zhuang Xiong et al. *Science* **390** (2025), pp. 638-642.
[3] Suo, J. et al. *Nat. Energy* **9** (2024), pp. 172–183.
[4] Liu, J. et al. *Nature* **635** (2024), pp. 596–603.

After Deadline Contribution

P40

Rapid volumetric imaging with dynamic Fourier-domain full-field optical coherence tomography

Austėja Trečiokaitė[1], Erikas Tarvydas[1] and Egidijus Auksorius[1]
[1]*Center for Physical Sciences and Technology (FTMC),*
Saulėtekio al. 3, Vilnius LT-10257, Lithuania
Email: egidijus.auksorius@ftmc.lt

Fourier-domain full-field optical coherence tomography (FD-FF-OCT) enables rapid three-dimensional imaging by acquiring depth profiles at all camera pixels in parallel. An implementation with reduced spatial coherence has been used for in vivo structural imaging of the human retina and choroid [1]. Here, we follow the complex OCT signal over time to derive dynamic contrast associated with intracellular motion [2], enabling label-free volumetric imaging of fresh mouse gut and kidney in 3.3 s.

An 803–878 nm swept source illuminates a Linnik interferometer with 20×, NA = 0.5 water-immersion objectives. A deformable membrane and multimode fibre reduce spatial coherence to suppress coherent crosstalk. A camera operating at 60,000 frames/s records 512 spectral images per volume, providing 117.2 volumes/s over a 512 × 448 µm field of view sampled by 512 × 448 pixels [2]. Fourier transformation of the spectral interferograms reconstructs the complex volumes. Spatial filtering and digital refocusing improve image quality and extend the usable axial range beyond the optical depth of focus. Temporal Fourier analysis of 389 consecutive volumes generates dynamic RGB contrast, with colour representing relative fluctuation frequency.

In the small intestine, dynamic images reveal villi from the mucosal side and crypts from the serosal side, as shown in Fig. 1 (a) and (b), respectively. Kidney images show putative renal tubules in transverse, oblique and longitudinal orientations, shown in Fig. 1(c). These results demonstrate rapid, label-free volumetric imaging of tissue architecture and intracellular dynamics across a wide field of view.

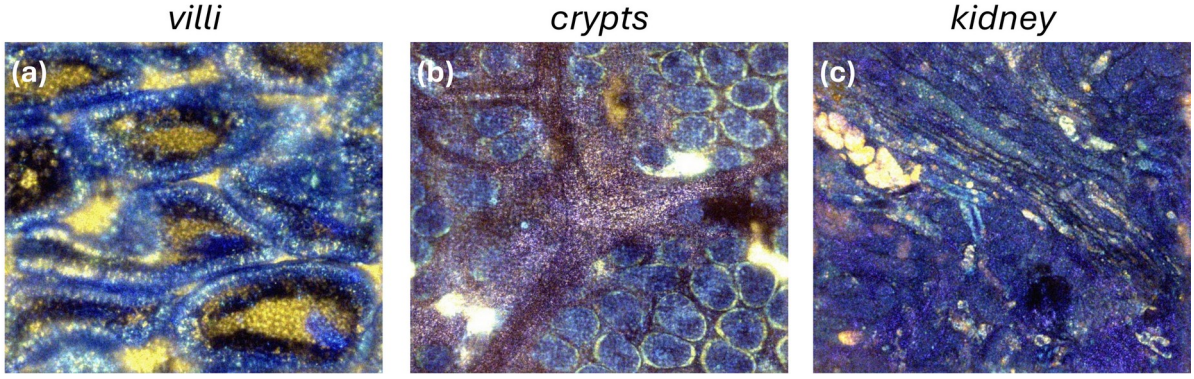


Fig. 1. Dynamic FD-FF-OCT images of mouse intestinal villi (a, 40 µm depth), crypts (b, 40 µm) and kidney (c, 30 µm). Field of view: 512 × 448 µm per panel. Colour encodes fluctuation frequency.

REFERENCES

[1] E. Auksorius et al., “Spatio-temporal optical coherence tomography provides full thickness imaging of the chorioretinal complex,” *iScience* 25 (2022) 105513.
[2] A. Trečiokaitė, E. Tarvydas and E. Auksorius, “Dynamic Fourier-domain full-field optical coherence microscopy,” *Optics Letters* 51 (2026) pp. 3581–3584.

After Deadline Contribution

P41

InAs/AlAsSb Mid-Infrared Quantum Cascade Lasers and Narrowband Thermal Emitters for Industrial Process Monitoring and Hazardous-Gas Detection.

Jan Devenson[1], Karolis Stašys[1], Jaunius Berškys[1], Giedrė Čepurnaitė[1], Viktoras Vaičikauskas[1], Viktorija Nargelienė[1]

[1]*Center for Physical Sciences and Technology, Vilnius, Lithuania.*
Email: E-mail: jan.devenson@ftmc.lt

Antimonide-based mid-infrared (mid-IR) optical sources offer a versatile platform for demanding sensing applications in the molecular fingerprint region. Here, we report advances in the molecular beam epitaxy (MBE) of InAs/AlAsSb heterostructures for both quantum cascade lasers (QCLs) and spectrally selective narrow-band thermal emitters, implemented within a common material system and epitaxial technology.

A central aspect of this work is an optimised MBE process for antimonide heterostructures based on an indirect arsenic-supply scheme. This approach markedly suppresses the formation of extended defects and provides a robust foundation for high-performance mid-IR device structures. Using this platform, we design and grow application-specific QCLs, including devices emitting near 8 µm for monitoring industrial curing processes and longer-wavelength structures operating around 11.5 µm for the detection of toxic gases, including phosgene. All QCLs employ InAs/AlAsSb active regions and are mounted epi-side down. The devices exhibit high maximum operating temperatures and maintain operation over a broad range of pulsed driving conditions, supporting their further development towards quasi-continuous-wave operation.

We also demonstrate metal-free, narrow-band mid-IR thermal emitters comprising heavily doped InAs active layers separated by AlAsSb barriers. Although their operating principle differs fundamentally from that of QCLs, these emitters exploit the same antimonide material system and MBE processes, offering a simple and attractive source architecture for compact sensing systems. Their emission wavelength can be engineered through the active-layer design, enabling spectrally selective emission without external optical filters

These results highlight the versatility of the InAs/AlAsSb antimonide platform for realising complementary mid-IR sources tailored to industrial process monitoring and hazardous-gas detection. The use of a common epitaxial technology for both coherent and thermal emitters also provides a promising basis for future integrated mid-IR sensing systems.

After Deadline Contribution



BEST STUDENT AWARDS:

Best oral presentation:

Chia-Ming Mai from National Tsing Hua University, Taiwan

Best poster presentation:

Justas Berškys from FTMC, Lithuania

Young student encouragement:

Simonas Driukas from FTMC, Lithuania

In the photos (next page): (top) Dr. Dovilė Čibiraitė-Lukenskienė (left) Prof. Shang-Hua Yang on behalf of his PhD student Chia-Ming Mai (center) and Chair Prof. Dr. Irmantas Kašalynas (right); (middle) PhD student Justas Berškys (left) and Dr. Dovilė Čibiraitė-Lukenskienė (right); (bottom) Chair Prof. Dr. Irmantas Kašalynas (left), PhD student Simonas Driukas (center) and Dr. Dovilė Čibiraitė-Lukenskienė (left). Photo credits: top and bottom Gabrielius Mackevičius, FTMC; middle Dr. Domas Jokubauskis, FTMC ▼


BEST ORAL PRESENTATION


BEST POSTER PRESENTATION


YOUNG STUDENT
ENCOURAGEMENT AWARD

Author Index

Aalto, Timo, 72
Abedi-Varaki, Mehdi, 91
Abramavicius, Darius, 92
Abramov, Sergiy, 105
Abramova, Viktoriia, 105
Adigun, Deborah, 46
Aleksiejūnas, Ramūnas, 56
Alesenkov, Aleksandr, 57
Aliyev, Raul, 80
Anbinderis, Maksimas, 80
Antanavičius, Romaldas, 57
Ardaravičius, Linas, 78, 82
Aslam, Zabeada, 20
Augulis, Dominykas, 114
Auksorius, Egidijus, 118
Ayyagari, Surya Revanth, 64
Ašmontas, Steponas, 104, 106

Babusci, Alfredo, 67
Baidya, Arunjyoti, 92
Balčytis, Armandas, 17, 76
Bauer, Maris, 54
Beard, Matthew C., 56
Belous, Anatolii G., 69
Berger, Christian, 14
Beršky s, Jaunius, 119
Beršky s, Justas, 100, 113
Białek, Marcin, 40
Bibi, Ifra, 50
Biswas, Joydeep, 88
Bičiūnas, Andrius, 83
Boiko, Vitalii, 97, 98
Bubilaitis, Vytautas, 92
Bukauskas, Virginijus, 86
But, Dmytro B., 93
Butkutė, Renata, 28, 83, 87, 99

Cernescu, Adrian, 58, 75
Charrouj, Noureddine, 40
Cojokari, Maria, 73
Conconi, Maria Teresa, 94
Couteau, Christophe, 67

Daraei, Mohammad Esmaeil, 91
Dasgupta,Shyantan, 35
Daugalas, Tomas, 29
Dermauskas, Eimantas, 74
Dettin, Monica, 94
Devenson, Jan, 86, 119
Dhillon, Sukhdeep, 20
Dinh, Hiep X., 76
Doerner, Ralf, 14
Driukas, Simonas, 22
Dub, Maksym, 26
Dudutienė, Evelina, 28, 83, 87, 99

Elertas, Gedminas, 70

Fedorov, Georgy, 46, 67, 73
Feiginov, Michael, 79
Filonenko, Elena, 31, 51
Fox, Nathan, 20
Franckevičius, Marius, 33, 117
Freeman, Joshua R., 20
Frogh, Abdullah Jan, 102

Gao, Feng, 35
Gelczuk, Lukasz, 35
Gečys, Paulius, 29
Gill, Thomas B., 20
Glubokov, Oleksandr, 14
Gläsel, Jonas, 14
Goldobin, Denis, 99
Golubewa, Lena, 98
Gonzalez, Marlene Patraca, 31
Gorbun, Mikhail, 73
Gradauskas, Jonas, 104, 106
Gregg, J. Marty, 20
Grigelionis, Ignas, 38, 39, 44, 81, 105, 109
Grishin, Mikhail, 57
Guimarães, Mateja, 31
Gulbinas, Vidmantas, 33, 35, 97, 98, 116, 117

Hagenmuller, David, 40
Haque, Md Azimul, 56
Heinrich, Wolfgang, 14
Hickey, Bryan J., 20
Horng, Ray-Hua, 29
Horoshko, Dmitri, 31
Hossain, Maruf, 14

Hreniak, Dariusz, 97, 98
Hsu, Chen-Peng, 62
Hussung, Raphael, 54
Hübers, Heinz-Wilhelm, 60

Ignatjev, Ilja, 29
Ikamas, Kęstutis, 80, 109
Indrišiūnas, Simonas, 29, 64, 75
Ivanauskaitė, Patricija, 63
Ivaškevičiūtė-Povilauskienė, Rusnė, 38, 39, 44, 109
Ivonyak, Yurii, 40

Janonis, Vytautas, 64, 73, 75
Januškevičius, Regimantas, 57, 75
Janušonis, Julius, 50
Jelezko, Fedor, 31
Johnson, Justin C., 56
Jorudas, Justinas, 29
Jovaišaitė, Justina, 56
Jukna, Vytautas, 112

Kaluza, Mateusz, 38, 39, 89, 93, 115
Kamarauskas, Mindaugas, 83, 86
Kamiński, Kamil, 68
Kananavičius, Robertas, 57
Kancleris, Žilvinas, 69, 90
Karaliūnas, Mindaugas, 34, 108
Karol, Mateusz, 68
Karpicz, Renata, 51, 94
Kasparavičius, Ernestas, 116
Kauppinen, Esko, 46, 73
Kawano, Shotaro, 21, 45
Kazakov, Alexander, 40
Kazlauskas, Karolis, 32
Kašalynas, Irmantas, 29, 34, 64, 67, 73, 75
Kašponas, Tomas, 57
Kersulis, Skirmantas, 110
Kimura, Wataru, 21
Kiprijanovič, Oleg, 78, 82
Klepeckas, Titas, 33
Knap, Wojciech, 26, 40
Komorowski, Paweł, 68, 89, 115
Konishi, Kuniaki, 21, 45, 46, 55, 67
Korotyeyev, Vadym, 26
Krotkus, Arūnas, 84, 85
Krozer, Viktor, 14
Kurowska, Marta, 93, 115
Kuzhir, Polina, 31, 46, 51, 73
Kwak, Joon Young, 82

Lamberti, Patrizia, 94
Laurinavičius, Klemensas, 111, 113
Le, Cheng-Siang, 62
Levinas, Ramūnas, 86
Liao, Zi-Xiang, 62
Lienqueo, Francisco Hernán Capdeville, 34
Lin, Hungyen, 62
Linfield, Edmund H., 20
Lisauskas, Alvydas, 15, 63, 80, 81, 109
Low, Mei Xian , 76
Lukin, Volodymyr, 105
Lukošiūnas, Julius, 57
Lukša, Algimantas, 86
Luther, Joseph M., 56

Maciejewski, Marcin, 68
Macutkevič, Jan, 64
Maffucci, Antonio, 67
Mai, Chia-Ming, 22, 62
Malinauskas, Tadas, 114
Malykhin, Sergei, 31, 51
Markauskas, Edgaras, 50
Masalskyi, Oleksandr, 104
Matoba, Mizuho, 45, 46
Mažeika, Kipras, 28
McCluskey, Conor J., 20
Menon, Aadya, 46, 73
Michailovas, Andrejus, 57
Mikhailikova, Iryna O., 27
Mindarava, Yuliya, 31
Minh, Duong Nguyen, 56
Minkevičius, Linas, 38, 39, 44, 81, 95, 105, 109, 112
Mitchell, Arnan, 76
Mohammadzadeh, Shiva, 54
Moorsom, Timothy, 20
Mosconi, Edoardo, 35
Moscotin, Maxim, 29
Motohashi, Kazuya, 45
Muggleton, Ben, 20
Muthamalingum, Karthickraj, 62

Nacius, Ernestas, 112
Nagatsuma, Tadao, 66
Naik, Nisha, 88
Nargelienė, Viktorija, 50, 86, 119
Nevinskas, Ignas, 22, 91
Nguyen, Thach G., 76
Nieradka, Adrianna, 38, 89
Nomeika, Kazimieras, 56
Norkus, Ričardas, 22, 84, 85

Ogrin, Feodor, 67
Orlita, Milan, 26
Orlov, Sergej, 95, 100, 109, 113
Otsuji, Taiichi, 24
Ourednik, Petr, 79

P J, Anand, 107
Padilla,Willie J., 42
Pakštas, Vidas, 98
Pashnev, Daniil, 34
Paulauskas, Tadas, 50, 74, 96
Pačebutas, Vaidas, 84, 85
Pałka, Norbert, 68
Petkus, Ričardas, 81
Petrauskienė, Virginija, 57
Petrokas, Jonas, 104
Piatrou, Pavel, 110
Pokaliuk, Karina, 86
Portnoi, Misha, 67

Ragulis, Paulius, 69, 90
Rao, Ashok, 88, 107
Rausch, Marko, 14
Razinkovas, Lukas, 52, 97, 101
Rehman, Ubaid ur, 74
Ren, Guanghui, 76
Rindzevičius, Paulius, 51
Robinson, Phoenix, 20
Rodz, Daniel, 97
Rogers, Matthew, 20
Runge, Patrick, 14
Rutkauskas, Danielis, 50, 94
Rämer, Adam, 14

Sadauskas, Modestas, 69
Sai, Pavlo, 26
Sakurai, Haruyuki, 21, 45
Sasaki, Satoshi, 20
Saushin, Aleksandr, 46, 73
Savitski, Stanislau, 100
Scheele, Patrick, 14
Seifert, Birger, 34
Seliuta, Dalius, 90
Shivan, Tanjil, 14
Siemion, Agnieszka, 38, 39, 89, 93, 115
Sieni, Elisabetta, 94
Silkinis, Rokas, 52
Silys, Vakaris, 74
Simniškis, Rimantas, 69
Singh, Dinesh Pratap, 34
Skapas, Martynas, 28, 99
Skaržinskas, Mantas, 96
Stacevičius, Lukas, 38, 39
Stalnionis, Giedrius, 29
Stanaitis, Kasparas, 44, 95
Stanionis, Benas, 84, 85
Stanionytė, Sandra, 28
Stankevic, Voitech, 110
Stankevič, Valdemar, 74
Starobrat, Joanna, 93
Stašys, Karolis, 119
Stefanski, Mariusz, 97, 98
Steponaitis, Matas, 117
Streckaitė, Simona, 97, 98
Stölmacker, Christoph, 14
Sunil, Dhanya, 88, 107
Sužiedėlis, Algirdas, 106
Svirskaitė, Lauryna M., 116

Tanaka, Koichiro, 61
Tarvydas, Erikas, 118
Todorov, Yanko, 40
Trečiokaitė, Austėja, 118

Ulbricht, Ronald, 49
Urbanowicz, Andrzej, 34, 67, 73

Vaitkevičius, Augustas, 28
Vaičikauskas, Viktoras, 119
Vaičiulis, Liutauras, 35
Valušis, Gintaras, 19, 22, 34, 38, 39, 95
Vasiliauskaitė, Dovilė, 116
Vitiello, Miriam Serena, 48
Vizbaras, Domantas, 63, 81, 109
V'yunov, Oleg I., 69

Wahaia, Faustino, 34
Waller, Erik Hagen, 54
Wojnar, Piotr, 28

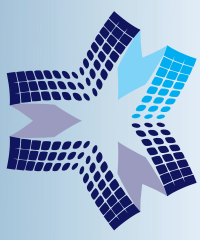
Yacoub, Hady, 14
Yagmur, Ahmet, 20
Yang, Shang-Hua, 22, 43, 62
Yang, YuLin, 62
Yavorskiy, Dmitriy, 40

Zagrajek, Przemysław, 68
Zamuner, Annj, 94
Zelioli, Andrea, 28, 83, 87, 99
Zenin, Vladimir A., 16, 75
Zhang, Muyi, 35
Zhang, X.-C., 18
Zhang, Xinwen, 56
Zharchenko, Ihor, 104
Zhenyu, Xu, 73

Čehavičius, Bronislavas, 22
Čepurnaitė, Giedrė, 119
Čerškus, Aurimas, 87, 99, 104, 106
Čibiraitė-Lukenskienė, Dovilė, 63, 81
Čirgelis, Vilius, 98
Čižas,Vladislovas, 44

Šermukšnis, Emilis, 82

Šilys, Vakaris, 50
Šilėnas, Aldis, 104
Šimukovič, Artur, 82
Širmulis, Edmundas, 106
Špokas, Aivaras, 28, 83, 87, 99
Štaupienė, Aistė, 99
Žalys, Ovidijus, 106
Žemgulytė, Justina, 69
Žurauskienė, Nerija, 82, 110
Žuvelis, Justas, 28, 83



CENTER
FOR PHYSICAL SCIENCES
AND TECHNOLOGY

ISBN 978-609-96355-1-4